

PAUL SCHERRER INSTITUT



PSI Scientific Report 2005

Volume 2

Life sciences
and medicine

Cover photo:

**Precise placing of a probe at the
SLS microtomography beamline.**

(Photo: H.R. Bramaz)



PSI Scientific Report 2005

Volume 2

Life sciences
and medicine

Imprint

PSI Scientific Report 2005 Volume 2

Volume 1 Condensed matter, photons,
neutrons and charged particles
Volume 2 Life sciences and medicine
Volume 3 Energy and environment

Published by
Paul Scherrer Institute

Concept and editorial work by
Juanita Schläpfer-Miller, Beat Gerber

Proof-reading
Terry Groves

Design and layout
Monika Blétry

Printing
Christoph Schütz

Available from
Paul Scherrer Institute
Communications Services
5232 Villigen PSI, Switzerland
Phone +41 (0)56 310 42 61
www.psi.ch

PSI public relations
pubrel@psi.ch

Communications officer
Beat Gerber, Phone +41 (0)56 310 29 16

ISSN 1661-7010

Copying is welcomed, provided
the source is acknowledged and an
archive copy sent to PSI.

Paul Scherrer Institute, April 2006

Table of contents 3

Volume 2
Life sciences and medicine

4 Foreword from the director

7 Research focus and highlights

- 8 Biomolecular research
- 18 Life sciences at large facilities
- 30 Radiopharmacy
- 36 Proton therapy

47 Technology transfer

Patents and licenses

53 Facts and figures

Research and user labs
Commission and committees

63 Publications

Lists and links to web

CD with publication lists and links to web



From ivory towers to alpine huts

Do scientists really occupy ivory towers? Do they live a comfortable, even luxurious life without contact to the real world? Researchers prefer to see themselves rather as hearty members of the Swiss Alpine Club, where, until recently, one needed special training and equipment to overnight in high mountain huts. Only those who were prepared for a difficult hike the next day could stay at the top of the mountain.

Earlier, a scientific experiment, like a mountain climb was done in the company of a few colleagues, without mobile phone contact, cut off from the rest of the world. This has changed dramatically in the last few decades. Even inexperienced hikers can stay overnight in alpine huts, transported to their destinations by cable-cars. Responding to the increasing interest of the lay public in research, science has also become more accessible and public-friendly.

Spectacular moments are rare

Mountain climbers were accompanied by live TV cameras for their ascent of the north face of the Eiger. In a similar search for the dramatic, TV crews install themselves in labs in the hope of broadcasting scientific first ascents. Yet spectacular discoveries are rare and often only years later achieve popular recognition and acclaim.

An excellent example of this is the ground-breaking work of Albert Einstein from 1905. One-hundred years later his works were exulted at PSI and around the world. During the International Year of Physics, Einstein theme tours for the public

were organised at PSI providing basic explanations of the three papers published in his “annus mirabilis”. Last year the number of visitors at the PSI open day was nearly 10,000 – illustrating that the world of science has learnt to present itself competently and attractively.

Research needs freedom

The question often emerges as to whether taxpayers’ money is being used efficiently for research. Perhaps the question should be more directly formulated as: can Switzerland compete globally for the best talent? The usual answers are thus; we need to join forces through better co-ordination, eliminate duplication of efforts and found centres of competence. However, often the most important factor is overlooked: excellence in research requires tolerance and space for unconventional ideas to flourish.

Competence requires time

The Swiss Nobel prize-winner Heinrich Rohrer used to say that; “One cannot establish a competence centre, at the most it is something that one can become.” In this sense the year 2005 was the start of a vision. Under the leadership of PSI, and supported by the accumulated intelligence of the ETH Domain, large energy research projects will be started which will lead to secure and sustainable energy solutions for Switzerland.

Creative heads will engage with projects to do with mobility, electricity and low temperature heat. We are very grateful for the financial support of the Swiss government and the Canton of Aargau.

Scientific success in 2005

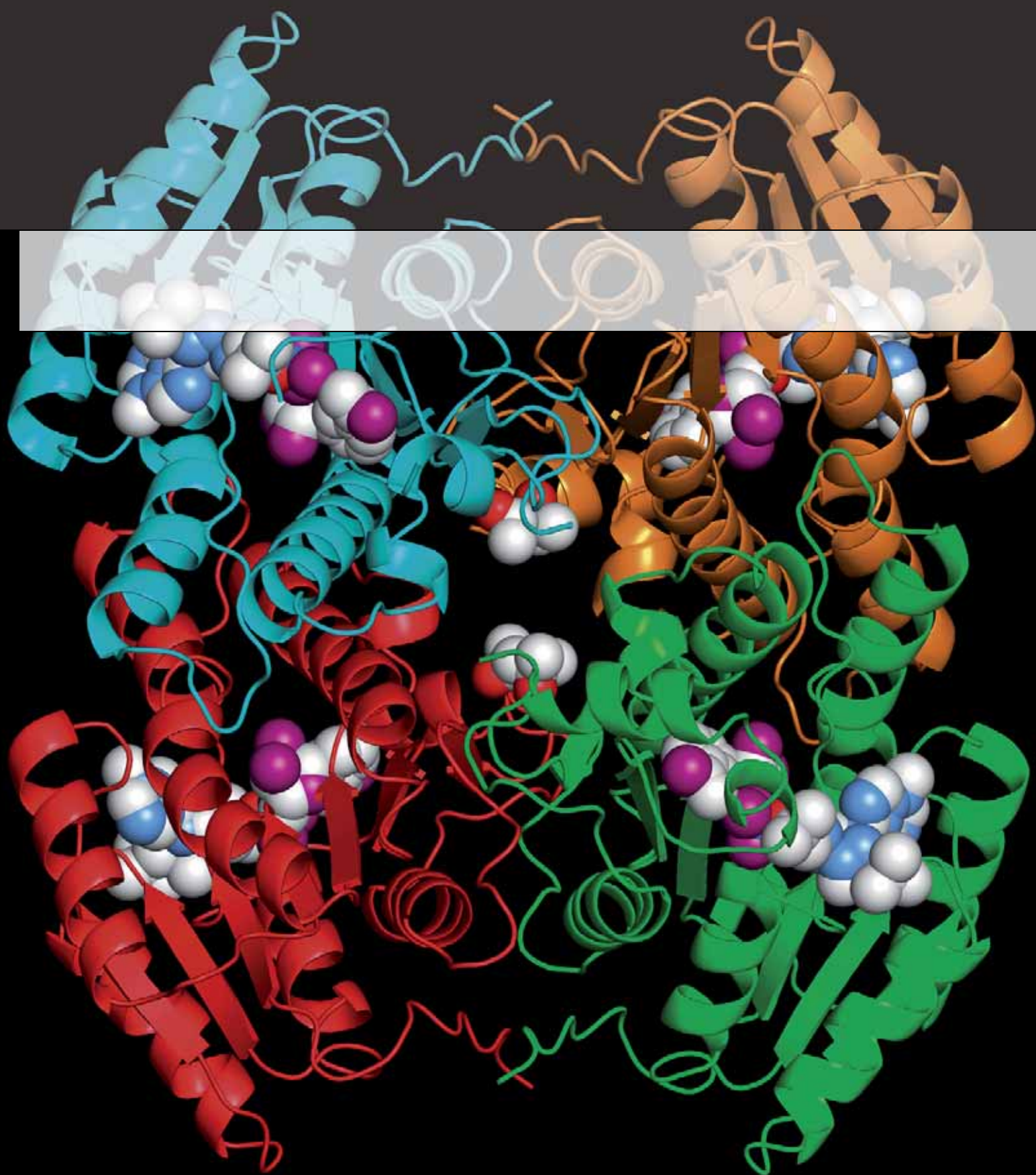
One scientific success was the rediscovery of uses for phase-contrast microscopy. Thanks to innovative ideas and technical skills, diffraction grating with an absorber of a few nanometers thick can be created for X-rays or neutrons which then produce razor sharp images after a few minutes exposure time. The potential applications for use with X-rays come from biology and medicine and for neutrons from the material sciences. Both techniques show promising applications for external clients of PSI, patents have been applied for.

This volume of the Scientific Report 2005, (Volume 2), highlights research undertaken in the areas of medicine and life sciences. Selected examples include research progress made in the structure determination of new targets for the design of anti-malaria drugs and in radio-immunotherapy for the treatment of cancers. The capabilities of the SLS were used in an international collaborative structural genomics project, for the analysis of very small crystals as present in insulin medication and for imaging possible effects on brain capillaries caused by Alzheimer's disease.

Scientific excellence is always the first priority of PSI and precisely because of this, science must be more accountable

to society. Visitor tours and science communication to the public have become part of daily business. The myth that researchers work in an ivory tower is obsolete. As testimony to this is PSI's positive reputation within the international scientific community, in Swiss national politics and in our local community. For this trust and recognition, our warmest thanks.

Ralph Eichler, Director PSI



Research focus and highlights 7

- 8 Biomolecular research
- 18 Life sciences at large facilities
- 30 Radiopharmacy
- 36 Proton therapy

PSI offers excellent facilities and support for competitive research and development activities in selected areas of the life sciences. These are used in collaboration with external partners as well as for in-house research. PSI's Life Sciences Department focuses on three areas: biomolecular research, radiopharmaceutical research and proton radiation therapy.

Biomolecular research investigates the structure and function of proteins involved in signalling and transport through biological membranes and studies protein-protein interaction networks. A highlight of last year's results is structural insights into interactions of EB1 a master regulator of microtubule dynamics. Using a microfocus setup, SLS scientists were able to determine the structure of insulin as present in very small crystals of the insulin drug Ultralente.

The Centre for Radiopharmaceutical Science is pursuing the discovery and characterisation of radiopharmaceuticals for treating metastatic tumours and presents imaging studies of folate radiotracers and an investigation of radiolabelled vitamin B12 uptake by tumours.

The Division of Radiation Medicine reports on further clinical successes with the unique compact scanning-Gantry for proton radiation therapy of deep-seated tumours. Progress made in the construction of Gantry 2 is described in the PROSCAN report.

Information about other ongoing projects can be accessed through our website, www.psi.ch (Research at PSI).

Atomic structure of the FabG enzyme of the malaria parasite. A potential target for anti-malarial drug design.

(Image: Dirk Kostrewa)

Protein EB1: a master regulator of microtubule growth

Srinivas Honnappa, Corinne John, Hatim Jawhari, Dirk Kostrewa, Fritz K. Winkler, Michel O. Steinmetz;
Biomolecular Research, PSI

The detailed characterization of proteins interacting with the microtubule cytoskeleton is a prerequisite to understanding their outstanding role in life organisms. EB1 has very recently emerged as a key player regulating microtubule growth in all eukaryotic cells. We have analyzed the protein by an array of structural methods including X-ray crystallography. Our findings provide a structural framework for understanding EB1-mediated interaction networks that enable microtubules to participate in fundamental cellular functions including chromosome segregation during cell division.

Cellular role of EB1

The ability of eukaryotic cells to adopt a variety of shapes and to carry out coordinated and directed movements depends on their cytoskeleton. The cytoskeleton is a complex and highly dynamic network of protein filaments. These filaments continuously grow and shrink and extend throughout the cell cytoplasm. Microtubule filaments are critical for many cellular processes including cell growth and division, cell motility, cytoplasmic transport and cell signalling, as well as for cell development and maintenance of cell shape. A central aspect of microtubules is their ability to interact with a variety of accessory proteins, which enable the same filament to participate in distinct functions in different regions of the cell. Microtubule tip tracking proteins (+TIPs) constitute a diverse subgroup of microtubule-binding proteins that associate preferentially with growing microtubule ends. They are implicated in many, if not all, microtubule-based processes including chromosome segregation, establishment and maintenance of cell polarity, cell migration, and anchoring of microtubules to different cellular structures. One key property of +TIPs is

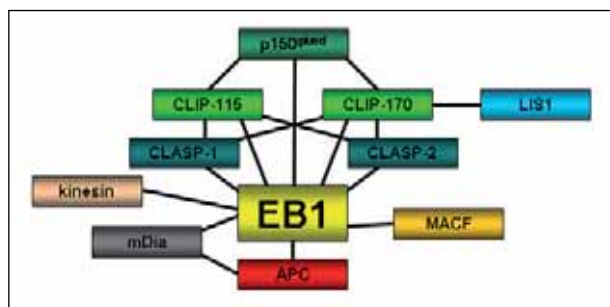


Figure 1: **Interaction network of +TIP proteins.**

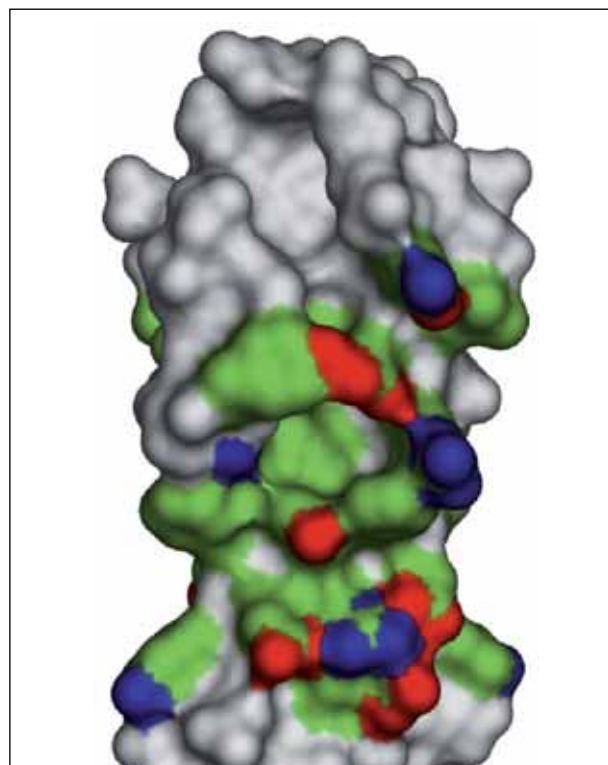


Figure 2: **Surface view of EB1-C. Highly conserved and surface accessible amino acids are indicated and coloured according to the atom type: blue, nitrogen; red, oxygen; green, carbon.**

their ability to form macromolecular microtubule “plus-end-complexes”. Recently, EB1 (end-binding protein 1) emerged as a master protein controlling +TIP interaction networks at microtubule tips. The molecule physically interacts with most prominent +TIPs including the adenomatous polyposis coli (APC) tumour suppressor, cytoplasmic linker protein 170 (CLIP-170), kinesins, and dynactin large subunit p150^{glued} (Figure 1).

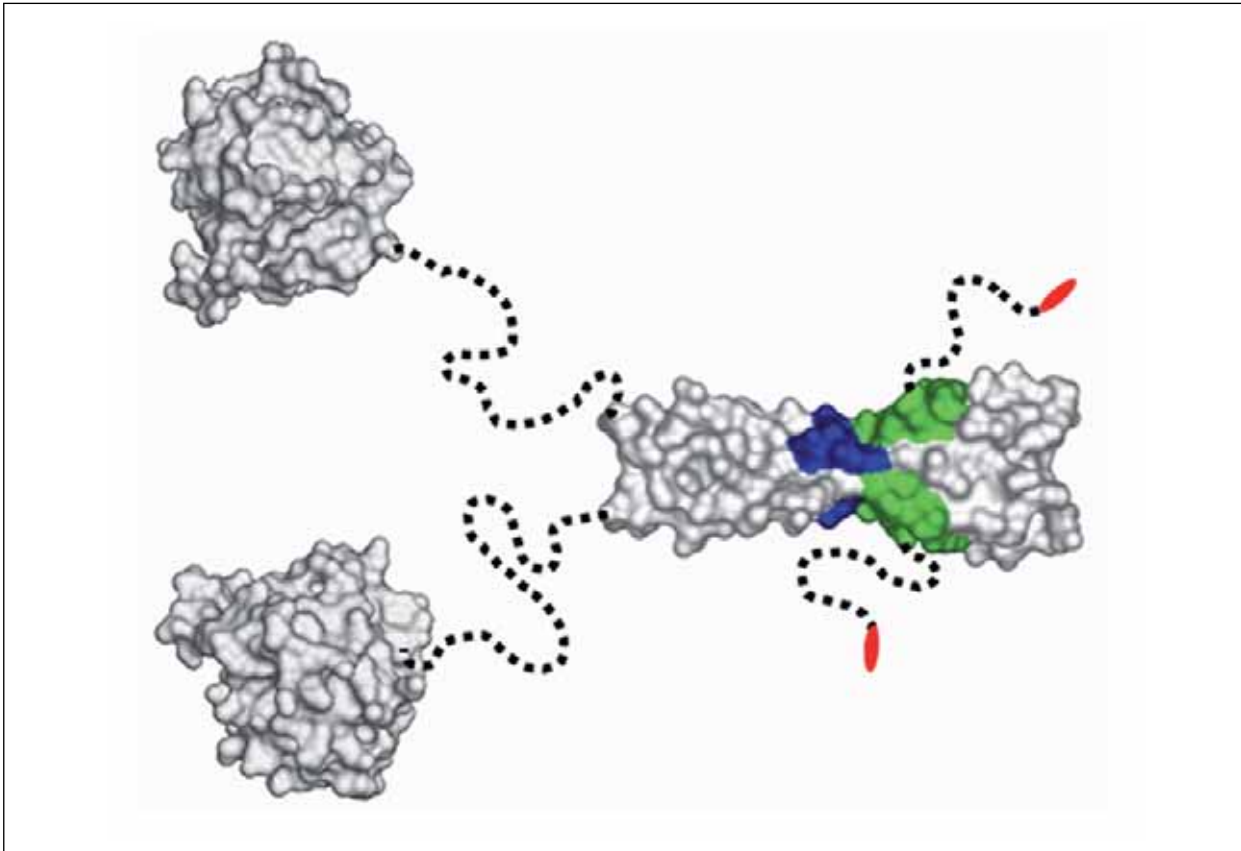


Figure 3: **Structural organization of full-length EB1 and mapped +TIP binding-sites.** The structures of the globular N-terminal microtubule-binding (top) and C-terminal EB1 (bottom) domains are depicted as surface views. Dashed and curved lines schematize flexible peptide segments of the dimeric molecule. The binding sites for APC (green and blue) and p150^{glued} (green, blue, and red) are highlighted.

A growing body of evidence suggests that the activity of many microtubule-binding proteins depends on their potential to interact with EB1. The detailed nature, specificity, and modes of regulation of EB1-mediated +TIP interaction networks, however, are poorly defined.

Structural studies on EB1

In order to provide a molecular basis for understanding how human EB1 organizes macromolecular microtubule plus-end-complexes we recombinantly produced and analyzed the protein by an array of structural methods including X-ray crystallography. We established that the C-terminal moiety of EB1 (EB1-C) represents a dimerization domain for the full-length protein. The crystal structure of EB1-C reveals that dimerization is essential for the formation of a highly conserved surface patch (Figure 2). The carboxy terminal 19 amino acids of EB1 were found to be unstructured and flexible. Mutational analyses suggested that the highly conserved surface patch as well as the last two conserved carboxy terminal EB1 amino acids act as binding sites for +TIPs interaction partners (Figure 3).

Our findings reveal that a central aspect of EB1-mediated protein-protein interactions is the involvement of a flexible polypeptide chain segment and a folded binding site. Such an interaction mode is well suited to recruit different molecular functionalities to a common location without imposing undesired structural constraints on the resulting assemblies. Moreover, as expected from *in vivo* observations, such regulated protein-protein interactions provide a basis for understanding the cross-talk among +TIP proteins at growing microtubule ends, the anchoring of microtubule tips to cellular structures, and the delivery of proteins to the cell periphery.

References

- [1] Honnappa et al., EMBO J. 24, 261 (2005)
- [2] Akhmanova and Hoogenraad, Curr. Opin. Cell Biol. 17, 47 (2005)
- [3] Vaughan, J Cell Biol. 171, (2005)
- [4] Bu and Su, J. Biol. Chem. 278, 49721 (2003)
- [5] Wen et al., Nat. Cell Biol. 6, 820 (2004)
- [6] Hayashi et al., J Biol Chem 278, 36430 (2003)

Structure-based design of a new receptor-specific VEGF-E variant

Michel Pieren, Andrea Prota, Fritz K. Winkler, Kurt Ballmer-Hofer, *Biomolecular Research, PSI*

Vascular endothelial growth factors (VEGFs) constitute a family of polypeptides that regulate blood and lymphatic vessel development upon binding to specific tyrosine kinase receptors (VEGFR-1, -2 and -3). We solved the crystal structure of a viral homolog, VEGF-E NZ2, and show that, similar to known structural homologs, the protein is dimeric and assumes a cysteine knot structure. Based on structures of various VEGFs we created chimeric VEGF-E proteins and tested their binding properties to both VEGFR-1 and -2. Our data show that receptor specificity of VEGFs is determined by a combined epitope formed by loops L1 and L3.

Introduction

Mammalian vascular endothelial growth factors constitute a family of polypeptide growth factors, VEGF-A, -B, -C, -D and PlGF, that regulate blood and lymphatic vessel development [1]. VEGFs bind to three types of tyrosine kinase receptors, VEGFR -1, -2 and -3, that are predominantly expressed on endothelial and some hematopoietic cells. Pox viruses of the Orf family encode highly related proteins called VEGF-E that bind with almost the same affinity to VEGFR-2. VEGF receptors consist of 7 extracellular Ig-like domains, a transmembrane helix, and a cytosolic kinase domain [2]. Receptor-specific

interactions have been described for PlGF and VEGF-B, which specifically bind only to VEGFR-1, while VEGF-E exclusively interacts with VEGFR-2 [3]. Mutation analysis of the extracellular domains of VEGFR-1 and -2 showed that the second and third Ig-like domains form the high-affinity ligand binding region for VEGF. Structural data are also available for specific VEGF ligands and ligand receptor complexes [4-6].

Structure determination of VEGF-E NZ2

Crystals of VEGF-E NZ2 contain two homodimers (named AB and CD) in the asymmetric unit that are related by non-crystallographic 2-fold symmetry (Fig. 1). The structure shows a highly conserved overall structure among all VEGF homologs with conformational differences in L1 and L3 (Fig. 2). The conformation of L3 in VEGF-E differs remarkably from those in the other VEGF family members.

VEGF receptor-specific chimera

We investigated the role of L1 and L3 in receptor binding by constructing chimeric VEGF-E variants in which L1 (VE_{L1}), L3 (VE_{L3}), or both loops (VE_{L13}) were replaced by the corresponding sequence from PlGF-1 (Fig. 2). In addition, we created a point mutant in L1 in which arginine 46 was replaced by isoleucine (VE_{R46I}). Competitive binding assays were performed on endothelial cells expressing either VEGFR-1 or -2. Data for VEGFR-2 are shown in Figure 3 (top panel). Cold VEGF-A competed radiolabeled ligand with an EC₅₀ of 1.0 nM (0.9-1.1 nM; 95% confidence interval), while for VEGF-E and VE_{R46I} values of 80.6 (71.7-90.6) nM and 16.2 (14.7-17.8) nM were calcu-

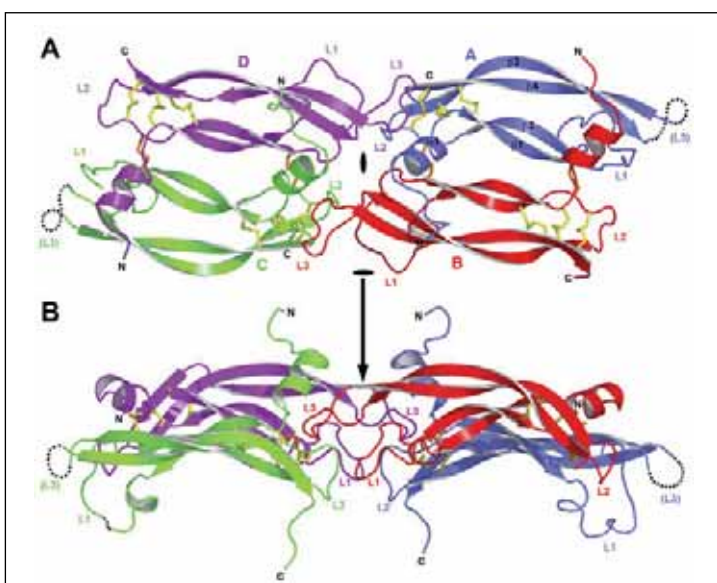


Figure 1: **Structure of VEGF-E NZ2. (A) Ribbon representation of the VEGF-E dimer of two covalent homodimers as observed in the asymmetric unit. (B) Same ribbon representation as in (A) viewed perpendicular to the central 2-fold axis.**

lated, respectively. Arginine 46 substitution resulted in a 5-fold decrease of the EC_{50} . Binding of radiolabeled VEGF-A₁₆₄ to VEGFR-2 was not competed with the loop mutants VE_{L1}, VE_{L3}, VE_{L13} or PIGF-1, demonstrating that exchanging either one or both loops destroyed binding to VEGFR-2.

Since our VEGF-E mutants contain L1 and L3 from PIGF-1, competition experiments with PAEC cells expressing VEGFR-1 were performed with ¹²⁵I-PIGF-1. PIGF-1, VE_{L13} and VE_{R46I} showed specific binding while single loop replacement completely abrogated binding. With an EC_{50} of 4.2 (3.7-4.7) nM the value for VE_{L13} was more than 8-fold lower than for VE_{R46I} (EC_{50} 34.8 (31.9-38.0) nM, Fig. 3, lower panel). PIGF-1 was competed with an EC_{50} of 0.17 (0.16-0.19) nM.

Discussion

The data presented here show that the distinct orientation of L1 and L3 determines VEGF receptor specificity and that subtle changes in the ligand-receptor interface alter receptor specificity of VEGF-E. VE_{L13}. This, to our knowledge, is the first artificially engineered VEGF mutant where such a minimal sequence replacement established a new receptor specificity. Receptor/ligand complexes analyzed from cocrystals of VEGFR-2 bound to various isoforms of VEGF are now needed for a final assessment of receptor specificity of VEGF family proteins and will be crucial for the development of receptor-specific VEGF antagonists.

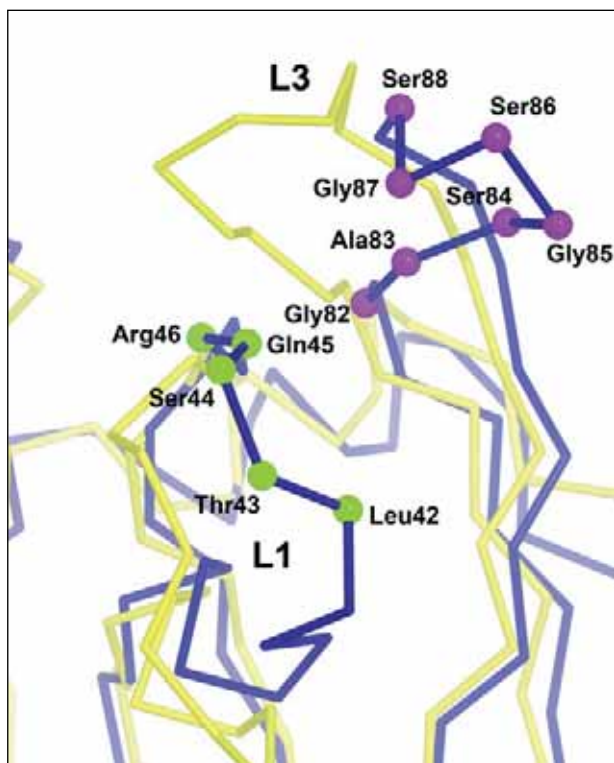


Figure 2: Loop structure of VEGF-E (blue) and PIGF-1 (yellow).

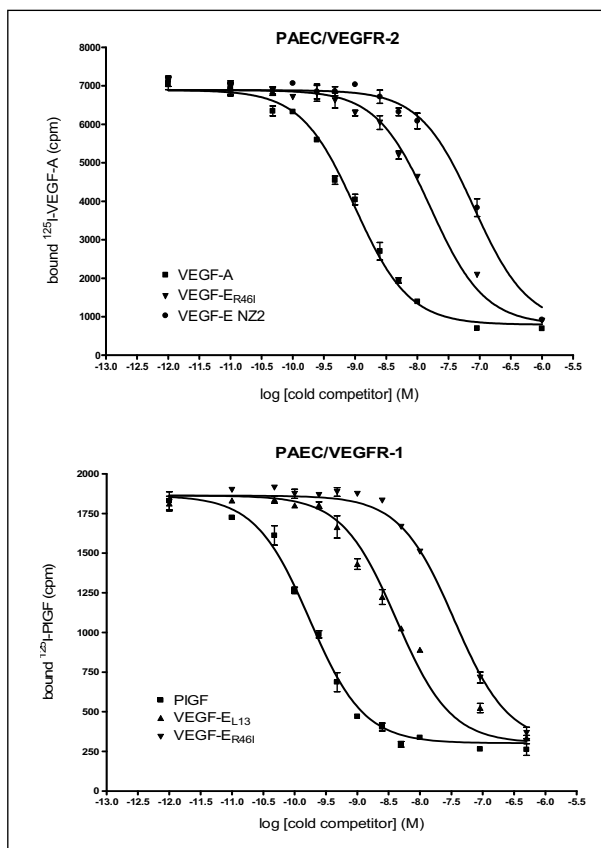


Figure 3: Binding data of chimeric VEGF mutants.

References

- [1] Ferrara, N. Vascular endothelial growth factor: basic science and clinical progress. *Endocr.Rev.*, 25: 581-611, 2004.
- [2] Cross, M. J., Dixelius, J., Matsumoto, T., and Claesson-Welsh, L. VEGF-receptor signal transduction. *Trends Biochem.Sci.*, 28: 488-494, 2003.
- [3] Mercer, A. A., Wise, L. M., Scagliarini, A., McInnes, C. J., Buttner, M., Rziha, H. J., McCaughan, C. A., Fleming, S. B., Ueda, N., and Nettleton, P. F. Vascular endothelial growth factors encoded by Orf virus show surprising sequence variation but have a conserved, functionally relevant structure. *J.Gen.Virol.*, 83: 2845-2855, 2002.
- [4] Christinger, H. W., Fuh, G., de Vos, A. M., and Wiesmann, C. The crystal structure of PIGF in complex with domain 2 of VEGFR1. *J.Biol.Chem.*, 279: 10382-10388, 2003.
- [5] Wiesmann, C., Fuh, G., Christinger, H. W., Eigenbrot, C., Wells, J. A., and de, V. A. Crystal structure at 1.7 Å resolution of VEGF in complex with domain 2 of the Flt-1 receptor. *Cell*, 91: 695-704, 1997.
- [6] Iyer, S., Leonidas, D. D., Swaminathan, G. J., Maglione, D., Battisti, M., Tucci, M., Persico, M. G., and Acharya, K. R. The crystal structure of human placenta growth factor-1 (PIGF-1), an angiogenic protein, at 2.0 Å

A new and highly effective anti-angiogenic therapy approach to tumour associated macrophages

Steffen M. Zeisberger, Bernhard Odermatt, Cornelia Marty, Ann Zehnder-Fjällman, Kurt Ballmer-Hofer, Reto A. Schwendener, *Biomolecular Research, PSI*

Tumour-associated macrophages (TAMs), play a pivotal role in tumour growth and metastasis by promoting tumour angiogenesis. Treatment of tumour-bearing animals with clodronate encapsulated in liposomes (clodrolip) and VEGF neutralizing antibodies efficiently depleted these phagocytic cells, led to a drastic reduction in vessel density and efficiently inhibited tumour growth. These results validate clodrolip therapy in combination with angiogenesis inhibitors as a promising novel strategy for an indirect cancer therapy and as a tool to study the role of inflammatory haematopoietic and dendritic cells in tumourigenesis.

Introduction

Solid tumours are not only composed of malignant cells, they are complex organ-like structures comprising many cell types, including migratory hematopoietic cells, resident stromal cells and TAMs [1,2]. TAMs are attracted to sites of tumour growth by vascular endothelial growth factor, VEGF, produced by tumour cells. TAMs produce a vast number of factors that

promote tumour growth, vascularization and dissemination to other organs [3]. Bisphosphonates such as clodronate are used in the clinic to inhibit the development of bone metastases and for the therapy of inflammatory diseases [4]. Here we use liposome-encapsulated clodronate in combination with anti-angiogenic reagents to block TAM recruitment.

Clodrolip therapy and VEGF neutralization

We combined clodrolip with a single chain antibody fragment, scFv, neutralizing VEGF to inhibit TAM recruitment in tumour-bearing mice (Fig. 1). Clodrolip treatment decreased tumour volume by 63%, treatment with the VEGF-specific scFvSZH9 by 59% and a combination therapy resulted in growth inhibition by 74%.

Analysis of TAM depletion

Histological analysis of A673 tumour sections showed reduced macrophage infiltration and vessel density. Three days after the end of therapy, tumour blood vessels were virtually undetectable and a significant reduction in vessel density was observed even 9 days later. Quantification of A673 tumour sections showed depletion of tumour associated F4/80⁺ macrophages by 93% and of MOMA1⁺ macrophages by 90% in clodrolip treated animals. CD11b⁺ TAMs were reduced by 24% after scFvSZH9 antibody treatment, by 59% after clodrolip and by 74% after clodrolip plus scFvSZH9 treatment, respectively. Finally, drastic depletion of CD11c⁺ tumour associated dendritic cells (TADCs) by 96% after scFvSZH9, by 99%

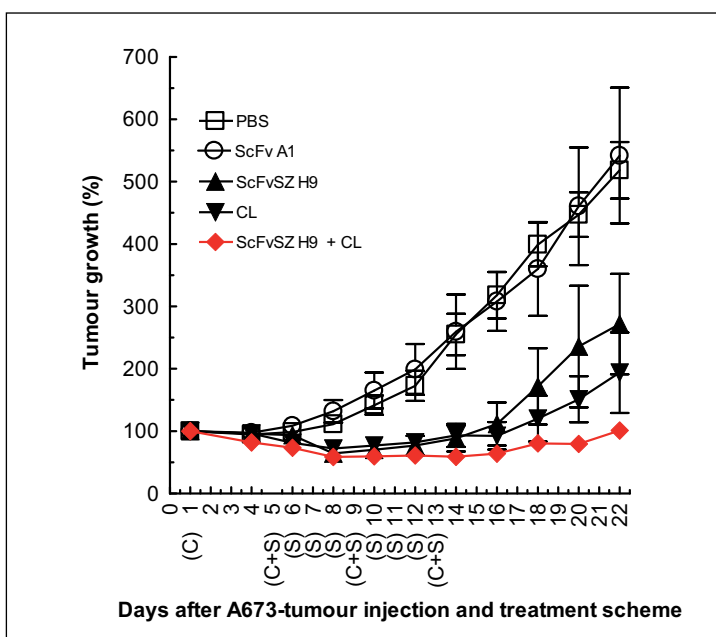


Figure 1: **A673 rhabdomyosarcoma tumour growth inhibition by clodronate and scFv antibody treatment.** Tumour bearing mice were treated with buffer PB, control scFvA1, VEGF-specific scFvSZH9, clodrolip plus scFvA1 or clodrolip plus scFvSZH9. Values represent the mean tumour volumes of treated mice \pm SEM (n = 6 – 8) normalized for tumour size on day 1.

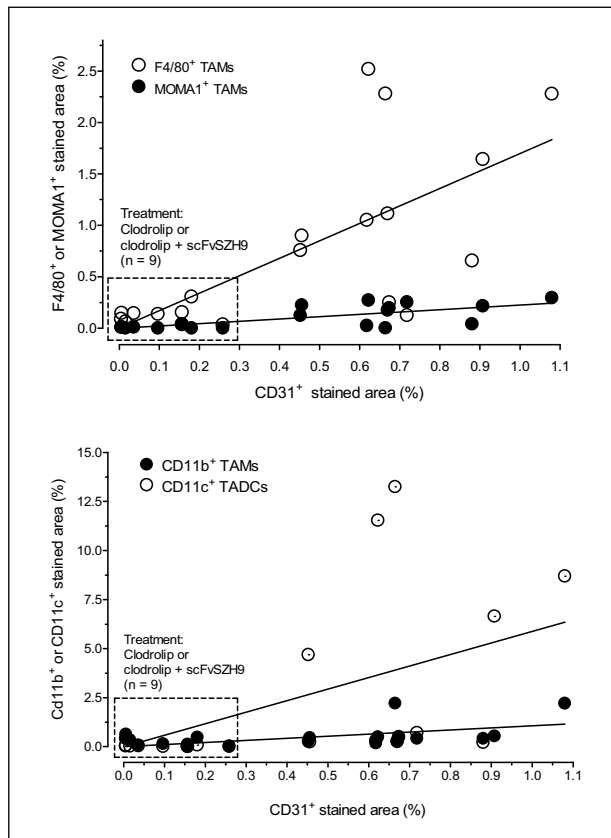


Figure 2: **Correlation of top panel, TAM (F4/80⁺, MOMA1⁺, CD11b⁺) and bottom panel, TADC (CD11c⁺) depletion versus vessel density (CD31⁺ cells). The dots represent values of positively stained areas from individual tumours and show clear separation of clodrolip plus scFvSZ9 treated (box) compared to PB, scFvA1 or single scFvSZH9 treatment. Statistical analysis Pearson correlation, $n = 20$: **F4/80**, $r = 0.701$, $P = 0.0006$; **MOMA1**, $r = 0.711$, $P = 0.0004$; **CD11b**, $r = 0.50$, $P = 0.025$; **CD11c**, $r = 0.531$, $P = 0.016$.**

after clodrolip and by 99% after clodrolip plus scFvSZH9 treatment, respectively, was observed. CD31⁺ staining specific for tumour vessels was reduced by scFvSZH9 monotherapy by 48%, by clodrolip by 89% and by a combined therapy by 85%. The correlation of F4/80⁺ and MOMA1⁺ macrophage density versus microvessel counts (CD31⁺ cells) showed a clear separation of tumours treated with clodrolip or clodrolip plus scFvSZH9 compared to tumours treated with scFvSZH9 alone, with the control antibody scFvA1 or buffer only (Fig. 2, top panel). Correlation of CD11b⁺ and CD11c⁺ cell depletion with vessel density (CD31⁺ cells) confirms these results (Fig. 2, bottom panel).

Discussion

TAMs, and TADCs, a subpopulation thereof, are among the many haematopoietic cell types recruited to sites of tumour

growth. These cells have been shown to play important roles in tumour growth and dissemination and were therefore proposed as potential therapeutic targets [5]. So far the idea to directly eliminate these cells in tumour tissue *in vivo* has not been exploited therapeutically. With the bisphosphonate clodronate encapsulated in liposomes we developed a powerful reagent for the selective depletion of tumour macrophages and endothelial precursors such as TADCs. Clodronate combined with anti-angiogenic therapy efficiently depleted TAMs and TADCs and inhibited tumour growth presumably by blocking tumour vascularisation. Depleting these stromal cell subsets apparently disrupts the cytokine network and results in an imbalance in the cell populations that are the source of tumour stimulatory chemokines and cytokines. We surmise that TAM depletion is indeed the cause of tumour growth inhibition.

TAM depletion, as with most therapies aimed at the tumour vasculature, ought to be regarded as an adjuvant treatment in combination with conventional chemo- or radiotherapy. Taken together, our findings provide solid evidence for the importance of TAMs, and possibly also of endothelial precursors such as dendritic cells, in the establishment of a micro-environment favouring tumour growth and dissemination.

References

- [1] Mueller MM, Fusenig NE. Friends or foes – bipolar effects of the tumour stroma in cancer. *Nat Rev Cancer* 2004;4:839-49.
- [2] Pollard JW. Tumour-educated macrophages promote tumour progression and metastasis. *Nat Rev Cancer* 2004;4:71-78.
- [3] Podar K, Anderson KC. The pathophysiologic role of VEGF in hematologic malignancies: therapeutic implications. *Blood* 2005;105:1383-95.
- [4] Ross JR, Saunders Y, Edmonds PM, et al. A systematic review of the role of bisphosphonates in metastatic disease. *Health Technol Assess* 2004;8:1-176.
- [5] Joyce JA. Therapeutic targeting of the tumour microenvironment. *Cancer Cell* 2005;7:513-20.

Single chain antibodies as diagnostic tools for SPECT, in tumour-bearing mice

Ann Zehnder-Fjällman, Alexander Hohn, Roger Schibli, Kurt Ballmer-Hofer, Reto A. Schwendener,
Biomolecular Research, PSI

Vascular endothelial growth factor receptor-3 (VEGFR-3) is required for lymphangiogenesis and plays a crucial role in tumour metastasis. VEGFR-3 is over expressed on tumour lymphatics and is therefore a good target for anti-cancer therapy. Single chain antibody fragments (scFv) specific for VEGFR-3 blocked signalling through this receptor and were successfully used for histological analysis of lymph vessels. Their potential for *in vivo* imaging in tumour-bearing mice was evaluated upon labelling with short-lived radioisotopes and single photon emission computerised tomography (SPECT) analysis.

Introduction

Today's cancer therapies consist mainly of a combination of surgery, radiotherapy, and chemotherapy. The major limitation for successful chemotherapy is a patient's tolerance of the highly toxic chemotherapeutics and the emergence of therapy-resistant cancer cells. The search for therapeutic alternatives that rely on new disease-relevant target molecules and on compounds with better tolerability is therefore of crucial importance. With a better understanding of the molecular basis of the pathophysiology of cancer, new potential targets are currently emerging. Growth and metastatic dissemination of tumour cells have been shown to depend on tumour vasculature. Anti-angiogenic and anti-lymphangiogenic therapy aiming at the destruction of the normal tissue which nurtures tumour cells is among the promising new strategies currently developed for cancer therapy [1-3].

In vivo distribution of scFv

We isolated a series of scFv antibody fragments recognizing VEGFR-3 from a phage display library. All antibody fragments bound the receptor with high affinity and blocked signalling by VEGF-C, a polypeptide growth factor implicated in lymph and blood vessel development. We also successfully used these scFv fragments for visualization of VEGFR-3 expression on cells by immunofluorescence microscopy and flow cytometry and for histological analysis.

The high affinity of these reagents for VEGFR-3 (K_D approximately 10 nM) made them good candidates for *in vivo* imaging of receptor-expressing tumour vasculature. To test this pos-

sibility we labelled one of these molecules, scFvAFC₅, with ¹³¹I followed by intravenous injection into tumour-bearing SV129 mice. After 2 hours the mice were sacrificed and analysed post mortem. The biodistribution was determined by SPECT, a method that allows non-invasive acquisition of multiple 3D images from the same live specimen over an extended time period. Control animals bearing no tumours or an F9 control tumour lacking VEGFR-3 showed background accumulation of the label in the stomach and the thyroid gland (Fig. 1). In animals carrying a VEGFR-3 expressing F9 tumour, the label rapidly accumulated at the site of tumour growth as illustrated opposite. Figure 1 E and F clearly show accumulation of the label in the neck region of the animal where F9-VEGFR-3 cells were injected and grew to large tumours.

Discussion

The data presented here show that scFv antibody fragments such as scFvAFC₅ are well suited for *in vivo* imaging of VEGFR-3-expressing cells. SPECT imaging in combination with X-ray tomography is a non-invasive and rapid method for imaging of tissues in live animals using target-specific reagents labelled with short lived γ -ray emitting isotopes.

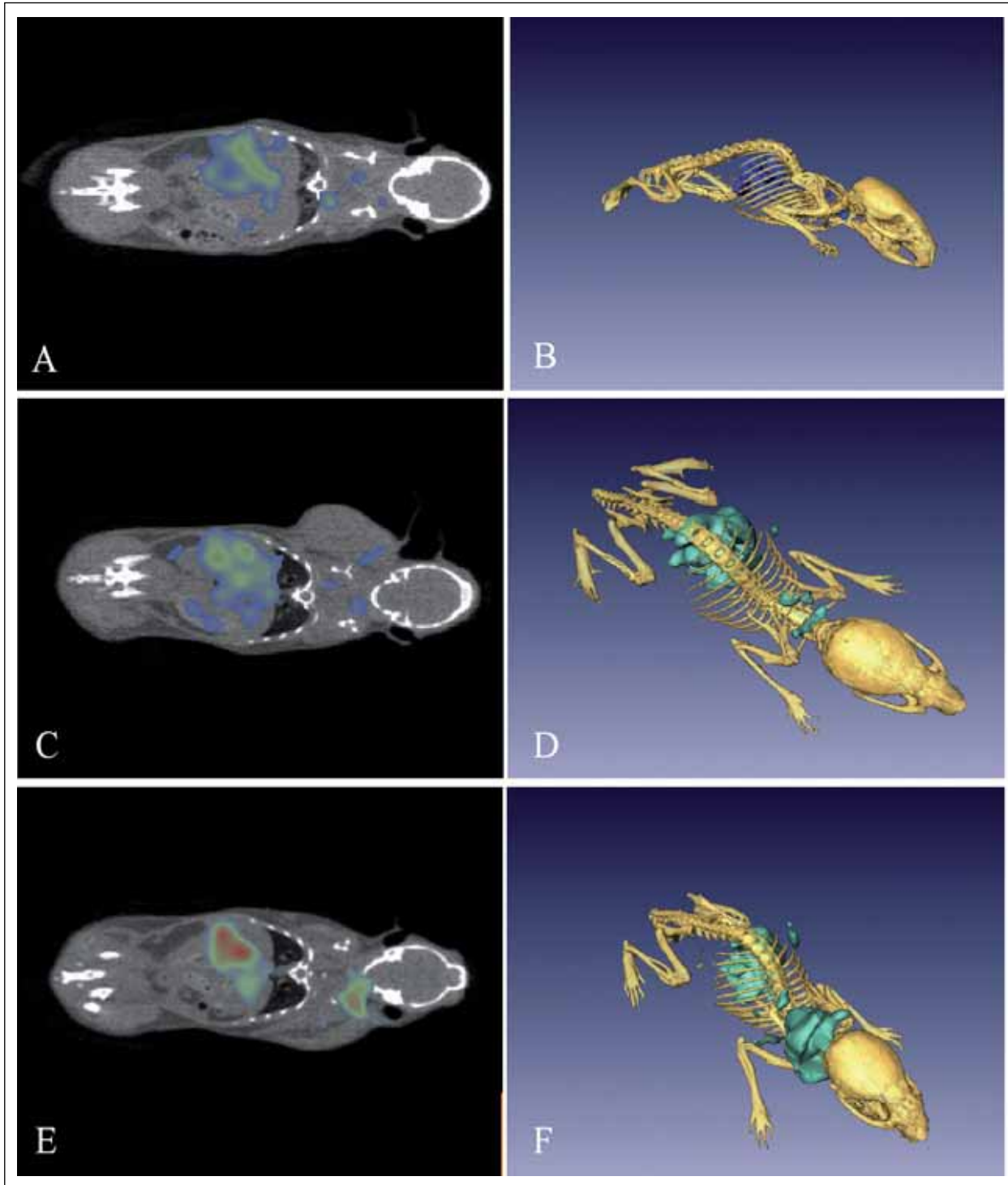


Figure 1: SPECT imaging in tumour-bearing mice. Accumulation of ^{131}I labelled scFvAFC5 specific for VEGFR-3 was determined in mice injected with 0.5×10^7 F9 tumour cells (C, D) or with stably transfected VEGFR-3-expressing F9 cells (E, F). Mice without tumours were used as controls (A, B). X-ray tomography images were superimposed with SPECT images. A, C, E show planar coronal sections and B, D, F 3 dimensional reconstructions.

References

- [1] Lymboussaki, A., Achen, M. G., Stacker, S. A., and Alitalo, K. Growth factors regulating lymphatic vessels. *Curr.Top.Microbiol.Immunol.*, 251: 75-82, 2000.
- [2] Tille, J. C., Nisato, R., and Pepper, M. S. Lymphangiogenesis and tumour metastasis. *Novartis.Found.Symp.*, 256: 112-131, 2004.
- [3] Ruoslahti, E. Specialization of Tumour Vasculature *Nature Rev.Cancer* 2, 83-902002

Atomic structures of two essential enzymes of the malaria parasite: new targets for drug design

Dirk Kostrewa, *Biomolecular Research, PSI*; Remo Perozzo, *Section of Pharmacy, University of Geneva*.

Malaria is one of the most dangerous diseases for humans with 40% of the world's population living at risk of being infected. Malaria occurs in tropical and sub-tropical regions and is caused by *Plasmodium* parasites which are transmitted to humans through mosquito bites. Resistance of mosquitos to insecticides and resistance of parasites to most of the existing antimalarial drugs, poses a severe problem in fighting malaria. We have determined the atomic structures of two essential metabolic enzymes of *Plasmodium falciparum* to provide a basis for the development of new antimalarial drugs.

Every year there are up to 500 million clinical cases of malaria with up to 3 million deaths. Most of these occur in Africa south of the Sahara, and mainly children under 5 years of age die.

Malaria is caused by *Plasmodium* parasites of which *Plasmodium falciparum* is the most dangerous one. These parasites are transmitted to humans through mosquito bites. Upon infection, the parasites enter the bloodstream, replicate in the liver for about 10 days before they return to the blood-

stream and invade red blood cells. They replicate until the blood cells burst and release even more parasites. Eventually, parasites are soaked up from the blood stream by another mosquito that will infect more people (Figure 1). The bursting of infected red blood cells occurs about every 48 hours causing the typical, periodically occurring malaria symptoms, that may return for several weeks. In extreme cases, death occurs within a few hours after the first symptoms.

Worldwide attempts to eradicate malaria have failed due to political and economic instability in the high-risk regions that is mostly a feature of very poor countries. Resistance of the mosquitos against insecticides and resistance of the parasites against almost all of the available antimalarial drugs further complicate this situation. There is a clear clinical need for new and potent antimalarial drugs.

Promising new antimalarial drug targets

In 2002, the complete genome of *Plasmodium falciparum* was determined. From its analysis, several important metabolic pathways of the malaria parasite were identified that could serve as potential targets for new antimalarial drugs. One of these metabolic pathways is the fatty acid biosynthesis whose proper function is essential for the parasite. Long fatty acids are major building blocks of the envelope of every living cell, and they are used for efficient energy storage. If the synthesis of fatty acids is blocked, the organism dies. Some very potent antibiotics block the fatty acid biosynthesis of bacteria. The genome analysis of *P. falciparum* revealed that its fatty acid biosynthesis is very similar to the one in bacteria and might thus provide promising targets for new antimalarial drugs.

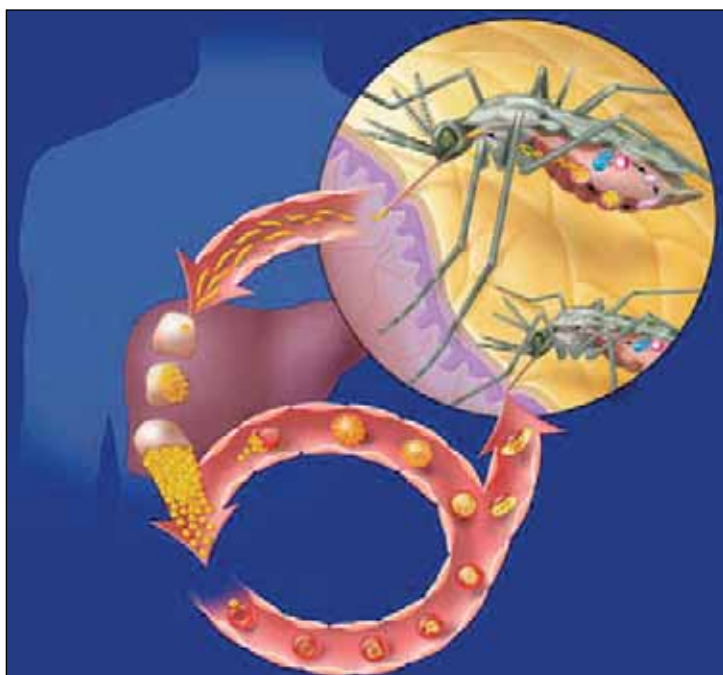


Figure 1: Life cycle of the malaria parasite. After injection through a mosquito bite, the parasite replicates first within the liver. Then it invades red blood cells and replicates there until the cells burst every 48 hours. Eventually, the parasite is taken up again by another mosquito bite.

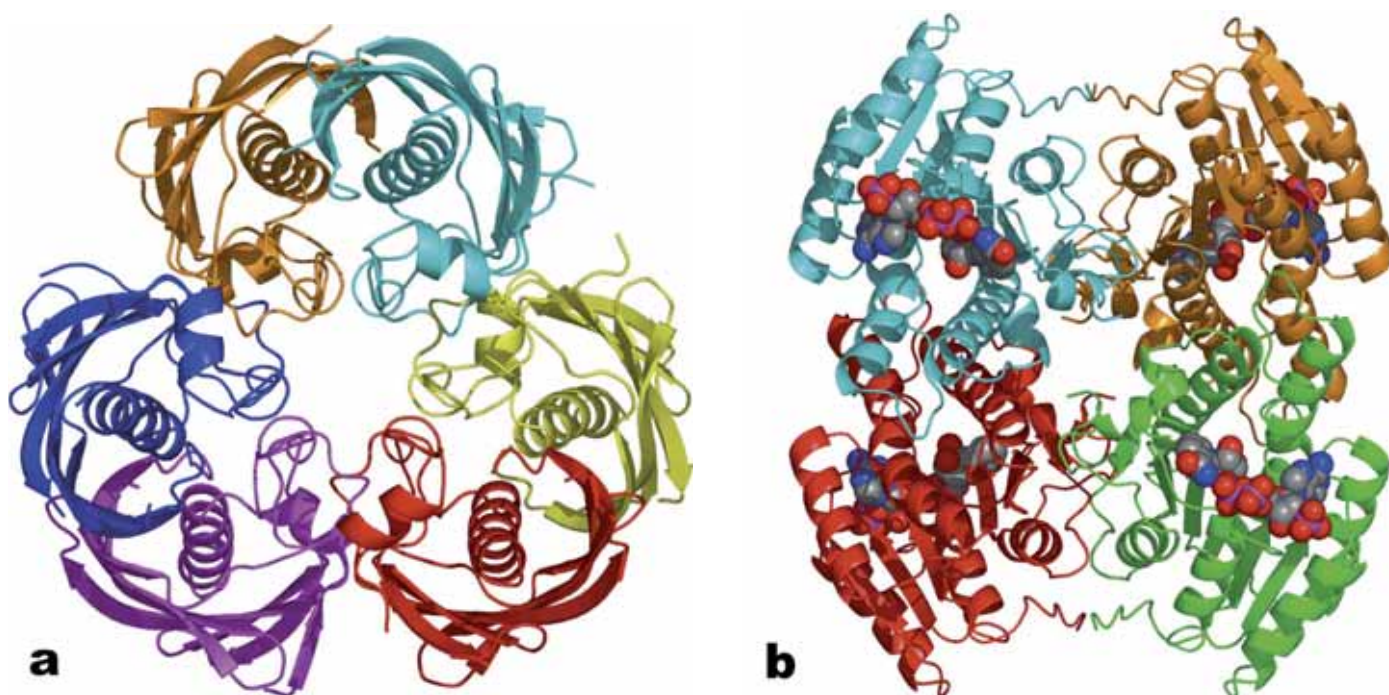


Figure 2: **Schematic illustrations of the atomic structures of two essential enzymes of the *Plasmodium falciparum* fatty acid biosynthesis. Alpha-helices are depicted as coils, beta-sheets are depicted as arrows (a) FabZ; shown are three dimers in orange/cyan, yellow/red and blue/magenta (b) FabG; shown is a tetramer in cyan/orange/green/red together with the four bound necessary cofactors (NADPH) as coloured spheres.**

Atomic structures of two essential enzymes of the malaria parasite

Fatty acid biosynthesis in *Plasmodium falciparum* is mainly done by five different enzymes. Exact knowledge of the atomic structures of these enzymes would help to find or design small chemical compounds that specifically bind to these enzymes and block their function. These chemical compounds would then serve as starting point “leads” for the development of new antimalarial drugs. In order to determine their atomic structures, we have overproduced and purified milligram amounts of two different enzymes of the *P. falciparum* fatty acid biosynthesis pathway using molecular biology techniques. We have then established specific conditions under which both enzymes form crystals. These crystals were then measured at the protein beamlines at the SLS to collect the best possible data sets. Using these data sets, we have determined the atomic structures of two essential enzymes of the *P. falciparum* fatty acid biosynthesis, named FabZ and FabG (Figure 2). The atomic structures give us a detailed view of the active sites, and more importantly, they provide us with a structural basis to help our ongoing search for new antimalarial drug candidates.

References

- [1] <http://www.who.int/malaria/>
- [2] M. J. Gardner et al., Nature, 419, 498–511 (2002)
- [3] D. Kostrewa, F. K. Winkler, G. Folkers, L. Scapozza, & R. Perozzo, Protein Science, 14, 1570–1580 (2005)

Structural genomics at the Swiss Light Source

Ehmke Pohl, Takashi Tomizaki, Santina Russo, *Research Department Synchrotron Radiation and Nanotechnology, PSI*; Judit Debreczeni, Frank von Delft, *Structural Genomics Consortium, University of Oxford, United Kingdom*

In April 2005 the SLS started an exciting collaboration with the Structural Genomics Consortium (SGC), Oxford University. The SGC is a non-profit organization funded by an international consortium of industry and public agencies, the largest being the Wellcome Trust. The aims of the consortium are to determine the 3D structures of human proteins with high medical significance. During the last year more than 50 structures were solved with data collected at the SLS. In addition, the collaboration includes methodical improvements around radiation damage, μ -crystal data collection and phasing.

Structural genomics

Today genomes of many species including eukaryotes and in particular humans have been completely sequenced. The next challenge lies in deciphering the function of the proteins that are encoded by the many genes identified. While a protein sequence alone may provide important clues about its function the detailed atomic structure, preferably in complex with ligands, co-factors and other interaction partners, can better illuminate a protein's function and its role in health and disease. The term *structural genomics* describes the large-scale effort of determining three-dimensional structures of biological macromolecules and their complexes by X-ray crystallography and NMR. The first generation structural genomics initiatives, launched in 1998–2000, concentrated mainly on the development of high-throughput methods and already resulted in an amazing increase in the number of crystal structures solved [1]. However, in spite of some spectacular successes and great advances in methods and technology, the overall success rate stayed below early, optimistic expectations [2].

One important goal of second-generation structural genomics initiatives, in particular the SGC, is to improve the per-target success rate to 20–30%. The SGC strategy is to focus efforts on the production of pure, soluble protein, while leveraging what material is produced to its maximum potential. In particular, this relies on the state-of-the-art beamline facilities of the SLS, which not only enable rapid experiments, but also the collection of high quality data from weakly diffracting or small crystals, or from samples that suffer radiation damage. Of the more than 80 crystal structures solved by the SGC, more than 70% required data collected at the Swiss Light Source and the majority of these represent novel structures. It is

important to note that all results of the SGC are immediately placed in a public domain without restrictions (<http://www.sgc.ox.ac.uk>).

Research of the SLS and the SGC

Because all of the SGC-UK targets are human proteins including a significant number of membrane proteins, a large proportion of crystals are expected to represent challenging crystallographic problems, an expectation that has been borne out in the first year. Therefore, members of the macromolecular crystallography group of the SLS and SGC scientists have joined forces to improve existing methods and develop new approaches to tackle particular problems. Current areas of research include experimental methods to monitor radiation damage in real-time during the diffraction experiment as well as the solution of the crystallographic phase problem in cases where only sub-optimal data are available. These difficult cases include data from small crystals, weak diffraction data and data collected from twinned or split crystals.

The crystal structure of the suppressor of cytokine signalling-2 (SOCS2) protein

One of the medically highly important structures determined in 2005 is the SOCS2 protein complex described below. This human protein regulates the growth hormone (GH) signal by recruiting the ubiquitinating E3 ligase to the receptor to flag it for internalization and degradation. SOCS2 is therefore of particular interest as a target for therapeutic alternatives to

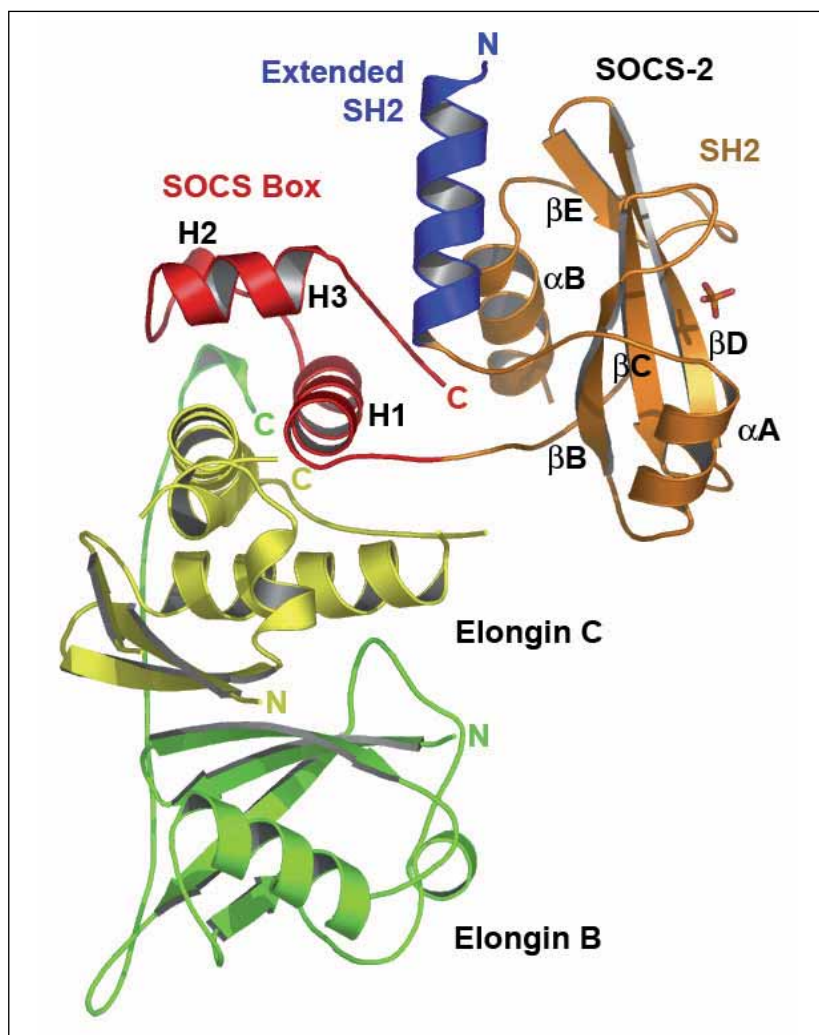


Figure 1: Ribbon diagram of the Suppressor of Cytokine Signalling (SOCS2) Protein in complex with Elongin C (yellow) and B (green).

growth hormone injections. Furthermore, GH and SOCS2 have been recently shown to regulate neural development, neural stem cell differentiation and neuronal growth - functions that might have important therapeutic implications for both repairing nervous system injuries and treating neurological disease.

The protein binds to growth hormone receptor with a well-known adaptor domain designated SH2 (spectrin homology 2) domain. The second domain called SOCS-box was thought (from homology models) to complex with other proteins (Elongins C and B and CULLIN), which in turn recruit the E₃ ligase. We have been able to confirm the latter binding model by unravelling the ternary complex of SOCS2 and Elongins C and B at 1.9 Å resolution. The structure, shown above as a ribbon diagram, was solved by molecular replacement using data collected at beamline X10SA [4]. Unexpectedly, the ESS helix (N-terminal to SH2), thought to bind directly to GHR, is instead seen to pack between the SH2 and SOCS-box domains, indicating that the ESS mutations known to interfere with GHR regulation do so by disrupting the intra-molecular SOCS2 packing. This crystal structure can now be used for the design of novel inhibitors and potential drugs.

Acknowledgements

We would like to thank all members of the SLS MX-group and the SGC protein crystallography group for their excellent work and great support.

References

- [1] Burley, S.K. An overview of structural genomics (2000). *Nat. Struct. Biol.* 7:932-934.
- [2] Service R.F. Tapping DNA for structures produces a trickle (2002) *Science* 298:948-950.
- [3] Abott, A. Protein structures hint at the things to come (2005) *Nature* 435:547.
- [4] Bullock AN, Debreczeni JE, Sundstrom M, Knapp S. "The Structure of the SOCS2-ElonginC-ElonginB Complex Defines a Prototypical SOCS-Box Ubiquitin Ligase", in preparation.

Atomic structure of Ultralente insulin

Armin Wagner*, Joachim Diez, Clemens Schulze-Briese, *Research Department Synchrotron Radiation and Nanotechnology, PSI*; Gerd Schluckebier, *Novo Nordisk A/S, 2880 Bagsvaerd, Denmark*;
*New address: *Diamond Light Source, Chilton, OX11 0DE, UK*

Ultralente insulin has been one of the most important long-acting pharmaceuticals in diabetes treatment since its introduction in 1953. The drug consists of a Zn containing suspension of rhombohedra shaped human insulin microcrystals which have to be injected subcutaneously by the diabetic. The long acting effect of Ultralente insulin is due to the slow dissolving of these microcrystals releasing a constant amount of insulin over and up to a twenty-four hour period.

Many attempts to characterize the structure have been undertaken during the last fifty years. Cell constants could be determined by powder diffraction and the hexameric arrangement of insulin dimers could be investigated by AFM. However, due to the small size of the crystals ($25 \times 25 \times 5 \mu\text{m}^3$) the X-ray crystal structure has so far been elusive. Using the microfocus setup at beamline Xo6SA of the SLS we were able to solve the atomic structure of Ultralente for the first time.

Ultralente production

The industrial production process of Ultralente can be separated into two steps. First, intermediate rhombohedral microcrystals are grown at high Cl^- concentrations (2 M). These crystals already show the morphology and size of the final Ultralente product. After crystal growth, the composition of the mother liquor is changed by dilution from high to very low Cl^- concentrations and the pH is changed from 5.5 to 7.4 without a change of crystal morphology during dilution. For conservation, methylparabene is added to the solution. The Ultralente microcrystals used in this study were directly taken from the final product, whereas the intermediate microcrystals had to be reproduced on a smaller scale because the production of Ultralente was recently discontinued.

Crystal handling

The standard crystal mounting technique using cryo-loops turned out not to be suitable for the insulin microcrystals. Especially in the case of the smaller “intermediate” crystals it was impossible to mount individual microcrystals from the crystal suspension. Thick drops of mother liquor in the loops made it very difficult to visualize and centre the crystals. Instead MicroMounts and MicroMeshes [1] were used throughout all experiments. Because of the relative hydrophobic

polyimide foil, the thickness of the solvent film could be significantly reduced leading to very low background scattering and to better visibility of the microcrystals. These supports allowed mounting and separation of several crystals from the suspensions at a time. Additionally, in the case of the micro-meshes a better separation of the single crystals could be achieved (Fig. 1).

Due to radiation damage it was not possible to collect complete data from one “intermediate” crystal, so that data from three crystals from the same preparation had to be merged. For Ultralente complete data could be obtained from one crystal.

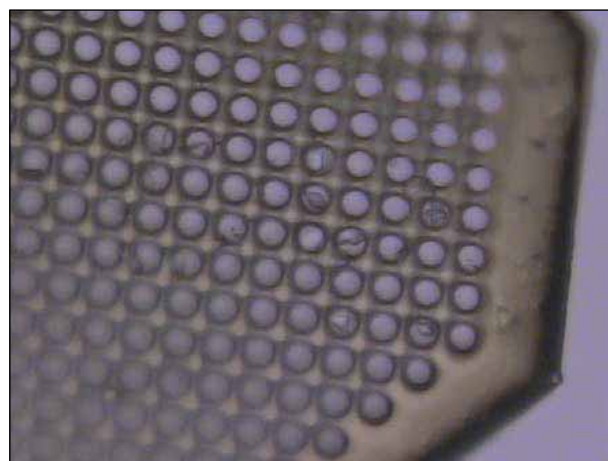


Figure 1: **Micromesh with “Intermediate” microcrystals (10 μm grid size).**

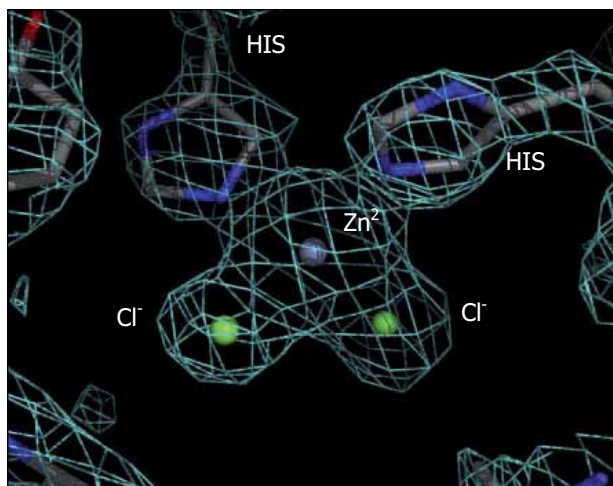


Figure 2: Off-axis Zn binding site in 4-Zn Insulin (2Fo-Fc, 2 σ).

Structure of 4-Zn insulin (intermediate)

The crystals were produced using the route taken in the industrial process, but scaled down to a standard laboratory scale. They turned out to be smaller, only around $8 \times 8 \times 3 \mu\text{m}^3$, compared to $25 \times 25 \times 5 \mu\text{m}^3$ in the industrial process. The dataset used for refinement was measured at a wavelength of 0.9183 \AA and processed with XDS. Data from three crystals up to 2.2 \AA resolution had to be merged with a R_{merge} of 8.7%, an average I/σ of 13.56, 100% completeness and a total redundancy of 4.45 (19943 total and 4483 unique reflections). The unit cell of $a=b=79.82 \text{ \AA}$ and $c=36.71 \text{ \AA}$ ($R3$) and the overall insulin conformation corresponds to $T_3R_3^f$ insulin, with the first 8 N-terminal amino acids of the B chain in extended conformation and the amino acids D1-D3 in extended and B4-B8 in helical conformation. However, this crystal structure differs from all other previous structures in that the off-axis Zn binding site is fully occupied and there is no evidence of occupation of the second on-axis binding site in this structure (Fig. 2). This leads to 4 Zn^{2+} ions per insulin dimer which was described already by Schlichtkrull in 1958 [2] but has never been observed in a crystal structure before.

2-Zn insulin (Ultralente)

Crystals were obtained directly from the production process at NovoNordisk. The dataset used for refinement was measured at a wavelength of 0.9786 \AA and processed with XDS. The data were useful up to 2.2 \AA resolution, with an R_{merge} of 6.9%, an average I/σ of 12.11, 99.6% completeness and a total redundancy of 3.18 (13240 total and 4161 unique reflections). The spacegroup was $R3$ with unit cell parameters $a=b=81.03 \text{ \AA}$ and $c=33.90 \text{ \AA}$.

The unit cell parameters correspond to known T6 insulin structures. However, the analysis revealed that in both B chains of the dimer the 8 N-terminal amino acids are disordered and could not be located in the electron density. Zn^{2+} cations occupy the two on-axis sites (3-fold axis) and are both tetrahedrally coordinated by the three N-atoms from His B10 and His D10, respectively, and one water molecule. Additionally one methylparabene molecule per dimer could be located in a hydrophobic binding site close to Tyr A14 (Fig. 3).

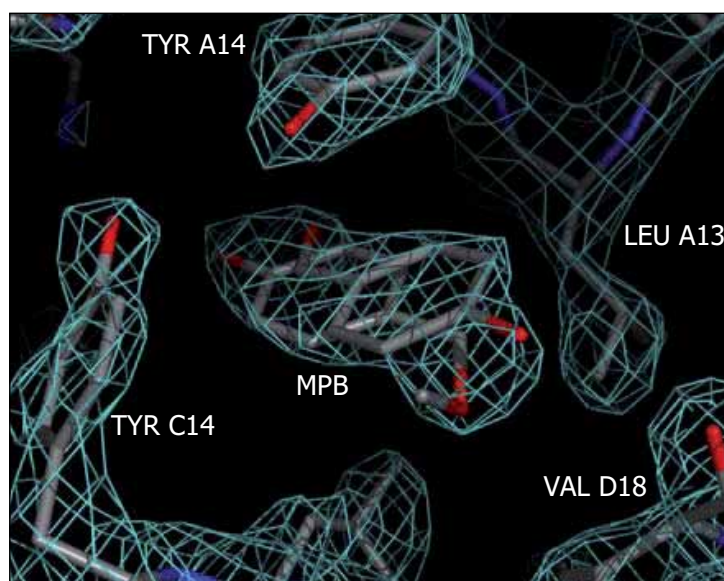


Figure 3: Methylparabene in Ultralente (2 alternative configurations, 2Fo-Fc, 2 σ).

Discussion

After more than fifty years of pharmaceutical use it has now been possible to determine the X-ray structure of Ultralente insulin microcrystals. The crystals undergo a phase transition during the industrial production process. High Cl^- concentrations within the initial crystallization conditions favour the $T_3R_3^f$ conformation with a fully occupied off-axis Zn^{2+} , tetrahedrally coordinated by two Cl^- and two N-atoms from His residues. This $T_3R_3^f$ conformation contains 4 Zn^{2+} cations as described in 1958 by Schlichtkrull [2], but has not been found in crystal structures until now.

References

- [1] www.mitegen.com
- [2] Schlichtkrull, J., *Insulin Crystals* (Munksgaard, Copenhagen, (1958)

How threonyl-tRNA synthetase regulates its own expression

Clemens Schulze-Briese, *Research Department Synchrotron Radiation and Nanotechnology, PSI*;
Lasse Jenner, Bernard Rees, Dino Moras, Gulnara Yusupova, Marat Yusupov, *IGBMC, Illkirch, France*;
Pascale Romby, Chantal Ehresmann, Bernard Ehresmann, Marat Yusupov, *IBMC, Strasbourg, France*;
Mathias Springer, *IBPC, Paris, France*

The bacterial ribosome was cocrystallized with initiator transfer RNA (tRNA) and a structured messenger RNA (mRNA) carrying a translational operator. The path of the mRNA was defined at 5.5 Å resolution. The ribosomal environment positions the operator stem-loop structure perpendicular to the surface of the ribosome on the platform of the 30S subunit. The positioning of mRNA regulatory domain relative to the ribosome elucidates the molecular mechanism by which the bound repressor switches off translation. Our data suggest a general way in which mRNA control elements must be placed on the ribosome to perform their regulatory task [1].

Translation relies on two selection processes: a) charging of tRNA by selection of the correct amino acid to be covalently bound to it, b) the selection of the tRNA as specified by the codon of the mRNA. Aminoacyl-tRNA synthetases catalyse the first of these steps using hydrolysis of ATP. In the present study the ribosome of *Thermus thermophilus* was cocrystallized with initiator tRNA^{fMet} and a structured mRNA fragment which codes for threonyl-tRNA synthetase. The thrS mRNA fragment consists of the translation operator domain flanked by two single stranded regions which constitute the ribosome-binding site.

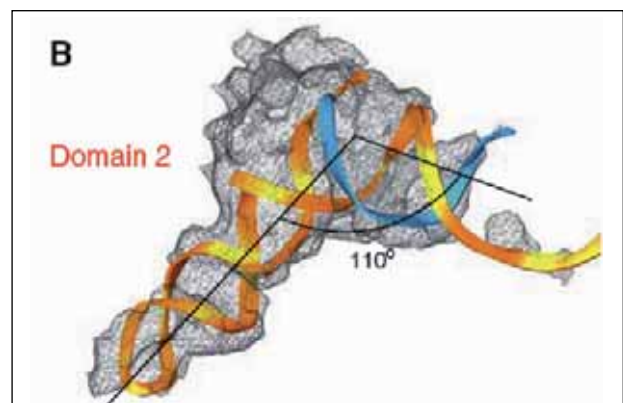


Figure 2: **Difference Fourier map of the SD and domain 2 helices at 5.5 Å resolution contoured at 3σ.**

The Shine-Dalgarno (SD) sequence, which is essential for the correct positioning of the mRNA with respect to the 16S-rRNA, is located adjacent to domain 2. In order to improve the binding, the complementarity between SD sequence and 16S rRNA was extended to 8 base pairs. Crystals containing functional ribosome in complex with initiator tRNA^{fMet} and either *thrS* mRNA, mk27 mRNA from the bacteriophage T4, or in the absence of mRNA were obtained under similar experimental conditions.

Highly complete and redundant data were collected from 300 to 5.5 Å at beamline X06SA. The collection of the low-resolution data was essential to obtain artefact free maps. Difference Fourier maps were calculated using phases derived from the *T. thermophilus* 70S model at 5.5 Å resolution completed by the high-resolution structures of the *T. thermophilus* 30S subunit and the *D. radiodurans* 50S subunit [2].

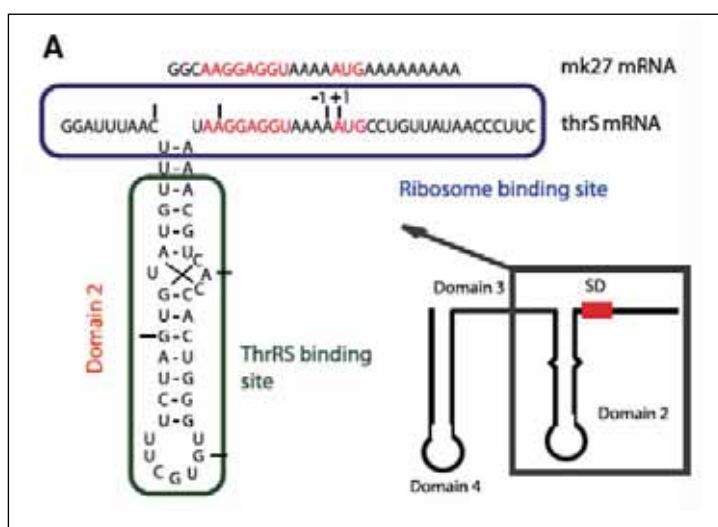


Figure 1: **mRNAs used in the experiment: The mk27 unstructured mRNA and the mRNA fragment encoding ThrRS, containing both the ribosome binding region and the stemloop responsible for binding ThrRS.**

The difference electron density corresponding to the regulatory domain 2 and the SD region has the form of a kinked helix. However, the electron density illustrated in Figure 2 shows a different conformation of the domain 2 stemloop structure when compared to the X-ray structure of the complex of domain 2 with ThrRS [3]. Domain 2 bound to the 70S ribosome adopts a conformation similar to the anticodon loop of a free tRNA. This result corroborates the proposal that the domain 2 stemloop binds ThrRS by an induced fit mechanism [3]. The SD helix forms an angle of 110° with respect to the stem of domain 2 (Fig. 2). The additional density on the opposite side may be assigned to the 15 N-terminal residues of protein S18, which are missing in the 30S high resolution structure due to disorder and therefore not included in the model. The constraints imposed by the SD helix and the ribosomal environment around the domain 2 stemloop place the regulatory domain on the platform of the 30S ribosomal subunit, protruding from the surface of the ribosome (Fig. 3)

Finally, the structure of the regulatory domain 2 bound to the 30S subunit reveals how the regulation of the translation of ThrRS works. Using the coordinates derived from the tRNA-ThrRS complex [4], it is not possible to dock the whole ThrRS enzyme on domain 2, when the latter is bound to the ribosome, because of a steric clash between the entire N-terminal domain and the 30S subunit (Fig. 4). Furthermore, it was reported in previous study, that the deletion of the N-terminal domain of ThrRS abolished translation control *in vivo*, although the truncated enzyme still efficiently binds to the thrS operator

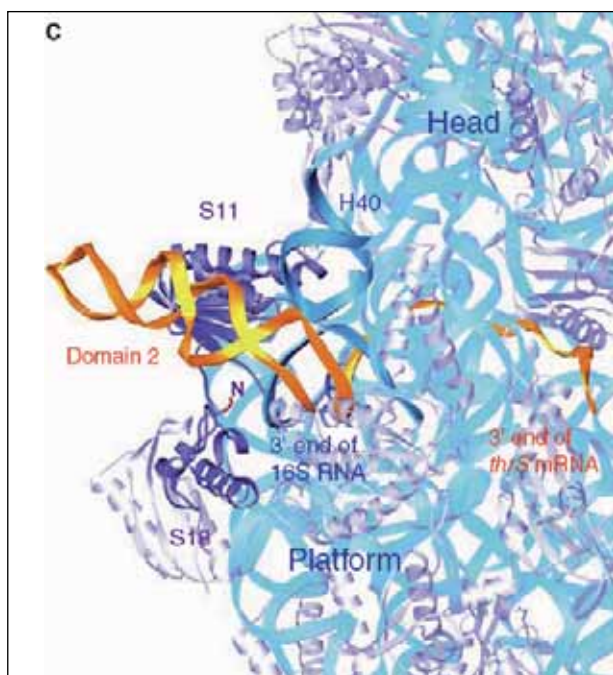


Figure 3: Solvent side view of 30S subunit. The 3' end of the 16S rRNA, forming base pairs with the SD helix and helix H40 are highlighted in cyan; proteins S11 and S18, in close contact with domain 2, are highlighted in blue.

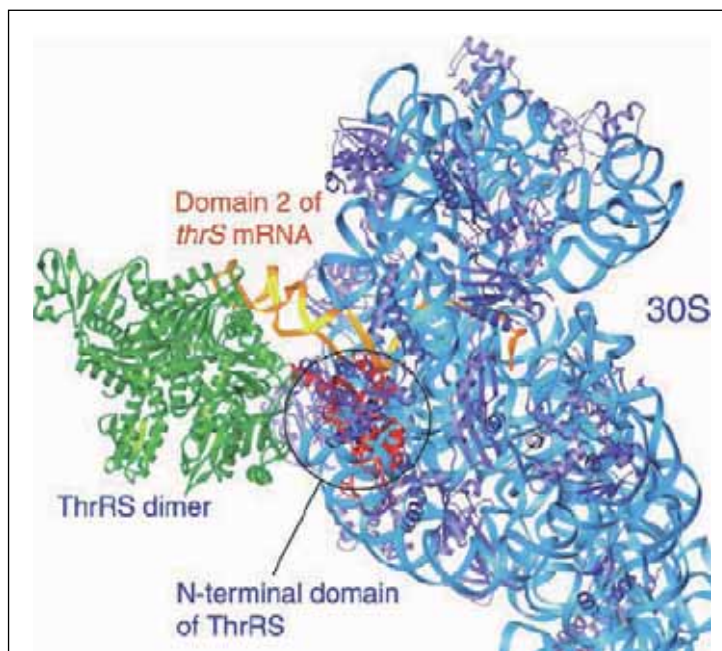


Figure 4: Superposition of ThrRS-*thrS* mRNA on the ribosome-*thrS* mRNA complex. The N-terminal domain of one of the ThrRS-monomers overlaps with the 30S subunit.

[5]. Therefore, the elongated structure of the enzyme and the positioning of the regulatory domain with respect to the 30S subunit form the basis for a competition mechanism. Such a mechanism does not impose stringent constraints on the protein structure, because the specificity of control can be readily switched from threonyl- to methionyl-tRNA synthetase. This type of regulatory mechanism is also kinetically controlled; that is, the repressor binds the mRNA faster than the 30S subunit binds to mRNA, and the non-translated mRNA is rapidly degraded, thus rendering the action of the repressor irreversible.

References

- [1] L. Jenner et al., *Science*, 308, 120-123, (2005)
- [2] Materials and methods of [1] as supporting material on Science Online
- [3] A. Torres-Larios et al., *Nat. Struct. Biol.*, 9, 343 (2002).
- [4] R. Sankaranayanan et al., *Cell*, 97, 371, (1999)
- [5] J. Caillet et al., *Mol. Microbiol.*, 47, 961, (2003)

Multiscale bioimaging using synchrotron light: vascular alterations in an animal model of Alzheimer's disease

Marco Stampanoni, Rafael Abela, *Research Department Synchrotron Radiation and Nanotechnology, PSI*; Stefan Heinzer, Ralph Müller, *Institute for Biomedical Engineering, University and ETH Zurich*; Eric P. Meyer, Alexandra Schuler, *Department of Neurobiology, Institute of Zoology, University of Zurich*; Thomas. Krucker, *Central Technologies, Novartis Institutes for BioMedical Research (NIBRI), USA*

Alzheimer's and other neurodegenerative diseases have been recently associated with alteration of blood flow in the brain. To evaluate this, vascular morphology and architecture in normal and pathological tissue from genetically manipulated animals modelling the disease were studied. A vascular corrosion cast (modified resin) was imaged with desktop and synchrotron-based microtomography. A hierarchical imaging approach allowed for non-destructive scanning and quantitative analysis of large vascular networks, and images were resolved of even the dense capillary networks of regions such as the cortex and the hippocampus.

Contrary to traditional hypotheses of Alzheimer's disease (AD) which focus exclusively on neuronal dysfunction, recent findings indicate that a vascular component contributes to the cognitive decline and neurodegeneration in AD [1]. In fact, reduced blood flow has been reported as a consistent physiological deficit in late stages of the disease [2]. However, it remains unclear whether this is a response to neuronal damage or a factor initiating the characteristic neuropathology [3]. The aim of our study is to develop imaging and evaluation tools that allow age-dependent alterations in the cerebral vasculature of a mouse model for AD to be determined. We use the APP23 transgenic (tg) mouse line that carries a human APP gene with the Swedish double mutation under the control of a neuron specific promoter. Initial characterization revealed that the tg mice develop age dependent formation of amyloid plaques, associated with inflammatory processes and neuronal degeneration, the typical hallmarks of the disease [4]. Vascular corrosion casts (VCCs) from tg and age-matched littermate controls of different ages were produced and analyzed using scanning electron microscopy [5]. Such analysis provides an insight into the architectural and morphological changes of the brain vasculature at submicron resolution, however, it is limited to a qualitative description of structures at the surface of the brain. Therefore a hierarchical imaging framework based on VCC and multiscale computed microtomography was developed to directly assess the three-dimensional (3D) architecture of the microvasculature. The method allows 3D visualization of the entire mouse brain vasculature at medium resolution (conventional μ CT at 16 μ m), suitable for selection of regions of interest (ROIs) in the frontal cortex and the hip-

pocampus. The ROIs are re-scanned non-destructively with a resolution of 1.4 μ m using local synchrotron microtomography (SR μ CT), visualizing the smallest vascular features such as arterioles, venules and capillaries. Being able to resolve the microvasculature is an relevant achievement, because pathological angiogenesis may be an important aspect of the disease [6] and would primarily be apparent at the level of the smallest blood vessels, the capillaries. Compared to other methods that resolve capillaries such as conventional histology and confocal laser scanning microscopy, local SR μ CT is unique because it can acquire larger volumes of vasculature located at any spatial depth in the brain non-destructively. To assess vascular alterations in the APP23 tg model, we focused on hippocampal and cortical regions, the brain areas primarily responsible for learning and memory. Plaques and tangles, both histological hallmarks of Alzheimer's disease, are most

Parameter	Unit	Value
global: all vessels		
vessel surface	[mm ²]	7.0
vessel volume density	[%]	3.4
vessel thickness	[μ m]	15.6 \pm 12.6
vessel spacing	[μ m]	89.3 \pm 52.1
connectivity density	[1/mm ³]	2729
local: capillaries only		
length	[μ m]	35.2 \pm 29.5
diameter	[μ m]	6.1 \pm 1.1

Table 1: **Morphometry from the sample shown in Figure 1b.**

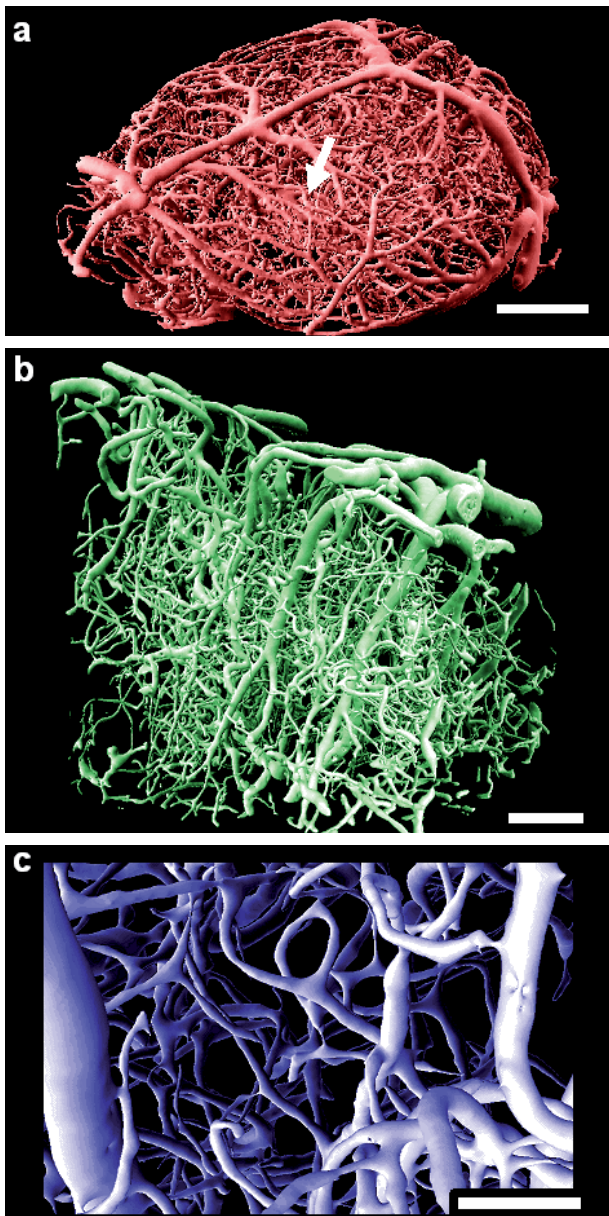


Figure 1: **Imaging of a selected area in a vascular cast from a mouse brain: (a) brain overview from μ CT, scale bar: 2 mm; (b) Area of interest indicated in (a) by an arrow acquired with SR μ CT, scale bar: 100 μ m; (c) detail from (b) showing the smallest vascular structures resolved at 1.4 μ m, scale bar: 50 μ m.**

commonly found in these two regions. Figure 1 shows the hierarchical imaging of a selected ROI: from the overview scan (μ CT at 16 μ m) a ROI can be selected and investigated with local SR μ CT at 1.4 μ m resolution.

Image data can be quantified using classical and advanced 3D morphometry. The analysis of the sample displayed in Figure 1b is summarized in Table 1 and is in good agreement with the literature but with the advantage of a fully automated analysis procedure.

To evaluate the vascular density within the frontal cortex of young animals (<9 months) the inter-vessel distance in selected ROIs of five tg and three control mice was determined

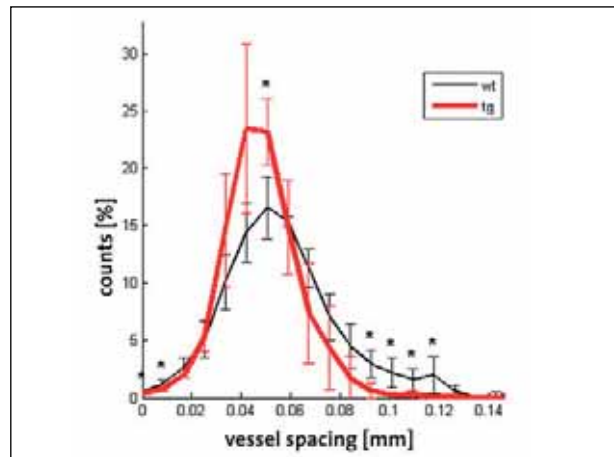


Figure 2: **Vessel spacing histogram of young wild type (wt) control and tg animals. Compared to age-matched wt mice, young APP23 tg mice exhibited an increased relative amount of shorter inter-vessel distances in the range of 40–60 μ m and a decreased relative amount of larger (80–120 μ m) inter-vessel distances in the cortical area.**

(see Fig. 2). It is namely at the age of about six months that these mice start developing amyloid pathology, followed later by vascular amyloid deposits [7].

Results

Our results indicate a significantly larger vessel density in young tg mice which are in accordance with our earlier findings of increased vessel connectivity in these animals. We hypothesize that amyloid over expression leads to additional angiogenic processes compensating for low perfusion in highly metabolic areas of the brain.

This new technology now allows detailed, hierarchical visualization of large vascular networks with unprecedented resolution and size using novel and more sophisticated quantification methods. This could open unique avenues on how to assess the vascular architecture in small animals modelling disease, with impact on drug discovery and therapy monitoring.

References

- [1] B. V. Zlokovic, *Trends in Neurosciences*, vol. 28, pp. 202-208, 2005.
- [2] J. C. de la Torre, *Stroke*, vol. 33, pp. 1152-1162, 2002.
- [3] C. Iadecola, *Nature Med.*, vol. 11, pp. 923-924, 2005.
- [4] C. Sturchler-Pierrat et al., *PNAS of the United States of America*, vol. 94, pp. 13287-13292, 1997.
- [5] T. Krucker, et al *Neurological Research*, vol. 26, pp. 507-516, 2004.
- [6] P. Carmeliet, *Nature*, vol. 407, pp. 249-257, 2000.
- [7] C. Sturchler-Pierrat and M. Staufenbiel, *Molecular Basis of Dementia*, vol. 920, pp. 134-139, 2000.

Reduction of radiation damage with X-ray data collection at 15 K

Alke Meents, Armin Wagner*, Roman Schneider, Claude Pradervand, Ehmke Pohl, Clemens Schulze-Briese, *Research Departement Synchrotron Radiation and Nanotechnology, PSI; *New address: Diamond Light Source Ltd., Chilton, Didcot, OX11 0DE, United Kingdom*

X-ray data collection at cryogenic temperatures around 100 K is a method routinely used as it can reduce radiation damage by a factor of approximately 70 compared to room temperature measurements. Lower temperatures are supposed to further reduce radiation damage thereby allowing more data to be collected from one crystal. However, only a few studies have been undertaken so far, and none of these were systematic studies. In the present study this effect was investigated on a solid statistical basis by comparing the radiation damage of 52 crystals at 15 K and 90 K. The results indicate that data collections at 15K can reduce the detrimental effects of radiation damage in favourable cases by up to 40%.

Introduction

X-ray induced radiation damage to biological samples is one of the main limiting factors for successful structure solution. Especially the most challenging projects in structural biology like membrane proteins or large complexes suffer significantly from radiation damage and a method to reduce its effects would be highly desirable. Apart from many other methods, cryocooling to 15 K is supposed to reduce radiation damage. In the present study this question is addressed for the first time on a solid statistical basis.

Experimental

Pig insulin and horse spleen ferritin were chosen as model systems. Cubic insulin crystals exhibit a high solvent content of around 68% and should therefore be more sensitive to radiation damage than proteins with lower water content. Cubic holo-ferritin is known for its radiation sensitivity which is mainly due to its 1764 atom iron core with a high X-ray absorption cross section. Thus, the chance to find any positive effect of 15 K data collection should be more likely for those two systems. Additionally, the cubic symmetry of both systems facilitates data analysis.

Data collection was carried out at beamline X10SA at the Swiss Light Source (SLS) at an X-ray energy of 13.5 keV. The incident beam was defocused to a size of 200 x 200 μm to bathe the crystals in the beam. The photon flux was determined to be 1.8×10^{12} ph/s. From all insulin crystals 360 images with a

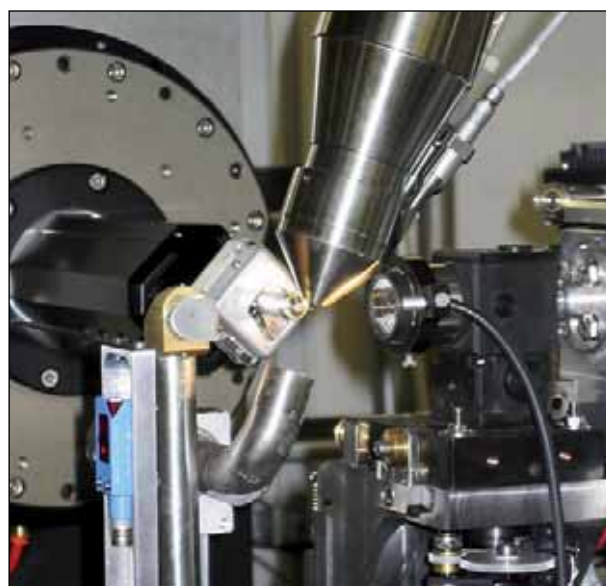


Figure 1: **Experimental setup for X-ray data collection at 15K using an open flow helium cryostat.**

rotation angle of 1° and from every ferritin crystal 270 images with a rotation angle of 0.5° per image were recorded. The exposure time was 1s per image for both proteins resulting in a total dose of approximately 2.7×10^7 Gy for the Insulin and 1.1×10^8 Gy for the ferritin crystals. The data collection temperature of 15 K was realized using an open flow helium cryostat system (Helijet) from Oxford Diffraction (Fig. 1). For the corresponding control experiments at 90K an open flow nitrogen cryostat from Oxford Instruments was used. Diffraction Datasets were collected from 26 Insulin crystals and 26 ferritin crystals at 15 K and 90 K, respectively.

The intensity data sets were subsequently processed in adjacent wedges of 30 images using XDS. This resulted in 12 independently processed datasets of 30° wedges for every insulin crystal and 9 datasets of 15° wedges for every ferritin crystal. Statistical parameters were determined in resolution shells of 0.1 Å.

Discussion

To monitor the radiation damage, three different parameters were chosen. The completeness of a dataset is the ratio of the number of observed reflections and theoretical possible number of reflections. Radiation damage causes a decay of the completeness with the absorbed dose. The R-merge value defines the agreement between symmetry related reflections and reflections measured more than once. Radiation damage should lead to an increase of R-merge values for higher wedge numbers. A crystal ideally consists of one well ordered domain. However, in reality a crystal is often composed of many small blocks, slightly misaligned with each other. This so called crystal “mosaicity” serves as another quality indicator. For analysis of the R-merge values and the completeness the corresponding values were taken from the highest resolution shell with an initial $I/\sigma(I)$ -ratio ≥ 6 . To be sensitive to X-ray induced radiation damage only and not any other factors, e.g. crystal size, all parameters were normalized to their corresponding initial values from the first wedge. The displayed data points in the following plots represent averages over the 13 crystals of a group.

Figures 2 and 3 show plots of the completeness and the R-merge values as a function of the exposure time. For both proteins a positive effect of cryocooling to 15 K compared to 90 K can be observed. The decrease of completeness is slower at 15 K. The same effect is found for the R-merge values,

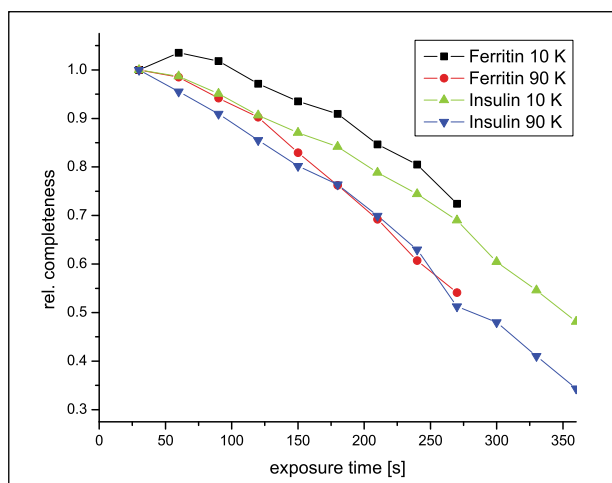


Figure 2: **Averaged relative completeness vs. exposure time for insulin and ferritin at 10 K and 90 K.**

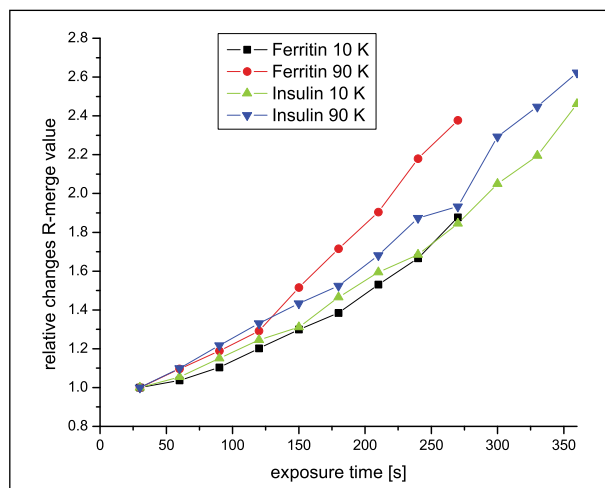


Figure 3: **Averaged relative R-merge values as function of the exposure time.**

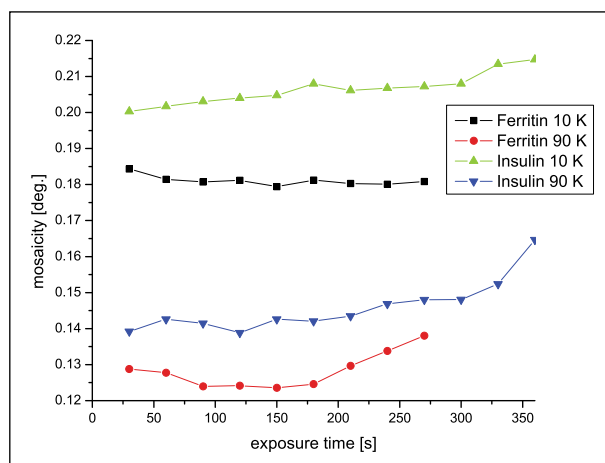


Figure 4: **Average crystal mosaicity as determined by XDS.**

where a steeper incline of the R-merge values indicates more severe radiation damage at 90 K.

Although the results are very promising, the mosaicity of the 15 K crystals was on average 0.055° higher than for the 90 K crystals (Fig. 4). An optimised cooling protocol for data collection at 15 K, therefore, needs to be developed.

This work, on a solid statistical basis, shows for the first time that data collections at 15 K can reduce radiation damage by up to 40%. Especially for challenging projects which often yield only very small or radiation sensitive crystals, this reduction of radiation damage should facilitate or even allow a successful structure determination.

References

- [1] Blake, C. C. F. & Phillips, D. C. (1962). International Atomic Energy Agency Symposium, Brno, Czechoslovakia, 2-6 July 1962, Vienna: IAEA, 183 (1962)
- [2] Hanson, B. L., Harp, J. M., Kirschbaum, K., Schall, C. A., DeWitt, K., Howard, A., Pinkerton, A. A., and Bunick, G. J., *J. Synchr. Rad.*, 9, 375 (2002)

Drug carrying nano-capsules characterised by small angle neutron scattering

Joachim Kohlbrecher, *Condensed Matter Research with Neutrons and Muons, PSI*; Andrea Rube, Gerd H. Hause, Karsten Mader, *Inst. f. Pharm. Technologie u. Biopharmazie, Germany*

The potential of nano-capsules in targeted and controlled delivery of drugs has received much interest in the past years. Their polymeric shell plays a predominant role in the protection of incorporated drugs as well as in the release profile. Small angle neutron scattering (SANS) at a contrast-matched interface with corresponding numeric simulation procedures yields a comprehensive model on the core-shell structure of nano-capsules that is demonstrated on poly[D,L-lactide] (PLA) nano-capsules. SANS has provided unique information about the PLA and Poloxamer shell thickness, which was previously not accessible by other techniques. The SANS method could be used to develop strategies for the optimization of the shell properties concerning controlled release and to study changes in the shell structure during degradation processes.

Nano-capsules, which fall as do nano-spheres, under the generic term nano-particles, are colloidal agent carriers consisting of biologically degradable plastics. Simplified they consist of oil droplets in which lipophilic pharmaceutical agents are solved (Fig. 1). This oil core is enclosed in a spherical polymer matrix. In the last ten years the study of these capsules in pharmacy, biology and medicine gained enormous significance due to many application possibilities, among other things for “drug targeting systems”. The interest in nano-capsules as agent carriers in medicine rose, because they allow a controlled release of the agent in the target tissue. The active agent included in the nano-capsules is transported by these capsules effectively to the target tissue where it is then released in a controlled manner. Therefore the use of nano-particles increases the therapeutic effectiveness of biologically active components as active agent carrier, while the side effects are reduced.

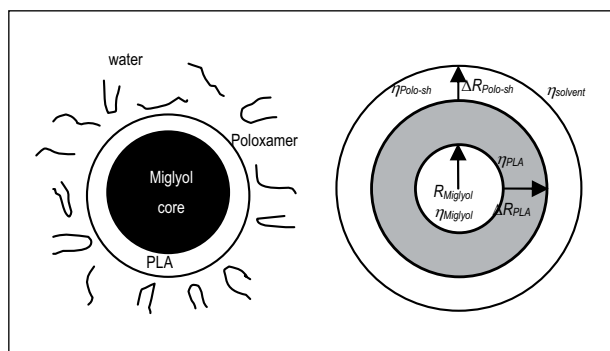


Figure 1: **Schematic representation of PLA nanocapsules (left) and a simplified nanocapsule model (right).**

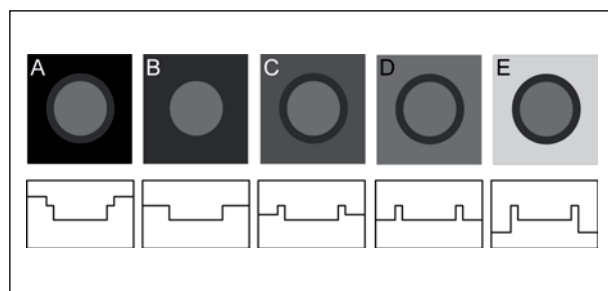


Figure 2: **A schematic sketch of a contrast variation experiment with different H₂O/D₂O mixtures on nanocapsules. The second row shows a schematic sketch of the scattering length density profile across the shell structure. By this method, one can highlight different parts of the capsules.**

Size of nano-capsules set by application

The size and the size distribution of the nano-capsules play a determining role, because depending upon the target organ the size of the nano-capsules must be selected accordingly. Several parameters need to be considered. Firstly, a narrow size distribution of the colloidal medicine form represents a factor which is crucial for the biological compatibility and for the desired effect of the preparation. Secondly, because of the large surface to volume ratio for nano-particles, interface effects play a dominant rule. The nano-capsules therefore exhibit new very interesting physical and chemical characteristics and offer a basis for new materials. As the characteristics of the nano-materials substantially depend on the particle characteristics, i.e. on their size, morphology, surface finish

etc., both the production processes and the characterization become very important.

Unfortunately the characterization of nano-capsule dispersions as drug carriers is not a trivial task for common analytical techniques. In the case of nano-capsules the polymeric shell plays a predominant role for the protection of incorporated drugs as well as for the release profile. Although the thickness of the Poloxamer wall is thought to be important, little is known about it.

Several groups estimated values of 10 nm using transmission electron microscopy (TEM), a technique that gives information about single particles and does not give statistically averaged values. TEM is therefore an inaccurate method for the determination of average shell thicknesses. On the other hand alternative methods, like small angle neutron scattering (SANS) or dynamic light scattering (DLS), which yield statistically averaged values, have to make assumptions about the particle shape in their analysis. Therefore it is beneficial to combine these two complementary methods. The aim of this study was to obtain a detailed picture of the inner structure of nano-capsules by SANS with additional information from DLS and TEM. As a model system poly(D,L-lactide) (PLA) nano-capsules were investigated.

The non-invasive SANS method at a contrast-matched interface was used to study the core-shell structure (Fig. 2). A SANS fitting program for the data analysis (Fig. 3) was developed based on the particle shape of nano-capsules gained from

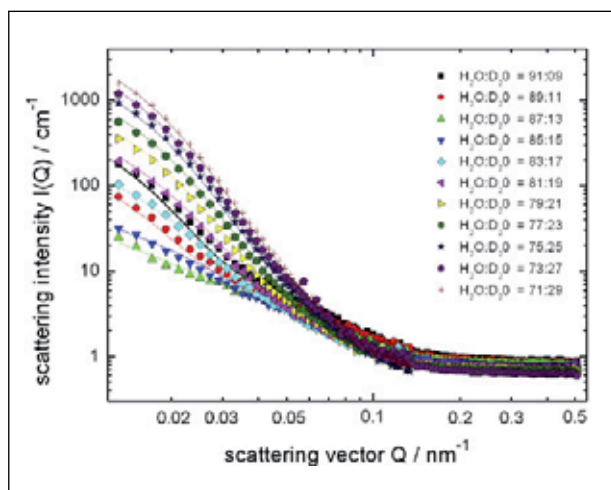


Figure 3: The results of the SANS experiment are shown together with the theoretical fit. In the contrast variation experiment the D₂O/H₂O was varied from 9/91 to 29/71. The scattering intensity is the lowest for a ratio of 13/87 as there, the volume times the contrast of the Miglyol core is about the same as for the PLA shell, but the contrast of the core and the shell have an opposite sign. The only free parameters of the fit were the thickness of the PLA shell and the parameters of the log normal size distribution of the Miglyol core. It was assumed that the shell thickness is constant and independent of the size of the core.

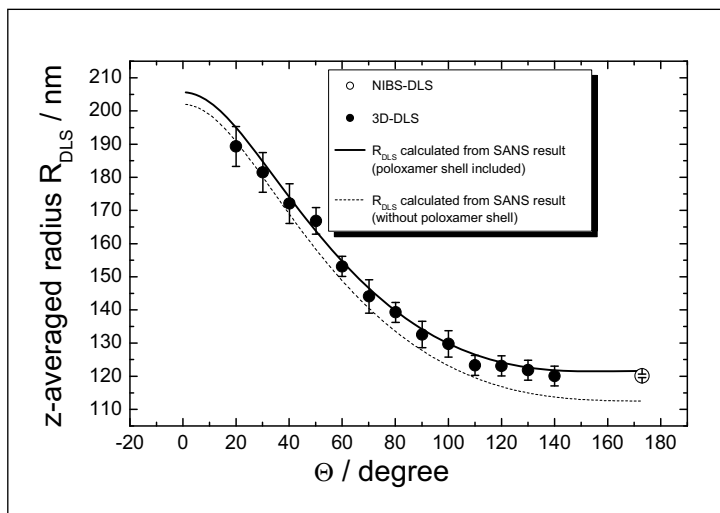


Figure 4: A comparison of the z-average radii obtained by DLS (3D-DLS + NIBS-DLS) and SANS measurements and the refined SANS fit model containing a second shell consisting of Poloxamer and solvent.

transmission electron microscopy. Information on the stabilizing Poloxamer shell were obtained by refining the SANS fit which was found to agree well with results from dynamic light scattering experiments (Fig.4).

The corresponding fit yielded a PLA shell thickness of 9.8 nm and an average miglyol core radius of 84 nm. The z-averages for the hydrodynamic diameter determined by DLS were systematically slightly higher than the values for the capsule diameter measured by SANS. When refining the model by introducing a second shell consisting of Poloxamer and solvent, SANS values and DLS values agreed well. The refined model provided a thickness of 17 nm for this additional shell and a Poloxamer content of 7%.

In summary, SANS has provided unique information about the PLA and Poloxamer shell thickness, which was not previously accessible using other techniques.

References

- [1] A. Rube, G. Hause, K. Mäder and J. Kohlbrecher, Journal of Controlled Release 107, 244-252 (2005).

Combination of radioimmunotherapy with growth inhibition for antibody-based therapy of metastases

Ilse Novak-Hofer, Jürgen Grünberg, Karin Knogler, Susan Cohrs, Kurt Zimmermann, Michael Honer, Simon Ametamey, P. August Schubiger, *Center for Radiopharmaceutical Science ETH-PSI-USZ, PSI*; Peter Altevogt, *German Cancer Research Center, Germany*

The objective of our work is to increase the efficacy of radioimmunotherapy for the treatment of metastases. We engineer antibodies with optimal pharmacokinetics, select effective radionuclides for tumour imaging and therapy and in this study, we combine growth inhibiting antibodies with Cu-67-radioimmunotherapy for ovarian carcinoma metastases.

The L1 cell adhesion molecule is involved in the control of growth and migration of several tumour types (neuroblastoma, renal carcinoma, melanoma). L1 is also overexpressed in ovarian carcinoma [1] and we found recently that our anti-L1 monoclonal antibody (mAb) chCE7 inhibits the growth of human ovarian carcinoma cells *in vitro* [2]. Figure 1 shows the effect of anti L1- mAbs chCE7 and 11A (a mAb binding to a different epitope of L1 than chCE7) on the growth of SKOV3ip human ovarian carcinoma cells. Proliferation is inhibited by about 50% and a control mAb HEA125, which binds to another cell surface protein (EpCAM), has no effect on tumour cell growth.

Positron Emission Tomography (PET)

In order to evaluate the ability of these mAbs to detect ovarian cancer metastases *in vivo*, we labelled the antibodies with

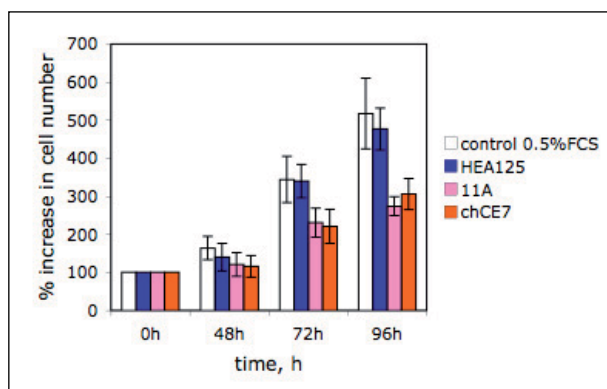


Figure 1: **Effect of anti-L1 mAbs chCE7 and 11A and anti-EpCAM mAb HEA125 on proliferation of SKOV3ip human ovarian carcinoma cells in culture.**

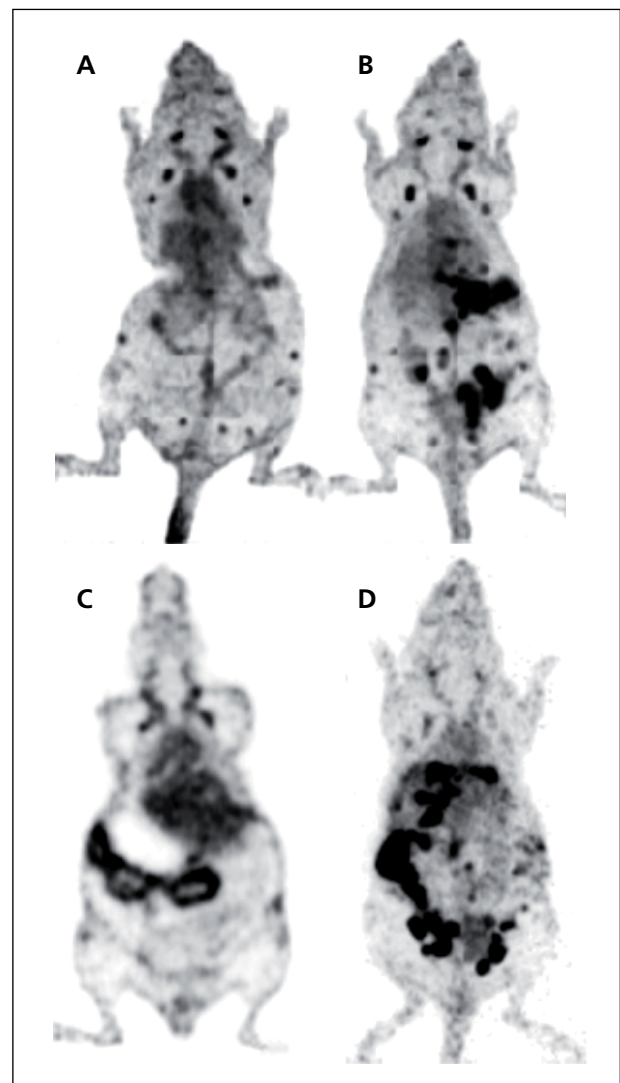


Figure 2: **Imaging of SKOV3ip metastases : PET images with ^{64}Cu -CPTA-mAb chCE7 (A,B) and mAb 11A (C) directed against L1 and mAb HEA125 (D) directed against EpCAM. A: control mouse without tumour.**

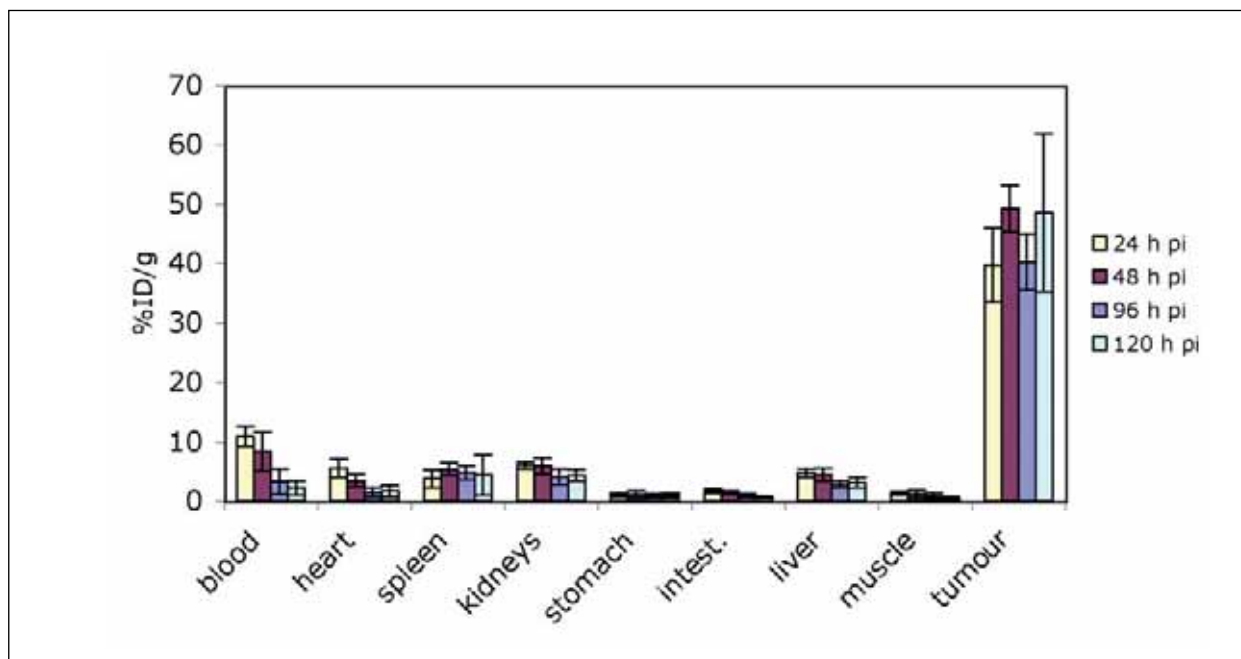


Figure 3: Tumour and tissue uptake of ⁶⁷Cu-CPTA-chCE7agl in nude mice with SKOV3ip metastases.

the PET nuclide ⁶⁴Cu using techniques we have developed over the years [3] and imaged mice with SKOV3ip metastases. Figure 2 shows a tumour-free mouse (A) and three different mice with metastases in the abdomen, imaged 22 h post injection of ⁶⁴Cu-labeled anti L1-mAbs chCE7 (B), 11A (C) and anti-EpCAM mAb HEA125 (D). The results show that the mAbs effectively target SKOV3ip tumour clusters *in vivo*.

In a subsequent experiment mAb 11A was found to reduce tumour growth *in vivo* in the SKOV3ip mouse model [2].

Combination therapy

These results prompted us to evaluate the efficacy of combining a single dose of radiolabelled mAb chCE7 with a biweekly treatment with unlabelled mAb 11A in prolonging the survival of nude mice with SKOV3ip metastases. We engineered an aglycosylated variant form of mAb chCE7 (chCE7agl) with more rapid clearance from the blood than the parent mAb chCE7 and produced it in high amounts in HEK293 cells [4]. The beta particle emitting nuclide ⁶⁷Cu, which we produce in house at the PSI accelerator, was chosen for radioimmunotherapy because of the favourable physical and biological properties of ⁶⁷Cu-immunoconjugates [5]. Figure 3 shows tumour uptake and distribution of ⁶⁷Cu-chCE7agl in normal tissues in nude mice with SKOV3ip metastases. The results indicate high (up to 45 %ID/g) and prolonged (up to 5 days) tumour uptake and low levels of the ⁶⁷Cu-immunoconjugate (below 2-4 %ID/g) in normal tissues such as blood, liver, or kidneys. Median survival of mice treated twice a week with 10 mg/kg of mAb 11A

was found to be less than 38 days. When the ⁶⁷Cu-chCE7agl conjugate was tested as a single low dose (5 MBq) it prolonged the median survival of SKOV3ip mice significantly from 29 days in untreated animals to 34 days. When ⁶⁷Cu-chCE7agl was combined with biweekly doses of 10mg/kg mAb 11 the median survival increased further to 49 days.

Our results provide proof of principle for combining radiolabelled and unlabelled anti-L1 antibodies for a more efficient treatment of ovarian cancer metastases.

References

- [1] M. Fogel et al., Lancet, 362, 869 (2003)
- [2] M.J.E. Arlt et al., Cancer Res., 66, 936 (2006)
- [3] K. Zimmermann et al., Nucl. Med. Biol., 30, 417 (2003)
- [4] J. Grünberg et al., Biotechniques, 34, 968 (2003)
- [5] I. Novak-Hofer, P.A. Schubiger, Eur. J. Nucl. Med. 29, 821 (2002)

Imaging studies of a ^{99m}Tc -folate-radiotracer for diagnosis and therapy of folate-receptor positive tumours

Cristina Müller, Alexander Hohn, P. August Schubiger, Roger Schibli, *Center for Radiopharmaceutical Science ETH-PSI-USZ, PSI; Department of Chemistry and Applied Biosciences of the ETH Zurich*

We report the pre-clinical evaluation of a new organometallic ^{99m}Tc -radiofolate. Combined SPECT/CT-studies showed the potential of this folate radiotracer to be used as imaging agent of FR-positive malignant tissue. Further experiments unveiled that pre-application of antifolates results in a significant reduction of the renal accumulation of the radiotracer, giving rise to an unprecedented improvement of the tumour-to-kidney ratio of accumulated radioactivity. These results potentially allow a therapeutic application of an isostructural radiotracer, when labelled with the β -radiation emitting ^{188}Re -radionuclide.

The folate receptor (FR) is a membrane-anchored protein, which is over expressed on a wide variety of cancer types but highly restricted in normal tissues.

Using folic acid as a “Trojan horse” for FR-specific tumour targeting has proved to be a promising strategy for selective delivery of folate-conjugated radionuclides into cancer cells [1].

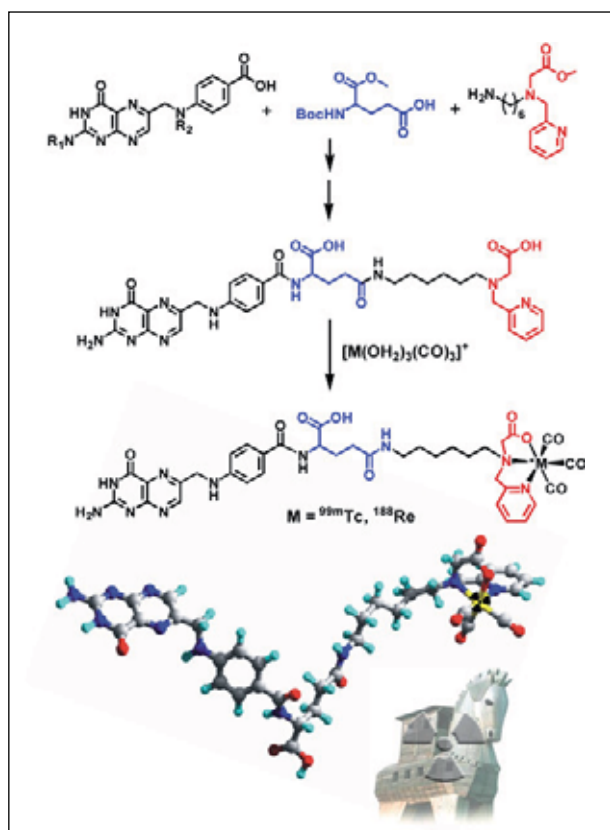


Figure 1: **Synthesis and radiolabelling of the folate conjugate with ^{99m}Tc - or ^{188}Re -tricarbonyl.**

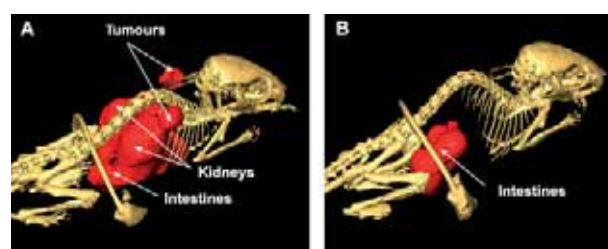


Figure 2: **SPECT/CT-images of an anesthetized mouse: (A) Tissue distribution of the ^{99m}Tc -folate radiotracer 24 h post injection; (B) Blocking study with excess folic acid co-injected.**

The aim of the present study was the development of folate-based organometallic radiopharmaceuticals, labelled with ^{99m}Tc (6 h half-life, 140 keV γ -radiation) or ^{188}Re (17 h half-life, 2.12 MeV β_{max} -radiation) for potential use in diagnostic and therapeutic nuclear medicine.

The tricarbonyl technique, developed in our laboratories, allows the preparation of isostructural Tc(I)- and Re(I)-complexes of high kinetic inertness and stability under physiological conditions [2-5].

SPECT/CT-studies

Recently, we reported the synthesis (Fig. 1) and *in vitro/in vivo* evaluation of a folate derivative, functionalized with the picolylamine monoacetic acid (PAMA)-chelating system for labelling with $[\text{M}(\text{CO})_3(\text{OH})_2]^+$ ($\text{M} = ^{99m}\text{Tc}, ^{188}\text{Re}$) [6, 7]. These experiments showed high specific accumulation of the radiotracer in FR-positive tissues (tumours and kidneys). *In vivo* studies were performed with an anesthetized mouse, 24 h post injection of the radiotracer using a dedicated small-ani-

mal SPECT/CT-camera. Figure 2 shows tomographic SPECT/CT-images: the folate radiotracer accumulated in both tumours positioned on the right and left shoulder.

A relatively high amount of radioactivity was found in the renal tissue as well as unspecifically distributed in the intestinal contents (Fig. 2A). Experiments with excess folic acid co-injected were performed with the same animal. An almost complete blockade of radiotracer accumulation in the tumours and the kidneys clearly confirmed FR-specific accumulation of the radiotracer in these tissues (Fig. 2B). These experiments unveiled the high specificity of our new folate-based ^{99m}Tc -radiotracer for visualization of FR-positive tumours. Renal uptake of radioactivity could be ascribed to substantial FR-expression in the kidneys. This issue was unfavorable, in particular with regard to a potential therapeutic application of the ^{188}Re -radiolabeled folate derivative since particle-emitting radiation could cause radiation injury of sensitive renal tissue. Therefore we aimed to develop a suitable method in order to increase the tumour uptake of the radiotracer or improve the tumour-to-kidney ratios.

Combined application with antifolates

Antifolates such as methotrexate or pemetrexed (PMX, Alimta[®]) are chemotherapeutics frequently used in the treatment of diverse cancers.

We hypothesized that a short treatment of cancer cells with an antifolate could positively influence the tumour uptake of the radiotracer as a consequence of cellular folate-deficiency. This hypothesis could be confirmed *in vitro*, when we found an increased accumulation of the radiotracer after incubation of the cancer cells with antifolates. Different results were observed *in vivo*. The tumour uptake of the radiotracer was

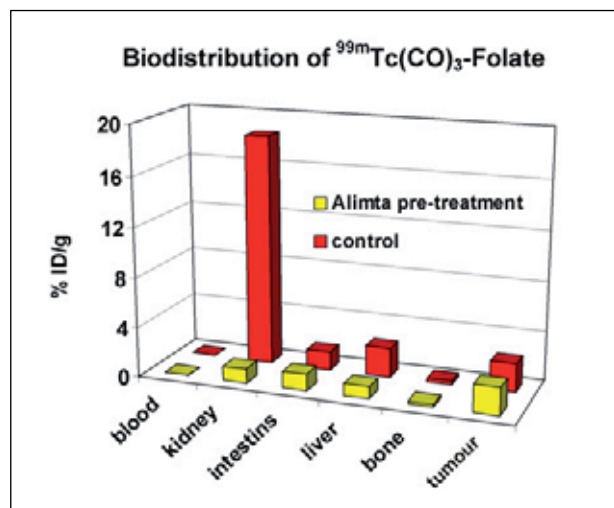


Figure 3: Biodistribution 4h post injection of the ^{99m}Tc -folate radiotracer in combination with Alimta[®].

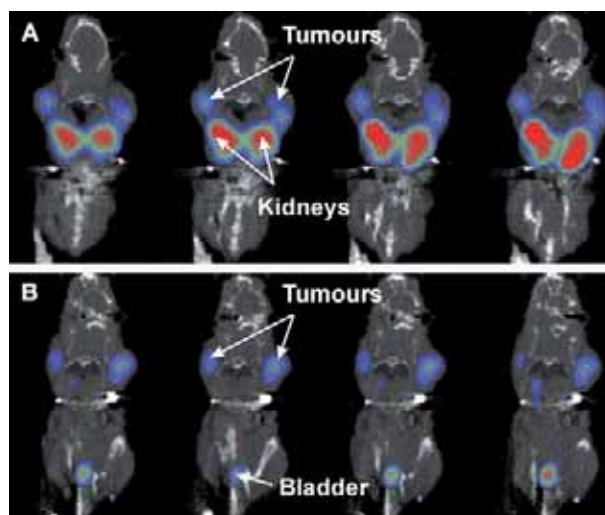


Figure 4: SPECT/CT-images: coronal sections of (A) a control mouse and (B) a mouse pre-injected with Alimta[®].

not increased, if mice were treated with antifolates for three days previous to the radiotracer administration. However, if antifolates were intravenously injected one hour before radioactivity, we observed a significant reduction of accumulated radioactivity in the kidneys, whereas the tumour uptake remained almost unaffected (Fig. 3).

This pre-treatment resulted in unprecedented tumour-to-kidney ratios of radioactivity, 10-fold increased compared to untreated animals. The *ex vivo* data could be confirmed via SPECT/CT-studies with an anesthetized mouse, pre-injected with Alimta[®] (Fig. 4). In contrast to control experiments (4A), the radiotracer accumulated selectively in the tumour tissue whereas kidneys were almost completely free of radioactivity (4B).

Hence, a therapeutic application of an isostructural radiofolate, labelled with high doses of the β -emitting ^{188}Re -radionuclide could for the first time become possible.

References

- [1] Ke CY, Mathias CJ, Green MA; Adv Drug Deliv Review 2004; 56:1143.
- [2] Alberto R, Schibli R, Waibel R, Abram U, Schubiger AP; Coord Chem Rev 1999; 192: 901.
- [3] Aebischer N, Schibli R, Alberto R, Merbach AE; Angew Chem-Int Edit 2000; 39; 254
- [4] Alberto R, Ortner K, Wheatley N, Schibli R, Schubiger AP; J Am Chem Soc 2001; 123; 3135.
- [5] Schibli R, Schubiger PA; Eur J Nucl Med Mol Imaging 2002; 29: 1529
- [6] Müller C, Dumas C, Hoffmann U, Schubiger AP, Schibli R; J Organomet Chem 2004; 689: 4712.
- [7] Müller C, Hohn A, Schubiger AP, Schibli R; Eur J Nucl Med Mol Imaging; manuscript submitted

New radiolabelled derivatives of vitamin B12 show preferential targeting of tumours

Robert Waibel, Dave van Staveren, Christine De Pasquale, Alexander Hohn, P. August Schubiger, Roger Schibli, *Center for Radiopharmaceutical Science ETH-PSI-USZ, PSI*; Stefan Mundwiler, Roger Alberto, *Institute of Inorganic Chemistry, University Zurich*; Hans-Jörg Treichler, Martin Kuenzi, Jakob Nüesch, *Solidago AG*

Rapidly growing cells show an increased demand for nutrients and vitamins. The objective of our work is to use the supply route of vitamin B12 to visualize hyperproliferative cells with radiolabelled derivatives. To date, radiolabelled (^{57}Co , ^{111}In) vitamin B12 derivatives showed labelling of tumour tissue, but also strong accumulation of radioactivity in normal tissue. By abolishing the interaction of vitamin B12 to its transport protein TCII and therefore interrupting megalin mediated uptake in normal tissue, preferential accumulation of the radiolabelled vitamin in cancer tissue could be accomplished.

All living cells require vitamins for survival. Cells undergoing rapid proliferation have been shown to have increased uptake of thymidine and methionine. Since vitamin B12 is an essential enzyme cofactor and is directly involved with methionine synthesis and indirectly involved in the synthesis of thymidylate and DNA, it is not surprising that vitamin B12 has been shown to have an increased uptake in rapidly dividing tissue. Studies dating back almost 40 years demonstrated high accumulation of ^{57}Co -vitamin B12 (cobalamin (Cbl)) in transplanted tumours in mice using whole-body autoradiography. However, high accumulation of radioactivity in the liver, pancreas and especially the kidneys was also observed. The authors state that “one practical consequence of this may be the possibility of using labelled vitamin B12 to locate tumours clinically” [1]. Unfortunately, the long half-life of 272 days of

^{57}Co limits the maximal dose in human investigations to 37 kBq (1 μCi) per study and therefore ^{57}Co -Cbl was useless for targeting studies. It is only recently that clinically useful, short lived radiolabelled Cbl derivatives have emerged. Occult tumours in humans could be visualized via ^{111}In - and $^{99\text{m}}\text{Tc}$ - radiolabelled diethylene-triaminepentaacetate Cbl analogs (DTPA-Cbl) [2]. However, tissue distribution showed unfavourably high renal accumulation (see Fig. 1). Because kidney tissue is easily damaged by high radioactivity we attempted to improve tumour to normal tissue levels of radiolabelled Cbl with different analogs (derivatization at the ribose part, the phosphor part or using a more stable chelating system) [3] but failed initially, due to the intrinsic properties of the vitamin to be stored in these organs.

Homeostasis of cobalamin

Mammals must acquire Cbl from food where it is present in extremely minute quantities. Its re-absorption is entirely based on the binding of Cbl with different soluble transport proteins in circulation and corresponding receptors. The cellular uptake of Cbl from plasma is facilitated by the carrier protein, transcobalamin II (TCII) which is bound by its endocytotic receptor TCII-R mediating ubiquitous internalisation of Cbl loaded TCII. Another receptor, megalin, is strongly expressed in the kidneys where it also mediates re-absorption and storage of TCII-Cbl. It has been estimated that this kidney tubular Cbl re-absorption is similar to the intestinal uptake. Megalin is also exclusively expressed in all glands and absorptive epithelia [4]. In healthy individuals TCII is essential for the transport and cel-

	Tc(2) Cbl	Tc(3) Cbl	Tc(4) Cbl	Tc(5) Cbl	Tc(6) Cbl	^{111}In Cbl**
TCII	–	–	–	+	+	+
Bl	0.1	0.1	0.1	1.8	2.5	1.0
Ki	1.3	0.4	1.4	11.1	13.3	16.0
Li	1.4	0.4	1.6	7.4	10.2	10.2
Tu*	0.7	1.6	7.5	3.9	7.3	6.4
Tu/Bl	7	16	75	2	3	6

* Values are % injected dose per gram of tissue;
Tu/Bl are tumour to blood ratios

** Ref. [2]

Figure 1: TCII interaction and bio-distribution of labelled Cbl 24h after *i.v.* injection in mice with melanoma tumours; Bl = blood, Ki = kidney, Li = liver, Tu = tumour.

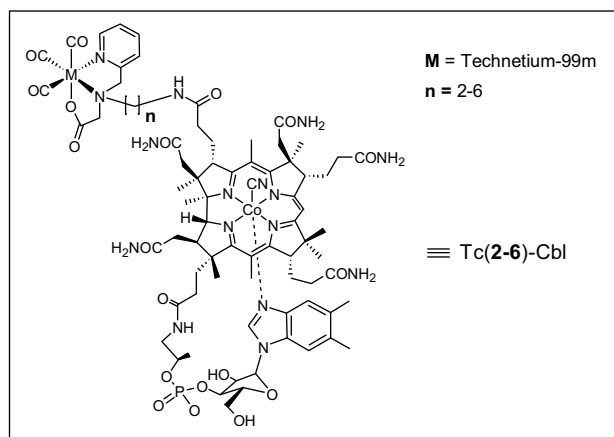


Figure 2: Structure of $^{99m}\text{Tc}(2-6)\text{-Cbl}$ derivatives.

lular uptake of Cbl. Congenital deficiency of functional TCII is an autosomal recessive genetic disorder that results in clinical Cbl deficiency within several months following birth [5]. The treatment of TCII deficiency by injection with high doses of cobalamin is generally successful, implying the presence of other mechanisms than TCII-binding for cellular uptake. We tried to exploit this alternate route by chemical tailoring Cbl with abolished interaction to TCII and therefore also abolished megalin receptor mediated uptake but still maintaining transport to tumour tissue.

Results

We synthesized a series of Cbl-derivatives with increasing linker length ranging from ethyl to hexyl (Fig.2). These conjugates are carrying mono-anionic ligands with a NNO donor set [6] and can be efficiently labelled with $[^{99m}\text{Tc}(\text{OH})_2(\text{CO})_3]^+$ at yields > 95% under mild conditions (50°C, 60 min.). TCII-non-binder derivatives Tc(2)-Cbl, Tc(3)-Cbl, and Tc(4)-Cbl, tested in mice carrying melanoma tumours display a significant diminution of systemic endocytotic uptake in healthy tissues, but still show high uptake in tumours (Fig.1). This allows the application of such non-binders as radiolabelled agents for tumour detection. Tumour to blood (Tu/Bl) ratio of 75 was reached with TCII non-binder molecules compared with 3 for a TCII-binder (Fig.1). Implanted tumours in mice showed autonomous uptake of free radiolabelled Cbl in circulation by bypassing established TCII dependent endocytosis (Fig.3). No unspecific uptake was observed except for some accumulation in the kidneys and liver. On the other hand, TCII binders reveal uptake in the tumour but also significant and high systemic uptake in other organs.

On conclusion we were able to demonstrate for the first time that specific and stringent structural modification of Cbl lead to selective targeting of tumour tissue and sparing normal

organs due to the circumvented TCII megalin receptor mediated uptake. Because of its superior pharmacological properties $^{99m}\text{Tc}(4)\text{-Cbl}$ has been selected for assessment in clinical Phase I studies at the University Hospital in Zurich.

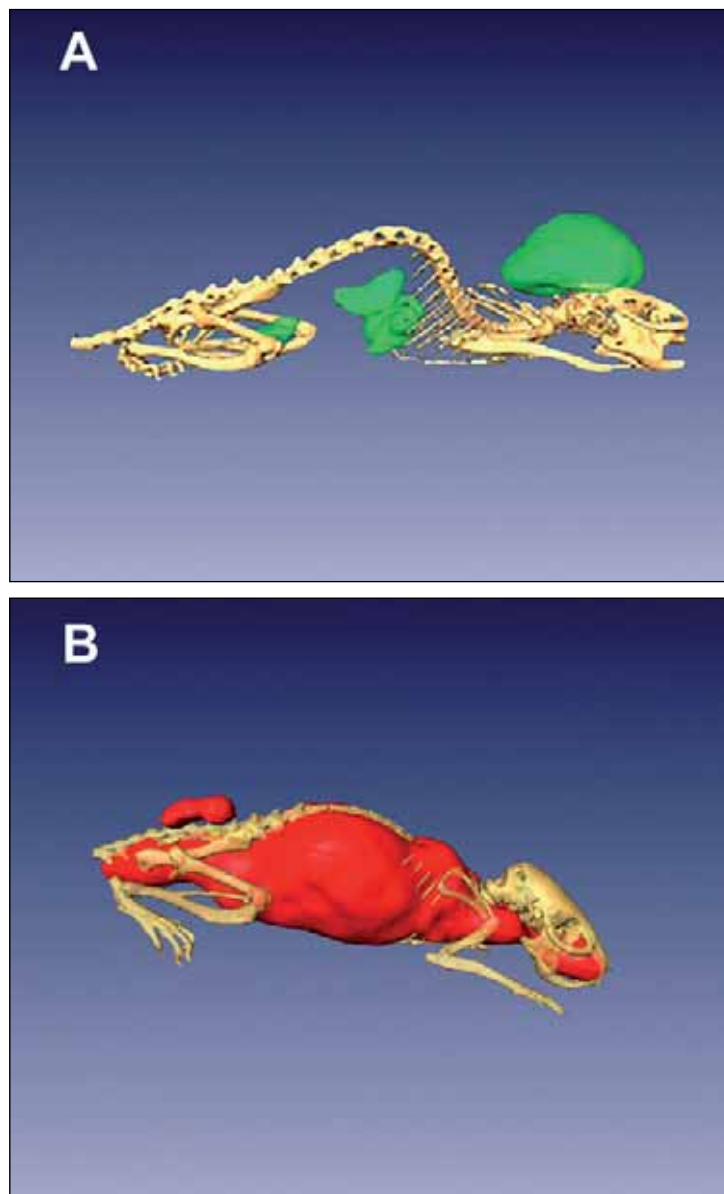


Figure 3: SPECT/CT scan of mice with $^{99m}\text{Tc}(4)\text{-Cbl}$ (A) carrying a tumour at the neck and with $^{99m}\text{Tc}(6)\text{-Cbl}$ (B) with a tumour at the tail.

References

- [1] H. Flodh and S. Ullberg, *Int. J. Cancer* 3, 694 (1968)
- [2] D.A. Collins et al., *Mayo Clin. Proc.* 74, 687 (1999)
- [3] D. van Staveren et al., *Helv. Chim. Acta* 88, 447 (2005)
- [4] E.J. Christensen et al. and H. Birn, *Nat. Rev. Mol. Cell Bio.* 3, 258 (2002)
- [5] N.Hakami et al., *N. Engl. J. Med.* 285, 1163 (1971)
- [6] A. Stichelberger et al., *Nucl. Med. Biol* 30, 465 (2003)

Treatment planning and clinical experience with intensity modulated proton therapy

Alessandra Bolsi, Francesca Albertini and Tony Lomax, *Division of Radiation Medicine, PSI*

During the 2005 beam season fifty-four patients were treated using spot-scanned proton therapy, a marked increase on previous years. This increase clearly reflects the work load of the staff of the department and, from the point of view of the medical physics group, is most clearly seen as a significant increase in the number of plans that have to be calculated, and the related patient and plan specific QA. In total in 2005, more than 330 different plans were calculated, of which 132 were subsequently delivered to patients, an average of 2.4 plans per patient. Of these plans, 44 (33%) were intensity modulated proton plans. In this year's report, we will summarise our experience of delivering intensity modulated proton therapy (IMPT), and will report on the more specific potential problems of weight gain and loss on narrow-angle IMPT plans.

Clinical experience with Intensity Modulated Proton Therapy (IMPT)

IMPT, which is the proton equivalent to IMRT, consists of the delivery of two or more highly modulated proton fields, with Bragg peaks being delivered and modulated in three dimensions within each field [1]. In this case, the combination of a set of individually in-homogeneous proton fields delivers a homogenous dose distribution across the target volume while selectively sparing the OARs which are included or close to the target.

Sixty-nine patients were treated with IMPT between 2002 and 2005 at our institute, for lesions in the skull base, spinal axis and head and neck.

Clinically acceptable IMPT plans have been found to require on average three, and no more than four fields. Before delivery for each patient every field was verified individually in a homogeneous-density phantom using a linear array of 26 ionization chambers (arranged as two orthogonal profiles) mounted underneath a water column. Those measurements have shown that the accuracy of the dose delivery is between +/- 3%. Different results were found for cases in which an organ at risk is completely surrounded by the PTV, where over-dosage of up to 10% has been measured. This effect is due to a halo of secondary particles from dose spots positioned near the PTV, and their effect should be included into the optimisation procedure [2]. For the clinical patient treatments, the IMPT plans have been discussed with the clinician and new IMPT plans have been calculated (with stricter dose constraints on the OARs) and applied, to reduce the dose to the critical structures below tolerance. These results show that IMPT is

a powerful treatment modality, which can be delivered accurately and safely with small numbers of fields.

Accurate patient positioning essential

For patients treated with this technique (and in general with proton therapy) daily positioning is crucial for the entire treatment since dose gradients are very steep and accurate patient positioning is essential for delivering the correct dose distribution. Positioning errors of more than 5 mm can cause significant under dosage in the target volume and over-dosage in the OARs.

We verify the daily patient position using two orthogonal topograms acquired with a CT *outside* the treatment room. In principle, this allows for the often time-consuming patient positioning process to be performed in parallel to the actual treatments, thus minimising lost time on the treatment machine. Reference topograms are acquired with the patient in the planning position; on these topograms we define reference points which will be checked every fraction on the daily images acquired. The table position in the treatment room is corrected according to the differences calculated between the reference and the daily images. Possible movements during irradiation have been analysed through the acquisition of post treatment topograms periodically. Applying this daily correction protocol positioning accuracies of 1-1.5 mm in the head region and 2-2.5 mm in the abdomen (SD) have been achieved. Differences in the patient position before and after therapy have been measured to be less than 2.5 mm SD in the abdomen/pelvic region, and of the order of 1 mm in the head.

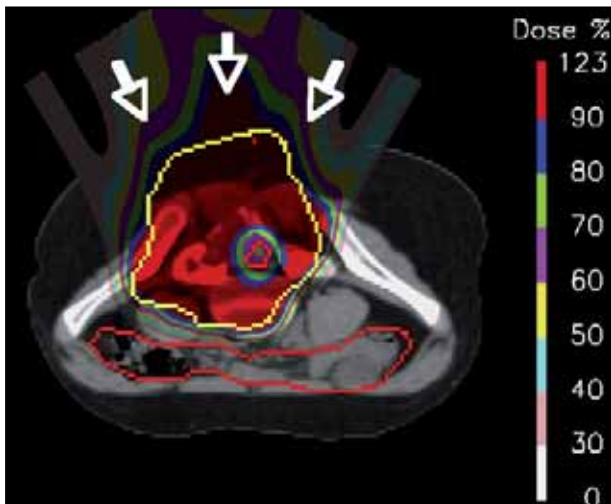


Figure 1: Example of IMPT dose distribution for the child: the beams are coming from the posterior with the following angles $(-20^{\circ};0^{\circ})$, $(0^{\circ};0^{\circ})$, $(+20^{\circ};0^{\circ})$; Notice the donut shaped configuration surrounding the spinal cord.

We can conclude that the daily imaging and correction protocol we use can reduce patient position inaccuracy below 2.5 mm, independently of the tumour site and the fixation device used. Since the CT is outside the treatment room, the position correction procedure does not affect the treatment room occupancy. As shown by computer simulation this could result in an increase of up to 30% of the patient throughput.

The effect of weight gain and loss on IMPT treatments along the spinal axis.

The accurate delivery of proton dose distributions depends on the correct positioning as well as on the accuracy of the definition of proton range in the patient body which is used for the planning and the dose calculation. To determine the range, we use a calibration curve that converts CT Hounsfield units into relative proton stopping power values. This provides a range precision of $\leq 3\%$ in typical treatment situations [3], [4]. However, it's very important to take into account any changes in patient anatomy during the treatment period because it could modify the range, and consequently the dose distribution.

We studied this effect on two patients (8 and 50 years old respectively) treated with an IMPT plan to paraspinal tumours that significantly gain and lose weight during treatment. Both patients were being treated in a so called "donut shaped configuration" with 3 fields coming from the posterior (see Fig 1). This is a configuration that allows maximal target volume dose coverage for targets encompassing a critical, dose limiting structure (i.e. the spinal cord) whilst delivering a minimal

dose to other healthy structures surrounding the target [5]. Based on the lateral topograms we observed a change in weight of both patients (+1.5 Kg for the child; -8 Kg for the adult) and a shift of the bony structures in respect to the planning CT. Although this shift could be corrected automatically by moving the treatment table, the change of the anatomy (due to fat variation) posterior to the target and spinal cord was expected to significantly affect the applied dose.

Both patients were re-CT'd and the plans optimised on the original CTs were re-calculated (but not optimised) on the new CTs to investigate the effect on the delivered dose, if the patients had not been re-scanned. The results were analysed calculating changes in the range and delivered doses in the spinal cord (SC) and in the target.

Maximum range differences over all fields in the spinal cord were 8 and 13 mm respectively for the child and for the adult, whereas the dose to the SC increased by less than 2%, indicating that both IMPT plans were relatively insensitive to substantial range uncertainties.

In both case, the IMPT plan delivered a "hole" around the SC which was mainly formed through modulation of the Bragg peaks in depth. Consequently, it could be expected that for both weight gain and loss, this hole would shift along the beam direction, substantially increasing the dose to the SC. Our analysis shows that this is not necessarily the case. Although we would always advise that patients are re-scanned if substantial weight loss or gain is observed, it appears that at least for these cases, IMPT is less sensitive than one may expect.

References

- [1] Lomax A.J. Intensity modulation methods for proton radiotherapy. *Phys. Med. Biol.*, Vol 44, pp 185 – 205, 1999
- [2] Pedroni E. *et al.* Experimental characterisation and physical modelling of the dose distribution of scanned proton pencil beams. *Phys. Med. Biol.*, Vol 50, pp 541 – 561, 2005
- [3] Schaffner B and Pedroni E, The precision of proton range calculations in proton radiotherapy treatment planning: experimental verification of the relation between CT-HU and proton stopping power (1998) *Phys. Med. Biol.* 43 1579-1592
- [4] Schneider U, Pedroni E, Lomax A. The calibration of CT Hounsfield units for radiotherapy treatment planning (1996) *Phys. Med. Biol.* 41 111-124
- [5] Rutz H.P. and Lomax A.J. Donut-Shaped High – Dose Configuration for Proton Beam Radiation Therapy. *Strahlenther. Onkol.*, Vol 181, pp 49 – 53, 2005

OPTIS – a developing programme

Jorn Verwey, Alessandra Bolsi, Gudrun Goitein, Ann Maria Schalenbourg, *Division of Radiation Medicine, PSI*;
Leonidas Zografos, *Hôpital Ophtalmique Jules Gonin*

The OPTIS programme was launched in 1984, and in 2005 treated 255 ocular tumours. The total number of patients treated by the end of 2005 was 4440. Clinical follow-up for our young retinoblastoma patients suggests that proton therapy may also become an important treatment modality for this ocular tumour. Technical improvements concerning the eye-surveillance system and the move away from Polaroid instant film in favour of flat panel digital imaging are completed and are progressing. The OPTIS2 project, continuing the ocular proton therapy programme at PSI using the new medical cyclotron COMET, officially started. First beam should become available in the OPTIS2 Areal in July 1 2007.

In 2005 a total of 255 patients were treated in 12 weeks of OPTIS operation. The following lesions were treated: 227 choroidal melanomas, 6 haemangiomas, 3 metastasis, 11 conjunctival melanomas, 5 iris melanomas, 1 age-related macular degeneration, 1 pseudo-tumour, and 1 endothelial lesion. There were no complications of any sort, technical or clinical, and all treatment weeks proceeded as scheduled. In 2002 and 2004, three young patients (4, 4 and 11 years of

age), had 4 retinoblastoma lesions treated at PSI. Retinoblastoma is a malignant eye-tumour that presents itself in early childhood (90% of diagnosis before 3 year's of age). External beam radiotherapy, albeit very successful in controlling the tumour, is currently controversial because of late effects caused by the beam's path having to traverse healthy extraocular structures. At PSI, for the first time ever, retinoblastoma lesions were treated using an anterior approach, avoiding all extraocular structures.

All three patients had undergone multiple treatments with a whole range of treatment modalities without achieving tumour control. Available follow up at 38, 15 and 13 months after treatment showed tumour control in three out of four lesions. One lesion proved to be radio-resistant and is progressing. All patients retained useful vision in the treated eye at the time of the last control.

PSI, together with the Hôpital Ophtalmique Jules Gonin, is working towards providing ocular proton therapy under anaesthesia to treat very young children with retinoblastoma, who cannot yet cooperate during the treatment.

Analogue to digital

Technical developments in the OPTIS programme focused on the eye-surveillance and clip-imaging system. Eye-surveillance is pivotal during treatment. Once the tumour, and hence the eye, is positioned correctly, it should no longer move. If it does, the operator has to interrupt treatment. The existing system is more than 20 years old and still relying on an analogue screen videopen combination. The pen allows the eye, as



Figure 1: A patient is positioned for treatment.

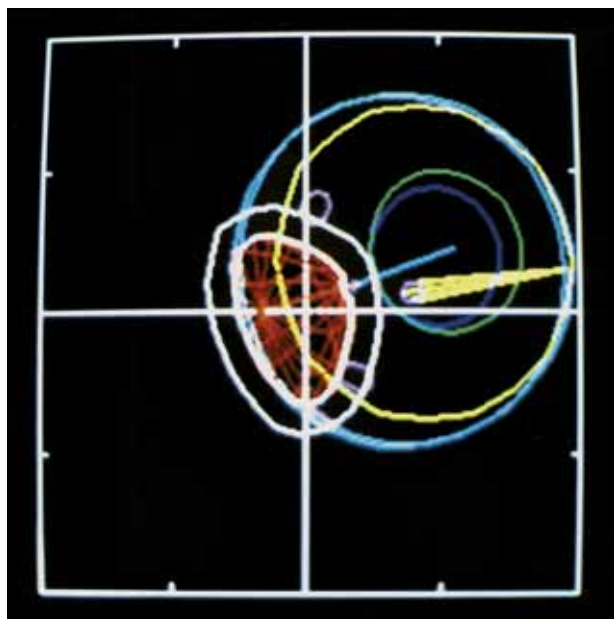
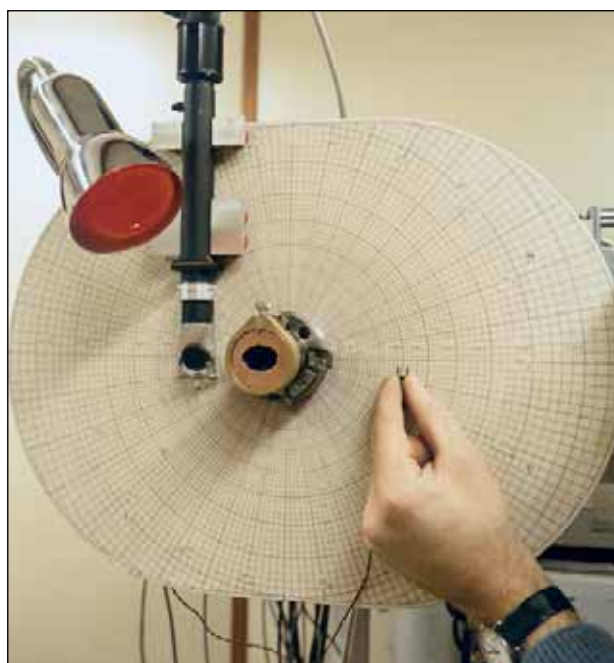
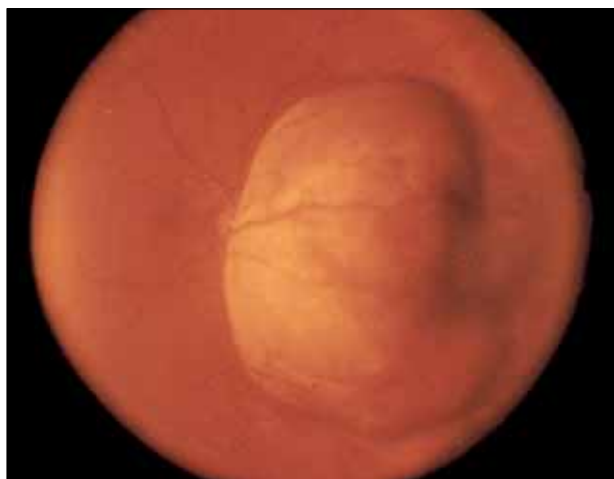


Figure 2: **Top: An eye tumour.**
Middle and below: Therapy planning at OPTIS.

captured by a camera, to be drawn on the screen. Once the correct position is found, this drawing, both visible in the treatment room and in the control room, then becomes the eye's "should-be" position. The age of the existing hardware made a switch to a digital system necessary. A PC-based system now allows the drawing to be done on a small flat-screen with an ever-present finger, which is also capable of capturing images for storage when so desired. In the future, automatic eye-movement detection may also be added.

The DISPOT project, replacing expensive Polaroid instant X-ray film with digital flat panels, is immense progress. Two 8x10 cm Hamamatsu flat panels have been ordered, and at PSI a sub-millimetre accurate panel-positioning system was designed and approved for manufacturing. The digital panels will be moved into position to image tantalum clips sutured to the eyeball indicating the tumour's position. They have to be driven out of the beam before actual irradiation commences. To prevent, as much as possible, image degradation due to neutron irradiation damage, the panels are located near the ceiling in a boronated polyethylene box. The replacement of analogue with digital images further allows computer-aided patient positioning. In this area PSI will cooperate with the Hahn-Meitner Institute (HMI), where computer-aided positioning is already in operation. The entire system is expected to be ready for routine operation in September 2006.

Development of OPTIS2

In 2005, PSI started focusing on the definite plans for OPTIS2, which is an important part of the PROSCAN project. First beam in the OPTIS2 Areal is scheduled for July 1, 2007. The main technical challenge for OPTIS2 is matching the OPTIS beam characteristics with a 25 times lower beam intensity *while limiting* the treatment time to 45 seconds. Dual scattering instead of OPTIS' single scattering, and intelligent placement of the beam-forming elements, have solved this problem on paper. Experiments with the COMET beam still have to confirm these calculations.

To have OPTIS2 ready for treatment in 2007, many pieces must fall into place. OPTIS2 is not a simple migration of OPTIS. From infrastructure to safety analysis, from the control system to treatment procedures, OPTIS2 will be designed and built from scratch. Experience gained from digital imaging and computer-aided positioning about to be introduced in OPTIS, will aid in preparing OPTIS2 for routine patient treatment already in 2007. Initiated in 2005, intensive cooperation with HMI in the fields of beam transportation, beam shaping, treatment procedure and dosimetry, will contribute significantly in helping us reach that goal.

Objectives of PROSCAN

Martin Jermann, *Head of Proton Therapy, PSI*

Based on the developments and successes of proton therapy, the PSI directorate decided in 2000 to expand the activities in this field and launched the so-called PROSCAN project. The objectives of PROSCAN are to further develop the PSI Spot-Scanning technology (i.e. with faster scan methods to overcome the organ motion problem) into a new gantry, which can be implemented in a hospital environment. Further aims are to optimize treatment methods, including the treatment of additional indications; the transfer of the technology and know-how to industry and to radiation therapy centres, including education and the training of specialised personnel.

With PROSCAN, PSI will implement and operate a base technology laboratory for the further development and advancement of proton therapy using proprietary system techniques and applications. The programme is based on the experience with the technology at the compact PSI Gantry for the treatment of deep-seated tumours and on the treatment of eye tumours at the OPTIS facility.

The PROSCAN project is an interdisciplinary development of several laboratories and divisions at PSI.

Expansion of the existing facility

The expansion of the PSI facility started in 2000 with the specifications for a dedicated proton accelerator which is able to deliver protons with high reliability and with the quality necessary for the implementation of the advanced scanning

features at the new PSI Gantry under development. PSI contributed to the design and development of the new accelerator, for example, by analysing the static and dynamic 3D magnetic and electric fields. Special effort has been put into the optimisation of the beam extraction region. Reaching high extraction efficiency, the activation of structures and production of radioactivity can be minimised.

In May 2001, the dedicated compact medical cyclotron COMET was ordered from the company ACCEL Instruments GmbH. The 250 MeV superconducting cyclotron was delivered during the second half of 2004 and the commissioning phase started at the end of the year. The machine was operational for acceptance tests in the middle of 2005. In October 2005 the specified extraction efficiency of 80% had been reached and it was routinely reproduced during further tests of the cyclotron. The beam intensity of 500 nA has been routinely extracted with high beam stability. Beginning in the second half of 2005 the test area for advanced scanning tests has been completed and first experiments with 250 MeV protons started at the end of July. Studies of the beam transport with the new profile monitors showed good agreement with the calculated beam widths. The transmission through the degrader and collimator system shows that losses due to multiple scattering in the degrader are slightly higher than expected, which implements a rather sophisticated and optimized design of the horizontal beam port and layout of the new OPTIS facility.

The new beamline to connect COMET to the existing Gantry 1 was realized and tested (without beam) in another building in the second half of 2005. Planning and preparatory work has been done to replace the existing beamline structure from the ring cyclotron to Gantry 1. The new beamline will be installed in the first half of 2006 and first patient treatment with COMET on Gantry 1 is scheduled for October.



Figure 1: **The new compact cyclotron, COMET.**

Before commissioning of the new proton therapy facility a new operating license will be required from the Swiss Federal Office of Public Health. The safety report for the licensing process has been delivered to the authorities and the commissioning of the COMET cyclotron has been approved.

Strengthening the medical programme

With the dedicated cyclotron and the expansion of the facility we expect to be able to treat about 200 patients with deep-seated tumours (i.e. about 5000 to 6000 fractions) per year. The existing OPTIS programme will also be transferred to the new cyclotron.

The extended clinical R&D programme, running in parallel with the various technological developments, will contribute within the international framework together with other centres to demonstrate the strengths and potential of this treatment method, including treatment of moving targets using scanning technology. In parallel, within the framework of a ten year programme, we aim to support the education of technical and medical specialists with regard to the introduction of this new and advanced therapy method in hospitals.

Improvement of scanning technology

The major challenge to proton therapy is coming from new sophisticated beam delivery methods developed in conventional radiotherapy (like IMRT= “intensity modulated radiation therapy”), which has been widely introduced in hospitals. The PSI scanning technology attracted world-wide interest, since it is presently the only system capable of providing intensity modulated radiotherapy with protons (IMPT). This approach could be essential if proton therapy wants to continue to play the leading role in precision radiation therapy in the future. Most of the further work for implementing IMPT into clinical practice is being done with the existing gantry, including the development of treatment planning, dosimetry and quality assurance methods. Gantry 1 will continue to play an important role in the development of proton therapy at PSI. Fifty-three patients were treated in 2005, of which fourteen were small children under anaesthesia. Based on the operational experience of the patient treatments, an improvement and revision programme is still in progress to improve reliability and comfort.

Beam-scanning methods are more sensitive to organ motions than passive-scattering foil techniques. For solving this problem a new Gantry 2 is under construction which allows faster beam scanning in order to apply multiple target repainting without compromising the size of the pencil beam. The new

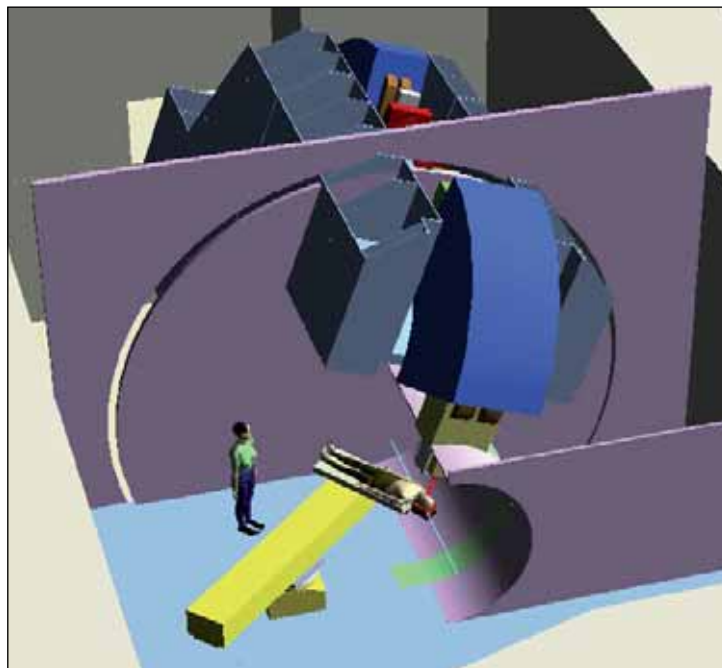


Figure 2: **Design plans of Gantry 2.**

options for improving scanning being considered in the frame of Gantry 2 are: a) double magnetic parallel scanning on the gantry, b) dynamic energy variation using the degrader, and c) use of intensity modulation at the ion source. The parallelism of the beam will bring practical advantages, i.e. for therapy planning, patching field techniques, use of collimators and compensators. A much faster beam scanning technique should allow multiple target-repainting in a single fraction, in order to be able to completely replace scattering foil options.

The construction of the mechanical structure started in the second half of 2005. The beamline inside the gantry was specified and will be ordered in 2006. First beam in Gantry 2 should be available in the middle of 2007. Patient treatment with Gantry 2 will start after commissioning of the facility and adaptation of the necessary therapy planning procedures at the end of 2007.

Conclusions

The expansion of the PSI proton therapy facility (with 2 gantry rooms for treatment of deep-seated tumours and one 70 MeV fixed beam room for eye treatment) will provide new interesting technological and clinical research opportunities. It will allow the investigation of advanced scanning features for the treatment of additional medical indications, including moving tumours and it will consolidate PSI worldwide as a technology base laboratory for advanced proton therapy applications.

A probabilistic safety assessment of the PSI proton therapy facility

Bernhard Reer, Vinh N. Dang, Luca Podofilini, *Laboratory for Energy Systems Analysis, PSI*;
Adolf Coray, *Division of Radiation Medicine, PSI*

A Probabilistic Safety Assessment (PSA) study has been undertaken to address selected potential sources of risk for patients attending the PSI proton therapy facility; namely, overdose accidents due to failure to switch off the proton beam, or to the inadvertent delivery of repeated doses to the same area of the body. Results indicate a low risk in both cases. Issues identified for risk minimization are the (fail-safe) design of the electrical power supply, fault detection, and human error. Overall, it has been demonstrated that PSA is a useful tool for obtaining insights into risks associated with medical treatment in complex facilities.

Introduction

The proton therapy facility at PSI relies on a complex control and safety (interlock) system to deliver a proton beam to deep-seated tumours, using the spot-scanning technique [1]. In connection with a planned upgrade of the facility, a Probabilistic Safety Assessment (PSA) has been initiated to identify potential vulnerabilities in the technical components of the facility, though the PSA has been directed at the facility in its current configuration.

Proton therapy at PSI

In the spot-scanning technique, a bundled pencil beam is scanned through the tumour from several directions succes-

sively. For each of these “fields”, the location of the peak energy deposition is controlled in three dimensions. This control is achieved by setting the various magnets on the beam line, as well as by adjusting mechanical devices, e.g. the range shifter plates and the patient table. The duration of the irradiation to each spot is controlled by real-time dose measurements. The risks from the technical components, i.e. the proton delivery system, are associated with incorrect location of the energy deposition, or with an incorrect dose.

The facility has an excellent safety record. Some 250 patients have been treated since 1997, and no accident (or a significant precursor of an accident) has occurred.

PSA: motivation and process

The risk associated with medical treatment is an issue of increasing importance. Today, systems are very complex, and the processes employed require a variety of actions to be performed by the operating personnel. The PSA methodology, with its scenario-based analysis and probabilistic perspective, complements the existing design and risk management processes.

PSA is the implementation of a systematic search for failures that could initiate accidents or fail systems. An accident sequence model is compiled to represent the resulting scenarios. The failure of the primary beam monitor (initiator) would lead to an overdose (>6 Gy) if all three defences (beam monitors 2 and 3, and time watchdog monitoring the duration of beam exposure) failed simultaneously, as indicated in Figure 1.

Parts of the facility’s control and safety logic are shown in Figure 2. Magnetic (SDW₁, AVK₁) and mechanical (BD₁, MDF₁)

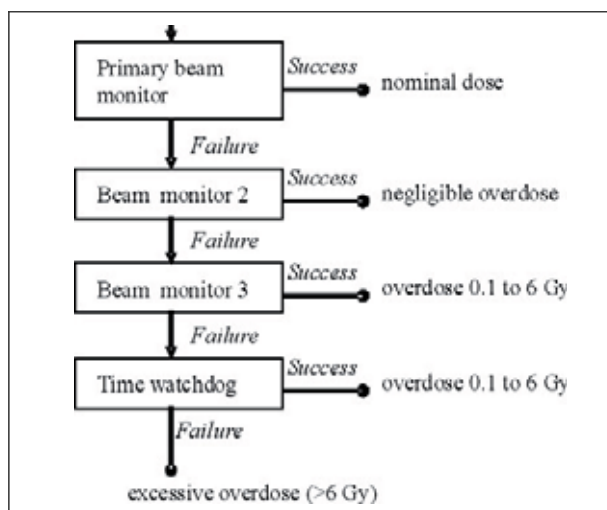


Figure 1: Accident sequence modelling (simplified).

devices serve to interrupt the beam. These devices are activated by various interlock (ILK) signals, such as zero-cross 2 (supported by beam monitor 2), dose watchdog (DWD), and time watchdog (TWD).

In turn, feedback data relating to proper functioning of the beam-stop devices are processed as additional signals (e.g. the kicker fault signal). Some important challenges for the application of PSA methods (e.g. event tree and fault tree analyses) were the modelling of signal timing and response times for beam-stop devices, as well as for the quantification of the components involved (especially the electronic components).

Overview of safety insights obtained

The PSA was carried out with emphasis on initiators related to the spot delivery system, which have the potential to result in overdose accidents due to failure of proton beam switch-off, or in repeated deliveries of doses to the same spot of the body. Other sources of risk, such as beam intensity excursions, were omitted from this phase of the PSA.

Results indicate a risk of about one accident with an overdose of 6 Gy or higher per one million patients. Safety insights and respective measures for risk minimization have been identified in the following areas: electrical power supply (e.g. a few gaps in the fail-safe system), fault detection (e.g. spurious counter reset not detectable by regular testing), and human performance.

HRA: process and insights

Operating experience with highly automated systems indicates that human errors frequently contribute to incidents or accidents. Human Reliability Analysis (HRA), which deals with the identification and quantification of human errors contributing to risk, is therefore an important component of PSA. The HRA performed here addressed potential failures to restore the proper standby states after testing, errors during start-up of beam delivery, and aggravating interventions (so-called errors of commission, or EOCs) after disturbances of normal operation.

EOC identification was carried out as follows. Plausible interventions with the potential for EOCs were first identified from reviews of operating procedures, logbook records, and from past incidents at the facility: for example, the procedure allows the treatment of patients with a disabled beam position check (of the software) in case of spurious activation. The process continued with a search for relatively frequent scenarios in which such an intervention is inappropriate (e.g. valid challenge of beam position check due to wrong beam position).

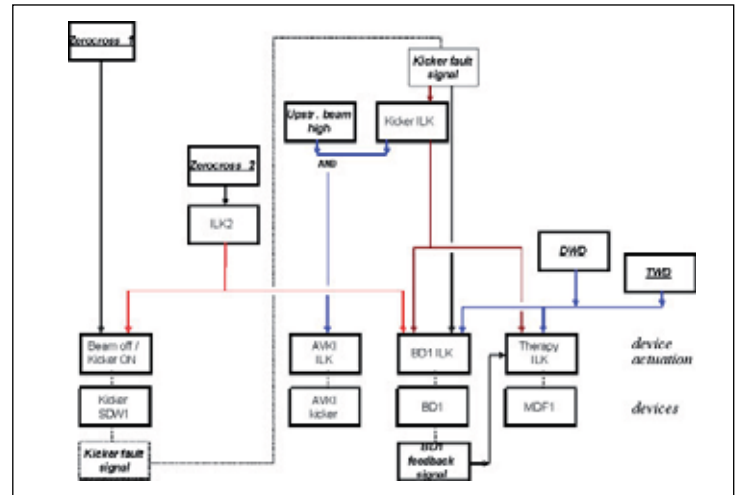


Figure 2: **Beam stop signals and devices.**

In such cases, potential operator errors in situation assessment (e.g. valid demand diagnosed erroneously as spurious) were quantified and integrated into the PSA model.

A total of 22 human errors were integrated into the PSA model. Five of them contribute more than 1% each to the risk of severe accidents. EOCs related to inappropriate bridging of software checks contribute about 10%. Respective suggestions for improvements are to provide interlocks that block bridging of certain checks, and the introduction of more explicit criteria in procedures regarding symptoms of valid challenges of beam position checks.

Conclusions

PSA has provided valuable insights into the safety of the proton therapy facility at PSI. Suggested additional measures for risk minimization have been implemented. Although the results indicate a low patient risk, further PSA applications in this field would still be useful to obtain insights into the risk from accident sequences that are difficult to foresee in advance. From the methodological perspective, software faults and reliability data, for electronic components in particular, are issues requiring further attention.

Acknowledgements

The authors would like to thank the PROSCAN Project contributors for sharing their systems expertise, and the VEIKI Institute (Hungary) for their contributions to the PSA model development.

References

- [1] E. Pedroni et al., *Medical Physics* 22(1), 37-53 (1995).

Progress in the development of Gantry 2

Eros Pedroni, *Representing the Gantry 2 development team, Division of Radiation Medicine, PSI*

A new gantry for proton therapy, Gantry 2, is being realized at PSI under the PROSCAN project, with the goal of increasing the speed of pencil beam scanning to deliver repeat doses on the target (target repainting) so as to reduce organ motion errors. This should permit the use of beam scanning in the whole patient body, including moving targets such as the lung area. Gantry 2 is characterized by an innovative isocentric layout, with an open patient-friendly treatment area and a permanent fixed floor. A new feature allows us to take X-ray images in the beam-eye-view direction simultaneously to the delivery of the proton beam.

Experience from Gantry 1

Gantry 1 is still the only proton therapy system in the world delivering the dose with a dynamic beam scanning technique. On Gantry 1 we introduced modulated proton therapy (IMPT), a new therapeutic method still possible only at PSI. Gantry 1 was designed in 1991 for the parasitic use of the 590 MeV beam of the PSI ring cyclotron. The system was adapted to the poor intensity stability of the split beam and to the slow selection of the beam energies which must be performed with a bulky degrader. The speed of scanning is limited; we can paint the dose on the target only once or just a few times. With Gantry 1 we can therefore only treat well immobilized lesions,

i.e. non-moving tumours attached to bony structures in the skull, spinal cord and lower pelvis.

The new Gantry 2 concepts

In order to extend the medical indications treated with beam scanning to the whole patient body, we are building a new gantry system designed specifically to deliver the dose in combination with the new medical cyclotron COMET. The accelerator, the degrader and the beamline to the gantry will be used as dynamic beam delivery devices in order to speed-up pencil beam scanning considerably as compared to Gantry 1.



Figure 1: **Simulated treatment with Gantry 2 (from a video still).**

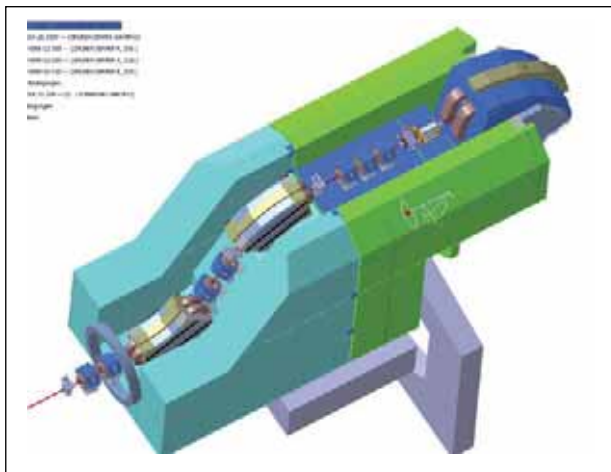


Figure 2: **Layout of the support and of the rotating beamline of the new Gantry 2.**

The beam scanning techniques of Gantry 2 will be based on a fast double parallel magnetic scanning, with rapid energy changes. We plan to modulate the beam intensity at the ion source of the cyclotron (using a deflector plate in the first turn of the cyclotron) as part of the dynamic therapy. We should be able to deliver the dose with a high number of target repaintings for treating moving tumours. Faster scanning will be applied with or without the additional options of using gating (synchronization of the beam delivery with a given phase interval of the breathing cycle) or tracking (correction of beam position to follow the motion of the tumour). On Gantry 2 we will also implement the possibility of mounting optional collimators and compensators on the nozzle for treating very superficial tumours (for example eye treatments in supine position). With a faster scanning technique we should be able to simulate and replace completely the traditional scattering foil technique. The goal is to demonstrate the feasibility of beam scanning as a universal beam delivery method for treating all possible indications for proton therapy using a conceptually simple compact isocentric scanning gantry.

Realization steps towards Gantry 2

The practical realization of Gantry 2 was started in 2005 by placing the order for the mechanical components of the system (rotating beam line, nozzle, patient table and patient handling equipment). We have chosen to realize Gantry 2 in the same way as Gantry 1, as a cooperative joint venture with the Swiss company, Schär Engineering Ltd. Figure 2 shows the finalized layout of the gantry support with beam line components. The system is similar to Gantry 1, the major differences being the isocentric layout. The rotation of the gantry is limited to 30° , $+185^\circ$ in the vertical direction in order to have a flat, fixed floor around the patient table.

After performing Finite Element Model (FEM) calculations to study the deformations of the mechanical support during rotation and their influence on the beam optics, the optimized structure of the system was finalized. The mechanics are now being designed in detail and the gantry support will be delivered in June 2006.

The most delicate component of the gantry beamline is the last 90° bending magnet. A laminated structure of the yoke will permit changing the energy of the beam in range steps of 5 mm very quickly, within 100 ms. The gap of the magnet has been frozen at 15 cm. This permits double parallel scanning of the beam over a scanning area of 12 cm x 20 cm. To save space in the gap for the beam we plan to use an integrated non metallic vacuum chamber. The yoke of the 90° bending magnet will be realized with a hole for taking X-ray pictures in the BEV direction simultaneously to the delivery of the proton beam.

First prototype

The realization of the technical components for the beam delivery (beam monitors) and the development of the control system are proceeding well. The first prototype of a new ionization strip chamber with 2 mm strips was built at CERN by the TERA collaboration and was successfully tested with the beam of Gantry 1. A first version of an electronic simulator system for developing the control system of Gantry 2 off-line has been realized in the context of a diploma work by two students of the University of Applied Sciences in Winterthur. Unfortunately beam time was not available in 2005 in the provisional test area for the practical developments of advanced scanning. Nevertheless the realization of the new Gantry 2 should be completed in the first half of 2007 and first patient treatments are expected by the end of 2007.

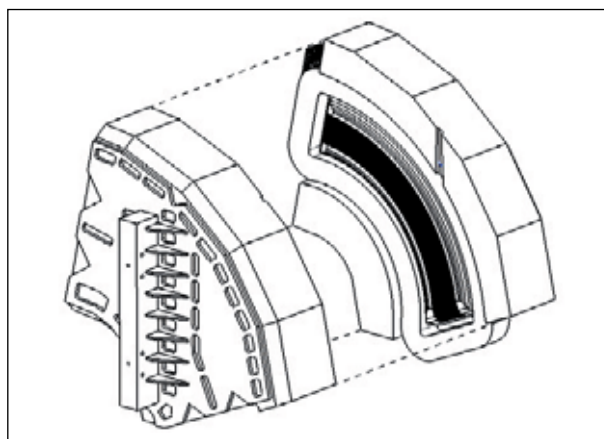
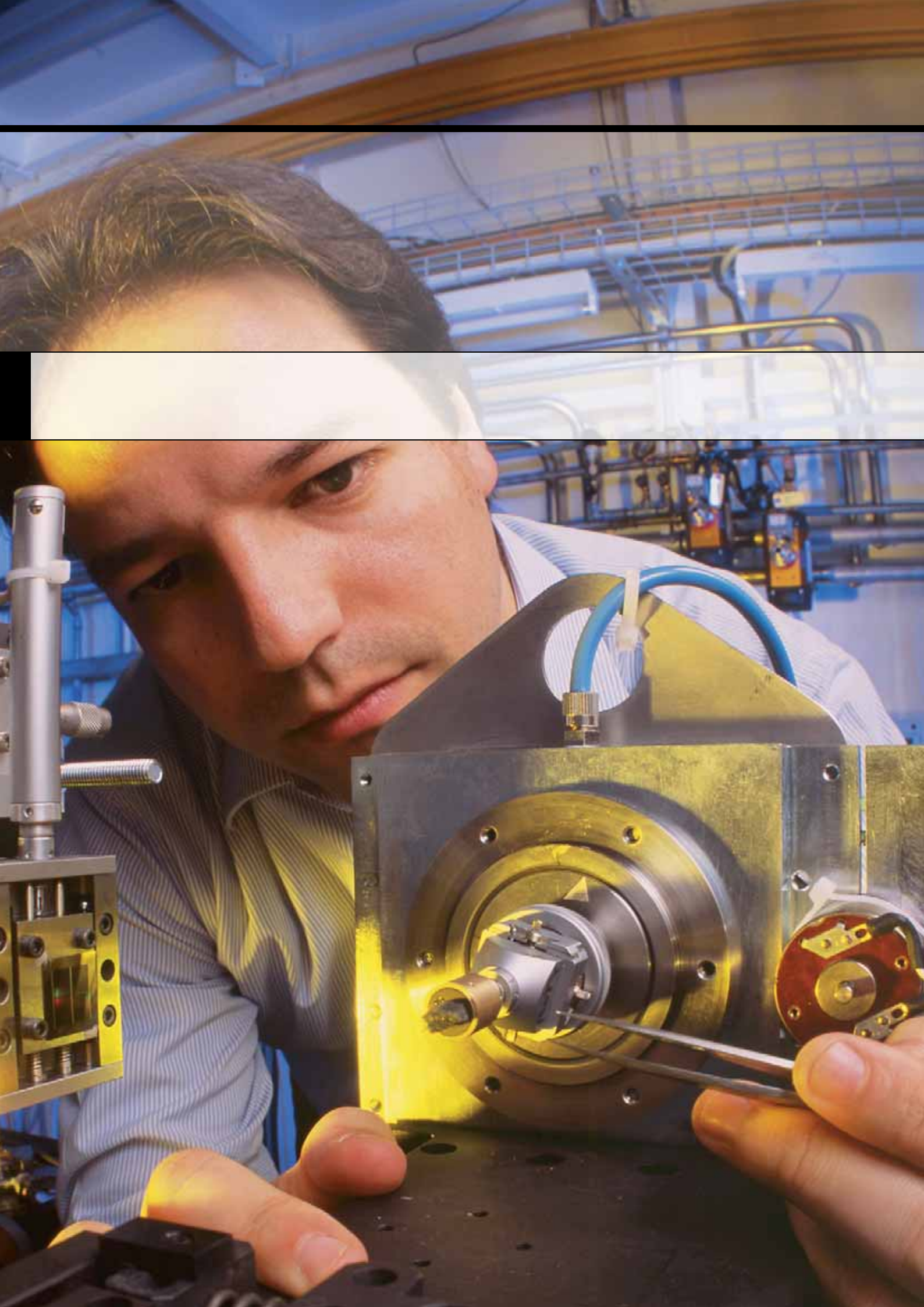


Figure 3: **Planned layout of the 90° bending magnet for double parallel beam scanning.**



Patents and licenses

The PSI technology transfer office aims to transfer inventions stemming from new research results or new technologies for industrial use, with the goal of either adding competitiveness to existing companies, or to create new jobs. This process has to be adapted for each technology transfer case because the majority of cases require person-to-person business where the specific needs of the industrial company have to be anticipated.

The most effective method of technology transfer is the transfer of persons, who not only possess specific know-how but also the spirit to transform an invention into an innovation. Along with this method, the transfer of know-how or protected intellectual property rights (IPR), mostly in connection with a collaboration, is a good way to sustain a successful transfer.

As we are a user lab operating large and complex research facilities, we generate not only scientific results but also new technological solutions, necessary for operating the facilities at the scientific vanguard. Experience has shown that these technologies can be beneficial in other fields of applications.

We always strive to generate a win-win situation for both the industrial customer and the scientific community. In 2005, PSI filed forty-two new applications for IPRs and completed seven new licence agreements.

The interferometer for X-ray radiation at the SLS opens up the prospect of unimagined applications in medicine.

(Photo: H. R. Bramaz)

Efficient Intelligent Patient TRANsport System – EIPATRANS

Daniel Lempen, Petra Rhiner-Rosansky, *Division of Radiation Medicine, PSI*; Robert Rudolph, *Technology Transfer, PSI*

PSI operates the first and only compact radiation therapy facility in the world treating deeply-situated tumours using spot-scanning proton radiation. To date, a total of 262 patients with brain, skull-base or spinal cord tumours as well as abdominal sarcomas were treated in the gantry. To increase comfort for the patients and the efficiency of the transfer of the patients between the stations of the facility, a self-propelled transport system has been specified and implemented together with an industrial partner.

During treatment the patient needs to be transferred between different stations such as the preparation room, computed tomography and proton radiation gantry. To facilitate the operation, the patients are fitted with a customized couch which is attached to a transporter. At the stations, the couch is transferred from the transporter to the installation using a precision clamping mechanism. Several factors limit the efficiency of the current system. Two persons are required to manoeuvre the transporter at and between the stations and the physical effort to move the transporter, which can weigh up to 500 kg including the patient, is quite considerable and thus a strain on the personnel. A major disadvantage is the non-adjustable height of the trolley, requiring patients to climb steps. This is difficult for the elderly and patients with mobility restrictions.

The new system which had to be integrated into the existing environment is based on an automated guided vehicle. A medical assistant selects a target station and initiates and

stops the motion of the vehicle via a wire control, thus accompanying the patient and the vehicle on its travel between stations. The vehicle follows a pre-programmed track by means of optical guidance. The mechanical coupling between the couch and the gantry is adapted for automated docking and operation. The adjustable height of the support offers convenience for the placing and preparing of the patient. The intelligence for these functionalities is located within the vehicle; it is flexible and is able to operate independently from the treatment infrastructure.

Increased patient flow

Children need to be anaesthetized for the treatment and the vehicle needs to be able to carry and supply the equipment for anaesthesia and monitoring. These features allow a reduction of personnel for the patient care and a speedup of patient handling at the gantry resulting in more patients being treated at the proton radiation facility.

The technical concept of the transport system has been done in cooperation with suppliers for the vehicle system and the mechanical coupling. License contracts have been signed with both suppliers to participate in the installation of the same type of patient transport systems by the supplier at other medical facilities.

The concept of this transport system is of interest to medical treatment and diagnosis facilities with defined tracks and the need for high throughput of patients, i.e. radiation and standardized high-tech surgeries. Based on these potential applications, PSI has filed a patent to protect the concept and possible variants of solutions for medical applications. Gantry 2, will be equipped with a similar system.

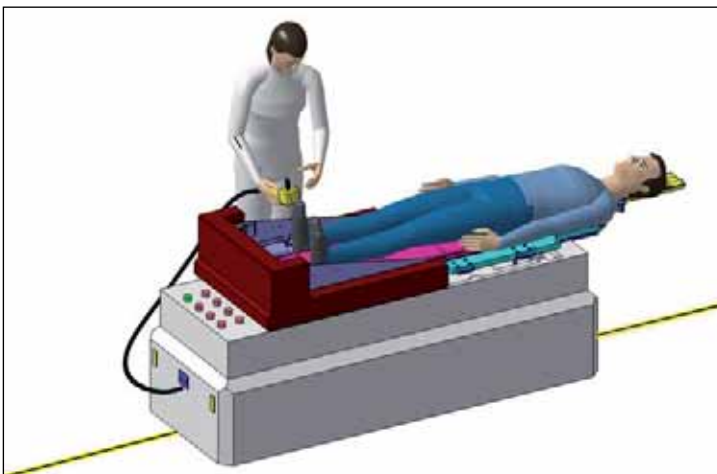


Figure 1: Patient transport system and the optical guidelines.

Lipid bilayer membranes on nanopore arrays

Louis Tiefenauer, *Biomolecular Research, PSI*; Peter Hardegger, *Technology Transfer, PSI*

The field of nanotechnology has created high expectations for new biotechnological products [1]. But where do nanosized dimensions provide added value? And where is there a big market for nano-based products? Recently, in collaboration with the industrial partner LEISTER, PSI established the procedure for mass fabrication of nanostructures. Based on the resulting nanopore array chips we launched a project aimed at developing analytical tools to investigate the function of membrane proteins. Understanding the function of membrane proteins is of high relevance to Life Sciences and also for industrial applications.

The big challenge in the development of novel drugs is the identification of more effective compounds that provoke specific biological responses with a minimum of side effects. The functional unit of all organisms is the biological cell which is generally surrounded by a 4 nm thick cell membrane consisting of lipids. The majority of future drugs will bind to proteins associated with this lipid bilayer membrane triggering biochemical reactions. The knowledge of the three-dimensional structure of such membrane proteins is currently a focus in structural biology, also at PSI. Several thousands of different membrane proteins of a cell cover many different essential functions. For instance, a hormone molecule which binds to a receptor protein on the outer surface of a cell induces a slight change to the protein structure resulting in a cascade of biochemical reactions inside the cell. Another two important classes of membrane proteins, the ion channels and transporters, control the passage of specific ions across cell membranes (see Fig. 1).

The function of each membrane protein has to be thoroughly investigated in order to understand its working mechanism on a molecular level as well as to identify drug compounds affecting its activity. Therefore, test systems are required which allow us to experimentally investigate the function of purified, reconstituted membrane proteins.

For four decades it has been known that artificial cell membranes spontaneously form bilayers in openings of about 0.1 mm diameter in Teflon sheets. Such bilayers are stable for several hours. Insertion of membrane proteins in lipid bilayers in a functional state is difficult. The major claim of our applied patent is that stability of bilayers will be significantly improved by reducing the diameter of pores to nanometer dimensions. Furthermore, a system of free-standing lipid bilayers which separate two fluid compartments simplifies the investigation

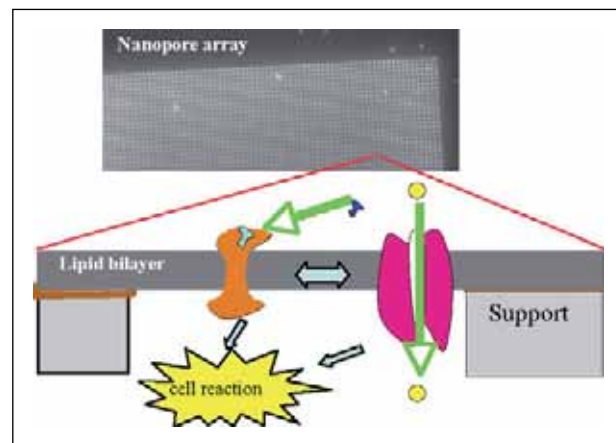


Figure 1: **Scheme of functional assay system.**

of transport processes across biological membranes. Free-standing bilayers supported by a regular pattern of nanopores mimic more closely the natural situation than bilayers immobilized on solid supports. We believe that integrating purified membrane proteins in such bilayers will lead to assay systems for the identification of new drugs and their side effects in early stages of the drug discovery process. Achievements will drive the related product development of our industrial partner.

The fabrication procedure for the mentioned silicon chips has been developed in a precedent TopNANO21 project at PSI in collaboration with LEISTER Process Technologies which is located in Sarnen, Switzerland. Our current research projects using biophysical and biochemical methods are supported by the Commission for Technology and Innovation (CTI) and PSI.

References

- [1] www.nanolife2.org "Envisioned developments in Nanobiotechnologies" Expert survey Dec. 2005.

PILATUS X-ray detectors

Christian Broennimann, Eric F. Eikenberry, Fredy Glaus, Beat Henrich, Miroslav Kobas, Philipp Kraft, Jana Lehmann, Markus Naef, Hermann Rickert, *Synchrotron Radiation and Nanotechnology, PSI*; Roland Horisberger, Daniel Luethi, Elmar Schmid, *Particles and Matter, PSI*; Michael Horisberger, *Condensed Matter Research with Neutrons and Muons, PSI*

The PILATUS Project [1] was initiated several years ago to overcome limitations of commercially available X-ray detector systems at synchrotrons. The hybrid pixel technology, successfully developed by PSI for high energy physics experiments, was adapted to the needs of experiments at modern synchrotrons. A prototype system, the PILATUS 1 M detector, was built in 2003 and delivered important input for a second iteration of detectors. The main goal of the project is the assembly of a 6 million pixel system for the SLS Protein Crystallography Beamline Xo6SA. As a side activity, a smaller system called PILATUS 100K was developed, which is successfully used at the SLS Material Science Beamline Xo4SA.

The PILATUS X-ray detectors are high quality large area hybrid pixel detector systems. They are adapted to the needs of experiments at synchrotrons as the CMOS chips and the sensors are radiation tolerant. The detectors operate in single photon counting mode, i.e. each incoming photon is counted.

The properties of the PILATUS detectors are:

- Dynamic range of 20 bit
- Highest sensitivity in the energy range of 3 – 20 keV
- Read-out times in the ms-range

The high dynamic range enables the recording of very strong and very weak X-ray signals with high precision. The short readout time allows the studying of dynamic processes. In order to demonstrate the potential of this new generation of digital X-ray cameras, the PILATUS 100K system was developed. It consists of one module with 500 x 200 pixels (pixel size 0.172 x 0.172 mm²). The system includes a power supply and a DAQ-computer.

The DAQ-system is based on the PSI Gigastar card, residing in the PCI bus of the computer. The PILATUS 100K can be operated at frame-rates of up to 50 Hz.

Except for the CMOS chips and the sensors, the components of the detectors are manufactured by Swiss companies. Manufacture of the detectors is partially out-sourced to nearby companies; the technologically demanding steps (the bump-bonding) are performed at PSI.

At the SLS, three different configurations of detectors will be available: the PILATUS 100k system for surface diffraction, a 21 module system (PILATUS 2M) for the cSAXS beamline X12S and the PILATUS 6M detector with 60 modules for protein crystallography. The main applications are:



The PILATUS 100K detector box. The active area of the detector is 84 x 34 mm².

- Protein Crystallography
- Surface Diffraction
- Small Angle X-ray Scattering (SAXS)
- Diffuse X-ray scattering
- Time resolved experiments

The market for the detectors lies in the field of synchrotron radiation. There are 39 synchrotron sources worldwide, some of them having up to 30 beamlines. Within the next five years, five new sources will go into operation. The field of material research diffractometers based on laboratory sources is also interesting, more efficient detector system create added values to such systems. Industrial contacts were established with major companies in the field of material research diffractometers, non-destructive testing and X-ray analysis.

References:

- [1] pilatus.web.psi.ch/publications

Mail-in crystallography (MIX) at the SLS – a successful new service for proprietary users

Joachim Diez, Clemens Schulze-Briese, *Research Department Synchrotron Radiation and Nanotechnology, PSI*;
Philipp Dietrich, *Technology Transfer, PSI*

In January 2005, a new service called Mail-in Crystallography (MIX) was established at the SLS. Companies now can send frozen protein crystals for analysis, thereby obtaining their data without having to buy entire shifts or to travel to the synchrotron. In 2005, around 250 crystals were measured and around 25,000 images were collected. So far, nineteen companies from Europe, USA and Japan have signed MIX-contracts. Starting in 2006, a third beamline will be built, where MIX service is planned on an even broader scale, thereby further improving turn-around. This bending magnet beamline will become available for users in the autumn of 2007.

The spectrum of potential customers for the MIX-service is very broad. Major companies with a large amount of crystals can benefit from this service as can small start-up companies with only a few samples, since the MIX service is available from one, to dozens of crystals. It is designed for customers who either do not have the time to go to a synchrotron, or would like to save on travel expenses. However, the main advantage of the MIX service is the speed at which results can be obtained. MIX beam time is, in most cases, available at short notice. If customers have urgent milestones or have new exciting projects, they do not have to wait for the next possibility to buy beam time at the SLS (e.g. industrial users book beam time up to 10 weeks in advance at the SLS). Once the customer has signed a contract with the SLS Techno Trans AG, to obtain access to the MIX service, they need only notify the MIX operator, who will reserve the next possible MIX shift for the measurements. If there is no shutdown, data is guaranteed within two weeks of submission.

Precise customer specifications

The whole information flow associated with the measurements is handled in the Digital User Office (DUO). The customers can specify the data collection parameters as precisely as they wish. For each crystal a form is filled out which provides the MIX operator with as detailed information as is needed. In addition, a customer can assign targets for each crystal including the minimal resolution limit, redundancy and I/σ . Data is collected by trained crystallographers. For every crystal a data collection strategy is calculated. This leads to minimal costs. On demand, the client can follow the data col-

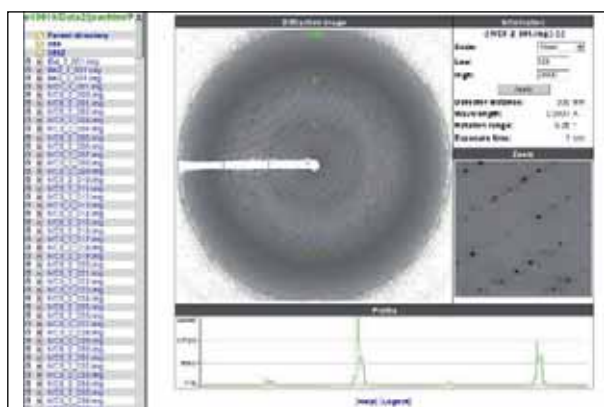


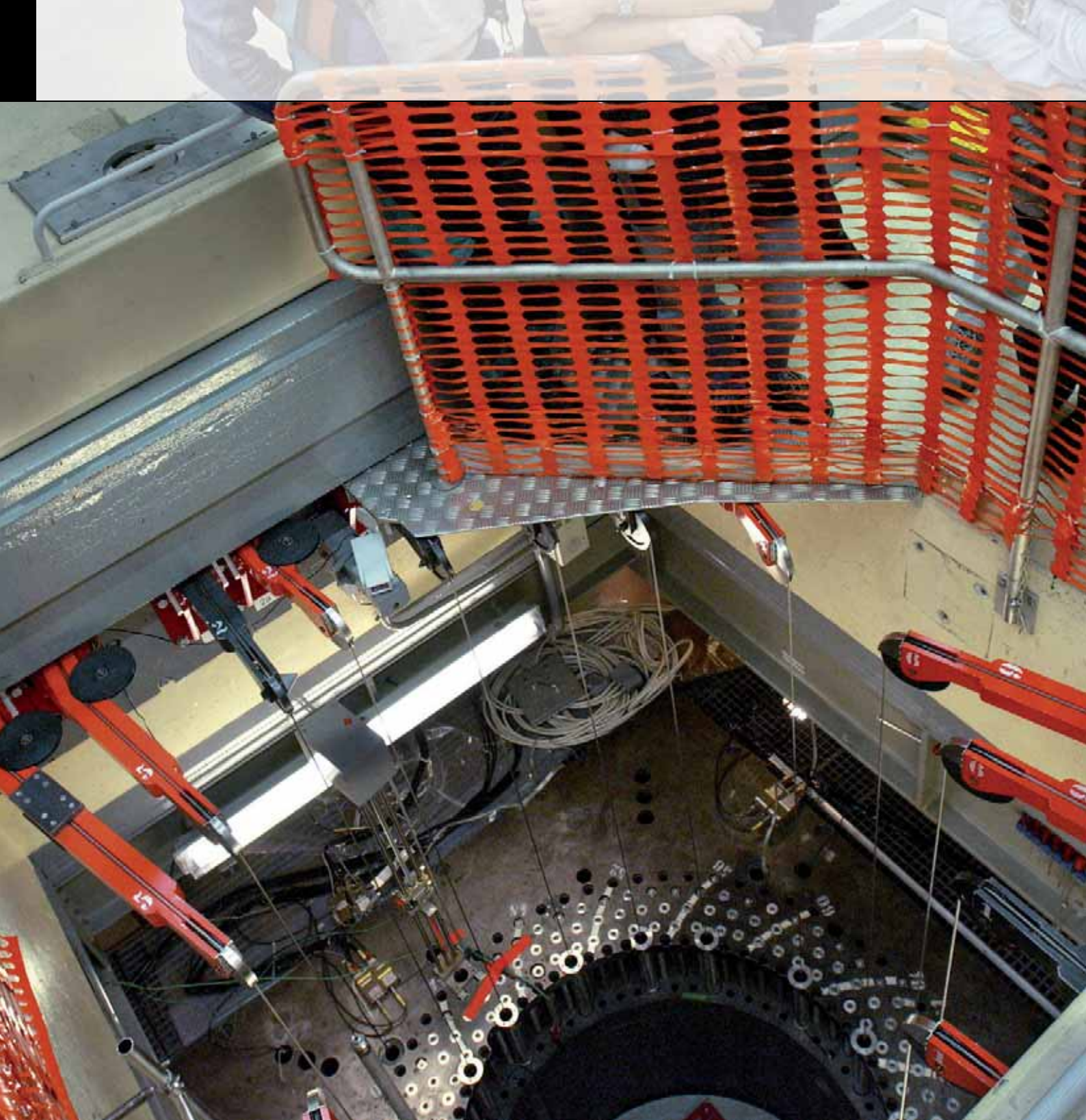
Figure 1: **The online image viewer. The customers can view their data live, as it is collected.**

lection online with a password protected image viewer (Figure 1). In addition, the customer has the option of interacting directly with the MIX operator by email or phone and discussing the strategy for the current measurement.

We also provide a crystal testing service. In this case, the customers may send a couple of crystals of the same type. The MIX operator will test all of them and select the best one. In addition, customers can send backup crystals of the same type together with a priority order, in case a crystal does not reach the desired data quality target (e.g. resolution) or suffers too early from radiation damage, so that the desired completeness or redundancy cannot be reached.

Data will be transferred on a hard disk to the customer by express courier. Moreover, there is the possibility to receive the data live by Rsync or FTP.

The increasing demand for MIX beam time allowed us to engage a logistics specialist, which leads to even faster return of the data and the dewars.



Research and user labs

Commission and committees

The Paul Scherrer Institute (PSI) is a multi-disciplinary research centre for natural sciences and technology. Research priorities lie in areas of basic and applied research, particularly in fields which are relevant for sustainable development, as well as of major importance for teaching and training, but which are beyond the capabilities of a single university department. In national and international collaborations with universities, other research institutes and industry, PSI is active in solid state physics, materials sciences, elementary particle physics, life sciences, nuclear and general energy research, and energy-related ecology.

The institute is committed to future generations by paving the way for sustainable development of society and economy. Through its research, PSI acquires new basic knowledge and actively pursues the application of this knowledge within industry.

With 1,200 employees, it is the largest national research institute and is unique in Switzerland. PSI develops and operates complex research installations which call for especially high standards of know-how, experience and professionalism, and is one of the world's leading user laboratories for the international scientific community.

Nearly 10,000 visitors poured through the doors at the PSI open day in 2005. The chance to glimpse into the experimental facilities, such as the PROTEUS reactor, was fascinating for all who came.

(Photo: Béatrice Devènes)

Research and user labs

PSI's total expenditure on R&D, construction and operation of research centres, infrastructure, and services in the year under review amounted to CHF 269.3 million. The Swiss Federal Government provided 83% of this sum.

Investments amounted to CHF 43.9 million (16%); HR costs (including scheduled work) comprised CHF 163.3 million (61%). Third party funding rose by some CHF 10 million on the previous year. As federal funding remained virtually constant (increasing by CHF 2.3 million or 0.1%), the increase in total expenditure to CHF 269.3 million represents funding provided by the private sector.

Third party funding in 2005 amounted to CHF 40 million, 63% of which came from private business and 20% from federal Swiss research programmes (Swiss National Science Foundation, Federal Office of Energy); 16% was linked to EU programmes.

PSI Financial Statement (in CHF millions)		
	2005	
Expenses		
Operations	225.4	84 %
Investments	43.9	16 %
Total	269.3	100 %
Thereof from:		
Federal government funding	224.3	83 %
Third party revenue	45.0	17 %
Third party revenue		
Private industry	25.5	64 %
Federal Research Fund	8.1	20 %
EU programmes	6.4	16 %
Total	40.0	100 %
HR (incl. trainees, staff continual-education and scheduled work)	163.3	61 %

High-end user lab

Some 70% of total expenditure in 2005 was again associated with our user laboratory. High pressure from the largely external body of users is currently restricting PSI's own research activities. Yet these activities are essential, because PSI can

only provide support and consultative services for external users if its own research remains competent and attractive. At year-end 2005 some 1200 people were employed at PSI. Most of these (77%) live in Canton Aargau; 11% live in Canton Zurich and 8% outside Switzerland. Women account for 14% of employees, and well over a third of all employees (37%) hold a foreign passport.

User lab 2005						
	SLS	SINQ	SμS	Particle physics	PSI Total	(2004)
No. of beamlines/instruments	8	10	6	11	35	(31)
No. of experiments	677	351	100	13	1141	(930)
No. of user visits	1805	557	433	230	3025	(2516)
No. of users	830	352	148	102	1432	(1399)

Training facilities in high demand

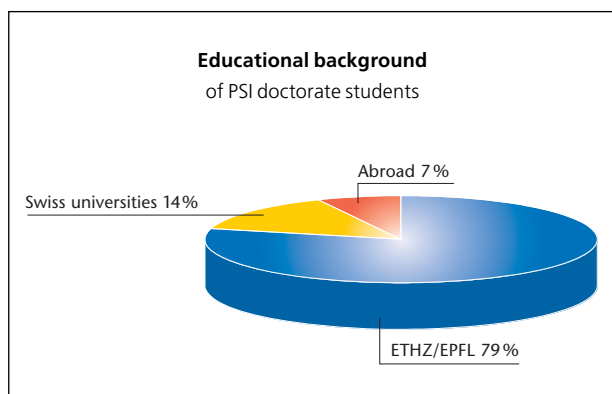
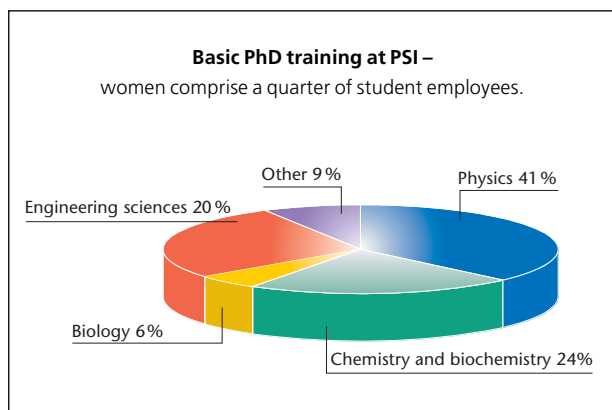
Approximately 270 PhD students are currently working in various internal and external PSI research groups. Of these some 170 are funded by PSI. The young doctoral students are mostly physics, chemistry or engineering graduates from the Swiss Federal Institutes of Technology (ETH) in Zurich and Lausanne, the Universities of Bern and Zurich or from abroad. In this way PSI provides a major input to ETH postgraduate programmes.

The largest group (58 students) are researching in the general energy (ENE) sector. Chemistry and biochemistry achieved the highest growth-rate in completed theses in 2005 (up 20% on the previous year); PhD's in biology, on the other hand, dropped 25%.

Thirty-two students, nine women and twenty-three men, completed their doctorates at PSI in 2005 with topics ranging from "Water Soluble Substances in the Atmosphere" and

“Experimental Investigations into Air Bubbles” to “Special Phase Transitions in Spin Liquids”.

As well as these PhD students, more than 40 graduates from classical or universities of applied sciences (Fachhochschulen), completed their final diploma or MSc dissertation at PSI in 2005. The institute is also a popular place for internships, with 76 students, some 70% from abroad and a third of them women, doing a laboratory trainee programme in the year under review.



With its commitment to doctoral education, as well as to teaching at the two Federal Institutes of Technology and at the classical and universities of applied sciences, PSI is a major source of input to graduate schools in the ETH sector. Our cutting-edge research, recognized the world over, as well as our globally networked user lab, guarantee that students are trained at internationally competitive levels. More than 70 PSI scientists had teaching commitments at classical and universities of applied sciences in 2005.

Support for Swiss universities

In 2005 PSI spent just over CHF 25 million on training and infrastructure facilities for PhD students and on university teaching. Some 80% of this outlay was allocated to post-graduates from Swiss universities and from the ETH institutes

in Zurich and Lausanne. By providing research training and lab facilities for external research groups, PSI takes a considerable financial and academic load off the shoulders of the Swiss universities.

Alongside academic and vocational training – PSI currently employs 77 apprentices in 12 different trades – the institute also offers courses on radiation protection and reactor technology. The special schools established for that purpose were attended by more than 2200 people in 2005.

Publications and impact score

Research at PSI is closely linked to the design, development and operation of large, complex research facilities. Unique in Switzerland, we are also, thanks to this specialty, the biggest national scientific research institute. Indications of our success and standing are on the one hand the number of papers published by our scientists in refereed journals, and on the other the impact score that tells how often publications are cited by other researchers.

Bibliometric data supplied by the University of Leiden shows that the output of scientific articles from PSI has risen slightly in recent years, reaching over 500 per year as against a ten-year average of 425. The impact score has likewise risen and currently stands at 2500 per year. In other words each paper is referred to on average five times by other scientists.

An attractive cooperation partner

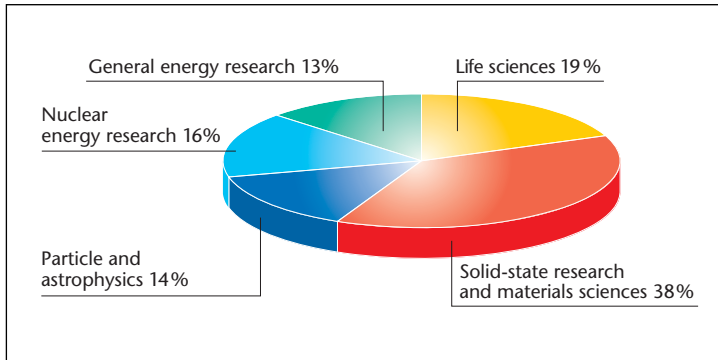
The main focus of this impact score coincides with our principal research fields – solid-state, particle and astrophysics, nuclear medicine and energy research. Some 80% of our



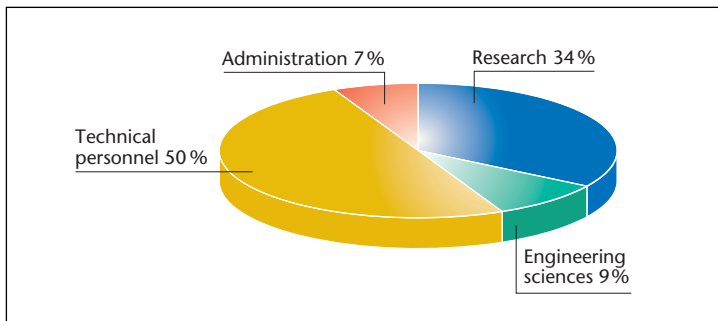
SLS

The Swiss Light Source (SLS) is a massive microscope and giant X-ray machine all in one. It accelerates electrons to nearly the speed of light and steers them with special magnets so that the characteristic high intensity synchrotron light is generated

straight ahead. This electromagnetic radiation spanning the wavelengths from infra-red to hard X-ray light is ideally suited to structural analysis of matter as well as spectrometry and to the ultra-fine structuring of material surfaces in the nanometer range.



Total budget distribution for 2004 (incl. non-governmental funding) across PSI's main research fields. The research facilities – in particular the accelerator, SLS and SINQ – were allocated to the various departments.



HR structure clearly reflects PSI's function as a user lab: the large scale facilities and complex research equipment require a large number of technical staff.

publications are in these areas. Analysis of publication activities shows that PSI is an attractive partner above all at the international level. Here too PSI achieved an impact score that puts us among the world leaders.

PSI as a user lab

PSI aims to continue attracting the best international scientists in their fields. This means that our employees, our research spectrum and infrastructure as well as our vital research culture must all meet the highest demands.

Nationally as well as internationally, PSI has established itself as a leading user laboratory. In 2005 we had some 3000 visits (previous year 2500) from more than 1400 scientists from 50 different countries. This meant one fifth more experiments than in 2004. Approximately 40% of lab users are from PSI and the Swiss universities, and more than half are from EU countries. Results of the research from the large facilities; SLS, SINQ, and S μ S resulted in 280 scientific publications, among them a larger number than ever in top journals like *Science*, *Nature*, *Cell*, *Langmuir* and *Physical Review Letters*. The Swiss Synchrotron Light Source (SLS) at PSI has been operating since 2001. In the year under review 830 scientists have conducted 677 experiments with this giant microscope, profiting from the exceptional qualities of a facility that is among the world's best.

Current research projects using the synchrotron's beamlines cover a wide area. They include the investigation of protein structures – crucial for the development of pharmaceuticals as well as for research into the function of the human genome – or the creation of 3-D reconstructions of biosystems, or the investigation of structures and properties of new materials and material surfaces.

Intense demand for SLS beam time

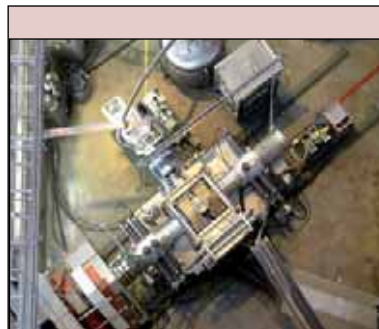
The high stability of the SLS beamlines has resulted in intense demand for user time, and we are stepping up our provision



SINQ

The **Spallation Neutron Source (SINQ)** is another oversized microscope. It produces neutrons, which at PSI are mostly used for experiments in materials research, solid-state physics (e.g. superconductors, magnetic and ferroelectric materials) and technology (neutron radiography). The neutrons are produced via spallation reactions induced by bombarding heavy metals (e.g. lead) with a proton beam from the accelerator.

superconductors, magnetic and ferroelectric materials) and technology (neutron radiography). The neutrons are produced via spallation reactions induced by bombarding heavy metals (e.g. lead) with a proton beam from the accelerator.



S μ S

Harnessed to the proton accelerator the **Swiss Muon Source (S μ S)** produces muons by directing the proton beam on a carbon target. When implanted in matter, these unstable elementary particles function like minute gyroscopes, providing precise information about local internal magnetic fields. Thanks to their spins, muons serve as highly sensitive probes used widely in materials and solid state research.

When implanted in matter, these unstable elementary particles function like minute gyroscopes, providing precise information about local internal magnetic fields. Thanks to their spins, muons serve as highly sensitive probes used widely in materials and solid state research.

to meet this as rapidly as possible. Eight beamlines were in use at the SLS in 2005, and a further eight were in various stages of planning, construction and commissioning.

Proton accelerator in demand on all fronts

The proton accelerator was originally developed more than 30 years ago for research into the basic physics of elementary particles. Today it is mostly used to produce neutrons in the Spallation Neutron Source (SINQ), the most powerful of its kind in the world. The facility comprises ten instruments for neutron experiments, used in 2005 by more than 350 scientists from Switzerland and other countries.

Central to SINQ research are solid-state physics and materials sciences. Significant for future applications are high-temperature superconductors (HTS), which at certain temperatures can conduct electricity without losses. At the moment the upper temperature limit is minus 125 degrees Celsius. In order to make further progress the origins of HTS have to be understood; a challenge for the researchers at SINQ. A speciality of SINQ is the further examination of materials which combine electrical and magnetic properties. This is usefully applied to the development of materials used in sensors, transducers and the performance of computer hard drives.

A third of the proton beam is used for producing the world's most intensive continuous muons, which are used as probes for structural research in materials sciences, solid-state physics and chemistry. Six instruments are currently available for this research. In 2005 they were used by 148 scientists in some 100 projects. The opening of the Low Energy Muon Facility (LEM) in 2005 opened up a completely new field of research, namely the depth dependent measurement of magnetic material properties in thin films, multi-layers and surfaces at nanometer scales.

Unique research offer

PSI's three major experimental research facilities, SLS, SINQ and $\text{S}\mu\text{S}$, offer an internationally unique combination of complementary methods for structural research, spectroscopy and materials structuring. The EU's Large Scale Facility Access programme supports this provision with funding to PSI of around CHF 1 million per year, which is used for operating the beamlines, ongoing development of the equipment, and training and support of researchers from EU countries working on these major facilities.

As the demand for laboratory places and instruments is up to five times what PSI can supply, only top research projects can be allotted time on the beamlines. Allocation is based on research proposals assessed for merit by an international board of scientific experts.

Active in environmental research

Research into environmental situations and the development of environmentally friendly technologies frequently demands complex facilities and equipment. PSI operates and develops large scale facilities that are in continuous intensive use in these sectors. For example, two SLS beamlines will soon be used for studying the mechanisms of dispersion and intensification of environmental pollutants, as well as questions relating to the long-term disposal of nuclear waste. The proton accelerators enable production of short-lived radio-nuclides for use in atmospheric chemistry experiments.

The SINQ facility is used for neutron radiography investigating the distribution of liquids and gases in fuel cells in order to establish fundamental processes for efficient energy conversion. Processes for the production of solar hydrogen as an



Particle physics

Particle physics investigates the fundamental building blocks of matter and their interactions. Many experiments have confirmed the standard physical model with great exactitude, but one element of this theoretical structure – the Higgs boson – has not yet been found. Particle physics is currently engaged on a twofold quest, on the one hand for this heavy particle and on the other for a new super-symmetry that will link elementary particles and their interactive forces, including gravity.

ment of this theoretical structure – the Higgs boson – has not yet been found. Particle physics is currently engaged on a twofold quest, on the one hand for this heavy particle and on the other for a new super-symmetry that will link elementary particles and their interactive forces, including gravity.



The hot-lab

The PSI hot-lab is home to applied materials research on highly radioactive probes and radioactive waste disposal. The only facility of its type in Switzerland, it provides backup for Swiss nuclear power plants as well as for university and industrial research groups.

plants as well as for university and industrial research groups.

environmentally friendly alternative to fossil fuels are undergoing further development in PSI's solar furnace.

A new accelerator-based mass spectrometer that enables radio-carbon dating (using the C 14 method) of very small samples is being used in climate research for analyzing ice cores. And in the PSI smog chamber scientists are simulating the formation of aerosols in order to investigate the behaviour of these climatically relevant suspension particles in air.

Top quality for atomic particle physicists

PSI's proton beam also functions as an intensive secondary source of pions and muons, which are used for experiments in particle physics. Because of their exceptional quality – they are the world's best – they are highly sought after by American and Japanese as well as European scientists. Researchers are currently investigating the basic properties of pions and muons, looking in particular at subtle details that are crucially important for present-day particle physics.

Important news from particle physics at PSI is the development of extremely sensitive detectors, used for example in the CMS experiment at CERN, which should prove the existence of heavy particles; as predicted by the standard model of physics. Conversely, fundamental symmetries are being challenged by a group at PSI working with ultra-cold neutrons (UCN).

The proton beam is also used to generate radio isotopes for pharmaceutical research into new diagnostic and therapeutic methods. A small quantity of accelerated protons was still being used in 2005 for cancer therapy, but this will be the last time, as proton therapy will in future be based on the new COMET compact cyclotron developed specifically for medical applications.

Tissue-sparing cancer therapy

More than three hundred patients profited in 2005 from PSI's globally unique proton therapy. In co-operation with Zurich Children's Hospital 14 small children (under 4 years old) suffering from cancer were successfully treated under anaesthetic with proton radiation – a particularly tissue-sparing procedure used on a total of almost 50 children and adolescents up to the end of 2005. From late 2006 proton therapy will be offered year-round, which will enable treatment of 400-500 patients annually.

The PROSCAN project for extending proton therapy to deep-seated tumours has seen major progress in 2005. The new superconductive compact cyclotron came on stream in April and is expected to be available for patient therapy, after comprehensive testing and specialized application runs, from October 2006.

A bonus for Swiss industry

PSI has granted industrial licenses for its precision radio-therapy scanning technology. An initial privately financed commercial facility using the scanning process and compact cyclotron developed at PSI will soon commence operations in Munich. Further projects are planned. With contracts in the double figure range (CHF millions) for the delivery of components and systems; Swiss industry stands to gain from this unique PSI-developed technology.

The compact cyclotron, COMET, soon to be in operation at PSI will be used for proton therapy of cancer tumours.

(Photo: H. R. Bramaz)



The solar furnace

PSI's solar concentrator, an 8.5 m diameter concave mirror, bundles solar radiation to an intensity of 5000 suns. The high temperatures (up to 2000° C) created in a reactor aperture are used for re-

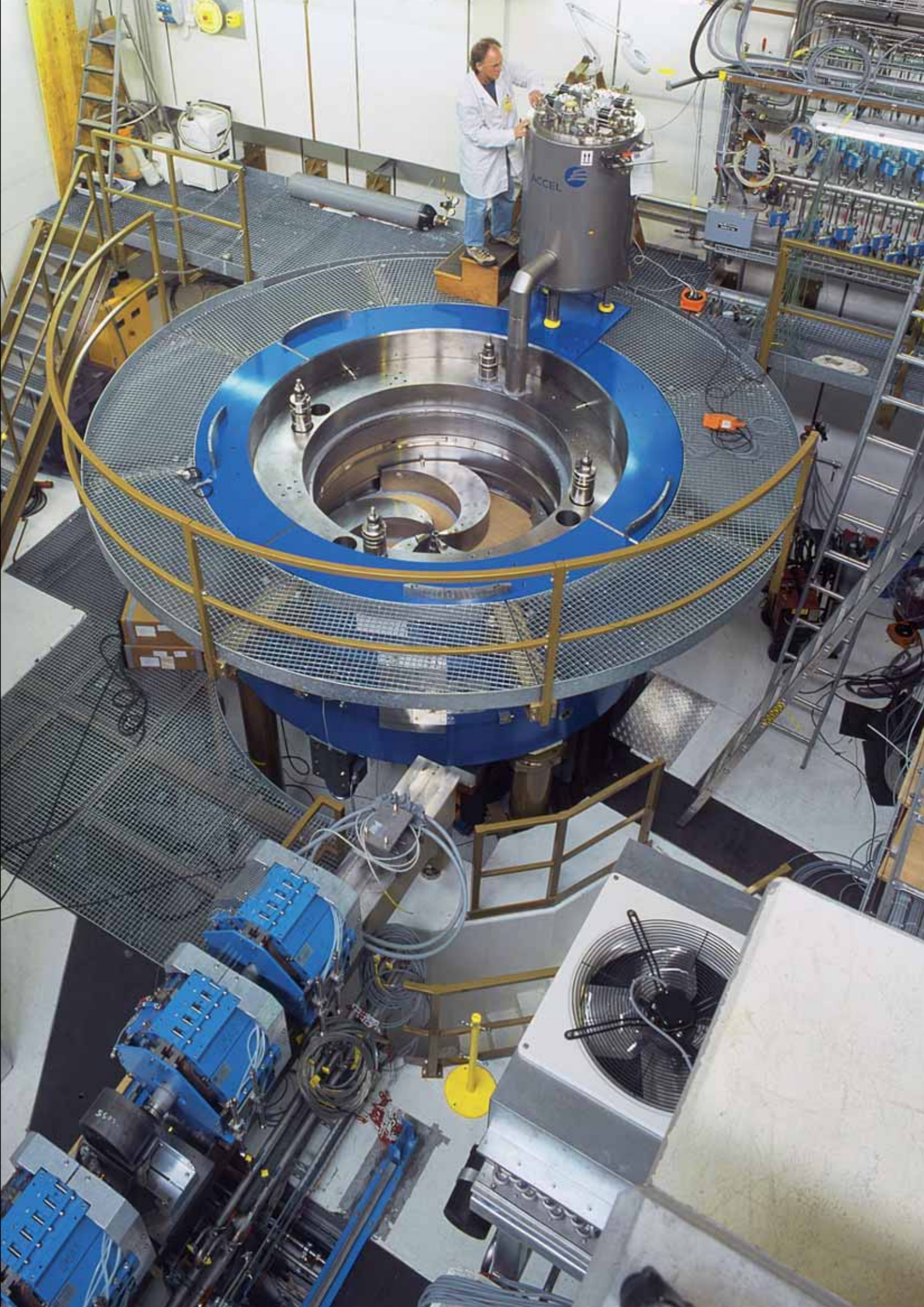
search into solar-chemical processes such as the efficient production of solar fuels and innovative materials. A high-flux solar simulator of double this power was recently installed for experiments into radiation under controlled conditions independent of the weather.



The smog chamber

The smog chamber simulates conditions for experiments in atmospheric chemistry. A 27 m³ Teflon sack can be filled, for example, with exhaust gases for exposure to artificial sunlight, and the ensu-

ing chemical reactions can be observed and measured. Results can be used for example, to determine how particulate matter transforms in the atmosphere.



Commission and committees

Research Commission

External Members

Prof. Dr. H.-R. Ott, President	Laboratory for Solid-State Physics, ETH Zurich, CH
Prof. Dr. U. Amaldi	University of Milano Bicocca, Mailand, IT
Prof. Dr. G. Aeppli	University College London, UK
Prof. Dr. W. Baumeister	Max Planck Institute for Biochemistry, Martinsried/Munich, DE
Prof. Dr. F. Carré	CEA, Gif-sur-Yvette, FR
Prof. Dr. Ø. Fischer	Department of Condensed Matter, University of Geneva, CH
Prof. Dr. B. Johansen	Research Center of Rossendorf, Dresden, DE
Prof. Dr. R. Klanner	Research Director, DESY, Hamburg, DE
Prof. Dr. D. E. Moncton	Nuclear Reactor Laboratory, MIT, USA
Prof. Dr. D. Richter	Institute for Neutron Scattering at the Institute of Solid-State Research, Forschungszentrum Jülich, DE
Prof. Dr. Th. Sattelmayer	Chair of Thermodynamics, TU München, DE
Prof. Dr. J.W. Tester	Laboratory for Energy and the -Environment, MIT, Cambridge, USA

Internal Members

Dr. M. Ammann	Particles and Matter (TEM)
Prof. Dr. K. Ballmer-Hofer	Life Sciences (BIO)
Dr. B. Delley	Condensed Matter Research with Neutrons and Muons (NUM)
Dr. R. Henneck	Particles and Matter (TEM)
Dr. I. Mantzaras	General Energy (ENE)
Dr. Joël Mesot	Condensed Matter Research with Neutrons and Muons (NUM)
Dr. W. Pfingsten	Nuclear Energy and Safety (NES)
Dr. G. Scherer	General Energy (ENE)
Dr. N. Schlumpf	Particles and Matter (TEM)
Dr. L. Simons	Particles and Matter (TEM)
Dr. U. Staub	Synchrotron Radiation and Nanotechnology (SYN)
Dr. W. Wagner	Condensed Matter Research with Neutrons and Muons (NUM)
Dr. P. Hasler, Secretary	Life Sciences (BIO)

Permanent Guest

Prof. Dr. A. Green	President of the ETH Zurich Research Commission; Institute of Geophysics, ETH Zurich, CH
--------------------	--

Research Committees

Synchrotron Radiation SYN*Scientific Advisory Committee (SAC)*

Prof. Dr. M. Altarelli, President
Sincrotrone Trieste, Trieste, IT

Prof. Dr. T. Baer
University of North Carolina, USA

Prof. Dr. P. Cramer
Ludwig-Maximilian University Munich, DE

Prof. Dr. W. Eberhardt
BESSY GmbH, Berlin, DE

Prof. Dr. R. Fourme
Synchrotron Soleil, Gif-sur-Yvette, FR

Prof. Dr. F. Farges
Université de Marne la Vallée, FR

Prof. Dr. J. Hastings
SSRL/SLAC, Stanford, USA

Prof. Dr. G. Margaritondo
EPFL, CH

Prof. Dr. G. Materlik
Diamond Project, Oxfordshire, UK

Prof. Dr. R. Prins
ETH Zurich, CH

Prof. Dr. T. Richmond
ETH Zurich, CH

Condensed Matter Research with Neutrons and Muons NUM*SINQ Scientific Committee*

Dr. A. Boothroyd, Chairman
Oxford University, UK

Dr. A. Arbe
University of San Sebastian, ES

Prof. Dr. C. Bernhard
University of Fribourg, CH

Prof. Dr. R. Caciuffo
Forschungszentrum Karlsruhe, DE

Dr. B. Fåk
CEA, Grenoble, FR

Prof. Dr. J. Löffler
ETH Zurich, CH

Prof. Dr. K. Mortensen
Danish Polymer Centre, Risø, DK

Dr. J. Rodriguez-Carvajal
Laboratoire Léon-Brillouin, Gif-sur-Yvette, FR

Dr. A. Wiedenmann
Hahn-Meitner-Institut, Berlin, DE

Dr. M. Würle
ETH Zurich, CH

Myon Spin Spectroscopy

Prof. Dr. H. Keller, President
University of Zurich, CH

Prof. Dr. A. Baldereschi
ITP, EPFL, CH

Prof. Dr. R. De Renzi
Università di Parma, IT

Prof. Dr. E. M. Forgan
University of Birmingham, UK

Prof. Dr. J. Gomez Sal
Universidad de Cantabria, Santander, ES

Prof. Dr. F. J. Litterst
IMNF, TU Braunschweig, DE

Prof. Dr. A. McFarlane
Univ. of British Columbia, Vancouver, CDN

Dr. F. Pratt
ISIS, RAL, Chilton, UK

Dr. B. Roessli
Paul Scherrer Institute/ETH Zurich, CH

Particles and Matter TEM*Experiments at the Ring Cyclotron*

Prof. Dr. C. Hoffman, President
LAMPF, Los Alamos, USA

Prof. Dr. A.B. Blondel
University of Geneva, CH

Dr. D. Bryman
TRIUMF, Vancouver, CDN

Dr. P. Cenci
I.N.F.N. sez. di Perugia, IT

Prof. Dr. S. Paul
Technical University of Munich, DE

Prof. Dr. M. Pendlebury
University of Sussex, UK

Prof. Dr. L. Tauscher
University of Basel, CH

Prof. Dr. D. Wyler
University of Zurich, CH

Life Sciences BIO

Prof. Dr. D. Neri, President
ETH Zurich, CH

Prof. Dr. Ch. Glanzmann
University Hospital Zurich, CH

Prof. Dr. M. Grütter
Biochemical Institute, Univ. of Zurich, CH

Prof. Dr. U. Haberkorn
Universitätsklinikum Heidelberg, DE

Prof. Dr. S. Werner
ETH Zurich, CH

Nuclear Energy and Safety NES

Dr. Ch. McCombie, President
Gipf-Oberfrick, CH

P. Hirt
Atel, Olten, CH

Prof. Dr. M. Giot
Université Catholique de Louvain, BE

Dr. P. Miazza
Nuclear Power Plant Mühleberg, CH

Dr. U. Schmockler
HSK, Würenlingen, CH

Dr. J.B. Thomas
CEA-Saclay, Gif-sur-Yvette, FR

Prof. Dr. K. Törrönen
Institute of Energy JRC Petten, NL

Dr. P. Zuidema
Nagra, Wettingen, CH

General Energy ENE

Prof. Dr. T. Peter, President
ETH Zurich, CH

Dr. T. Kaiser
Alstom Power Technology Center,
Baden-Dättwil, CH

Prof. Dr. A. Reller
University of Augsburg, DE

Dr. M. Schaub
CT Umwelttechnik AG, Winterthur, CH

H.U. Schärer
BFE, Berne, CH

Prof. Dr. L. Schlapbach
Empa, Dübendorf, CH

Prof. Dr. A. Voss
University of Stuttgart, DE



Lists and links to web

The publication lists for the PSI departments featured in this volume can be found on the accompanying CD and include the following:

- Peer reviewed publications
- Invited talks
- Dissertations
- Conference proceedings
- Lectures

Electronic versions of this volume (2) and volume 3 of the PSI Scientific Report 2005 and the Annual Report (Jahresbericht) in German are also included on the CD.

Upon publication, volume 1 will be available at www.psi.ch (Media/Annual Reports).

Links to other research activities not highlighted in the PSI Scientific Report 2005 can be found at www.psi.ch (Research at PSI).



PAUL SCHERRER INSTITUT

PSI

PSI Scientific Report 2005

Volume 2 Life sciences and medicine (ISSN 1661-7010)

Volume 3 Energy and environment (ISSN 1661-7029)

PSI publication lists

PSI-Jahresbericht 2005 (German) (ISSN 1423-7261)

The PSI Scientific Report 2005
comprises:

- Volume 1** Condensed matter, photons,
neutrons and charged particles
- Volume 2** Life sciences and medicine
- Volume 3** Energy and environment

PAUL SCHERRER INSTITUT



Paul Scherrer Institut, 5232 Villigen PSI, Switzerland
Tel. +41 (0)56 310 21 11, Fax +41 (0)56 310 21 99
www.psi.ch